

THE USE AND BEHAVIOR OF SORPTION MEDIA IN
MITIGATING EXCESSIVE DISSOLVED PHOSPHORUS IN
SURFACE WATERS

by

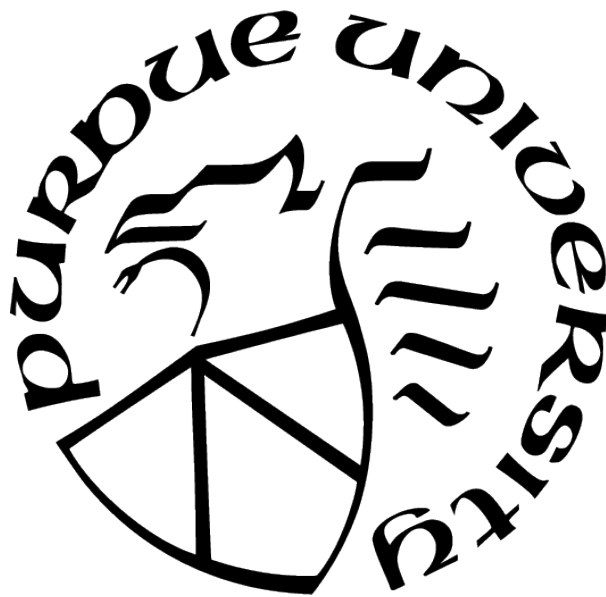
Isis Stacanelli Pires Chagas Scott

A dissertation

Submitted to the Faculty of Purdue University

In Partial Fulfillment of the Requirements for the degree of

Doctor of Philosophy



Agricultural and Biological Engineering

West Lafayette, Indiana

December 2020

**THE PURDUE UNIVERSITY GRADUATE SCHOOL
STATEMENT OF COMMITTEE APPROVAL**

Dr. Chi-hua Huang, Co-Chair

National Soil Erosion Research Laboratory

Dr. Laura C. Bowling, Co-Chair

Department of Agronomy

Dr. Chad J. Penn

National Soil Erosion Research Laboratory

Dr. Sara K. McMillan

Department of Agricultural And Biological Engineering

Approved by:

Dr. Nathan S. Mosier

“I have wandered to the limits of my understanding any number of times, out into that desolation, that Horeb, that Kansas, and I’ve scared myself, too, a good many times, leaving all landmarks behind me, or so it seemed. And it has been among the true pleasures of my life. Night and light, silence and difficulty, it seemed to me always rigorous and good.”

- *Marilynne Robinson, in Gilead.*

ACKNOWLEDGMENTS

I want to express my gratitude to my co-advisor Dr. Chi-hua Huang for his mentorship throughout my PhD. I take constant inspiration on how Dr. Huang approaches scientific questions, and I am thankful for the opportunity to learn from him. Thank you to Dr. Chad Penn for his invaluable support and teachings throughout this research. I am grateful for Dr. Penn's contributions to my growth as a student and scientist. I would also like to thank Dr. Laura Bowling for her academic guidance inside and outside the classroom. Thank you also to Dr. Sara McMillan, member of my advisory committee, for her encouragement and valuable inputs.

This research would not be possible without the support of the National Soil Erosion Research Laboratory (NSERL) staff and interns. In particular, I would like to thank Nancy Sanders, for her dependability, Rhonda Graeff, for her technical guidance, and Scott McAfee and Brenda Hoffman for their support with the experiments and analysis conducted in this research. I would also like to thank Dr. Kossi Nouwakpo, for being a constant source of inspiration throughout my work.

TABLE OF CONTENTS

LIST OF TABLES	9
LIST OF FIGURES	12
ABBREVIATIONS	16
NOMENCLATURE	17
ABSTRACT	19
1 INTRODUCTION	21
1.1 Rationale	21
1.2 State of the science on phosphorus (P) removal structures and P sorption materials	22
1.2.1 Definitions	22
Phosphorus Removal Structures	22
Phosphorus Sorption Materials	24
1.3 Knowledge gaps and research needs	25
1.3.1 Variability of the use of steel slags as PSMs	25
1.3.2 Development of a regeneration technique for Fe/Al-based PSMs	27
1.3.3 Behavior of PSMs under anaerobic conditions	28
1.4 Dissertation focus and organization	29
References	30
2 ESTIMATING THE VARIABILITY OF STEEL SLAG PROPERTIES AND THEIR INFLUENCE IN PHOSPHORUS REMOVAL ABILITY	36
2.1 Abstract	36
2.2 Introduction	36
2.3 Material and methods	40
2.3.1 Analysis of steel slags: chemical and physical characterization	42
2.3.2 Analysis of steel slags: P removal ability	42

2.3.3	Data analysis: effects of the variability of steel slag samples on P removal ability	43
2.4	Results and Discussion	46
2.4.1	Analyses of P sorption ability of steel slags in flow-through experiments	46
	Impact of residence time on P removal by uncoated steel slags	47
2.4.2	Differences between uncoated and coated steel slags under low RTs	48
2.4.3	Phosphorus removal capacity and origin of slag samples	50
2.4.4	Factors explaining P sorption capacity of steel slags	51
2.4.5	Coated slags	54
2.4.6	Environmental safety of steel slags	56
2.5	Conclusions	58
	References	59
3	DEVELOPMENT OF A REGENERATION TECHNIQUE FOR ALUMINUM-RICH AND IRON-RICH PHOSPHORUS SORPTION MATERIALS	78
3.1	Abstract	78
3.2	Introduction	79
3.2.1	Sorption of P by Al/Fe-Rich Materials	80
3.2.2	Desorption of P from Al/Fe-Rich Materials	81
3.3	Materials and Methods	83
3.3.1	Characterization of PSMs	83
3.3.2	Preliminary Evaluation: Flow-Through Experiments and Batch Isotherms	84
3.3.3	Sorption-Desorption Cycles: Testing Regeneration Treatments	85
3.4	Results and Discussion	87
3.4.1	Preliminary Experiments: Evaluation of P Removal Ability of Al/Fe-Rich PSMs	87
3.4.2	Regeneration Treatments	88
	Effect of P Concentration on Regeneration	90
	Effect of Residence Time	91
	Effect of Volume of Regenerative Solution	92

	Effect of Number of Recirculations	93
	Effect of Repeated Desorption Cycles	94
3.5	Conclusions and Implications	95
	References	97
4	THE USE AND BEHAVIOR OF PHOSPHORUS SORPTION MATERIALS IN ANOXIC ENVIRONMENTS	111
4.1	Abstract	111
4.2	Introduction	112
4.3	Material & Methods	116
4.3.1	Pre-incubation	117
	Characterization of media	117
	Flow-through experiments and batch isotherms	118
4.3.2	Incubation studies	119
4.3.3	Post-incubation: sample analysis and flow-through tests	121
4.4	Results and discussion	121
4.4.1	Characterization of PSMs	121
4.4.2	Incubation Analysis	123
4.4.3	Post-incubation analysis: P release and P removal ability of PSMs	125
	Analysis of incubated samples	125
	Post-incubation flow-through experiments	128
4.5	Conclusions and implications	129
	References	130
5	CONCLUSIONS	143
5.1	Summary	143
5.2	Recommendations	145
A	FLOW-THROUGH SYSTEM	148
B	STATISTICAL ANALYSIS OF THE STEEL SLAGS PERFORMANCES	149

C	ADDITIONAL CHARACTERIZATION RESULTS OF STEEL SLAG AND FLOW- THROUGH SAMPLES	157
D	EFFECT OF RESIDENCE TIME ON PHOSREDEEM	160
E	SUMMARY OF SORPTION-DESORPTION CYCLES	161
VITA	165

LIST OF TABLES

Table	Page
2.1 Origin and particle sizes of steel slag samples.	64
2.3 Characterization of steel slag samples: specific parameters tested and their respective levels.	65
2.2 Methods for characterization of steel slag properties.	65
2.4 Analysis of variance: the effect of slag sample and level of coating on the cumulative P removal response (data was previously transformed due to heteroscedasticity).	66
2.5 Mean estimates of cumulative P removal (%) for the coating groups and comparison between the marginal means of coating levels.	66
2.6 Mean estimates of cumulative P removal for the slags and comparison between the marginal means of different slag samples. ¹	67
2.7 Single linear regression models (uncoated steel slags): each of the variables was tested against the residuals of the EC versus P cumulative removal model (data shown in Figure 2.5b). We also show the variables for which the model was significant (indicated by the asterisk), i.e., variables that were able to explain the variability of the residuals.	68
2.8 Summary of multiple linear regression predicting cumulative P removal of uncoated steel slags: original and corrected (ridge estimators) parameter estimates.	69
2.9 Single linear regression models (Al-coated steel slags): each of the variables were tested against the residuals of the EC versus P cumulative removal model. We show the variables for which the model were significant (indicated by the asterisk), i.e., variables that were able to explain the variability of the residuals.	70
2.10 Summary of multiple linear regression predicting cumulative P removal of coated steel slags: original and corrected (ridge estimators) parameter estimates.	71
2.11 Range of micro-constituents of steel slag samples and water quality criteria for freshwater systems and for heavy metals applied to soils: evaluating the environmental safety of steel slag according to drinking water and soil amendments standards.	72
3.1 Chemical characterization of PSMs: Average elemental composition and pH.	100
3.2 Preliminary performance and subsequent maximum phosphorus (P) removed (P_{Max}) by three P sorption materials (PSMs) under flow-through conditions of 0.5 and 50 mg P L ⁻¹ inflow and 0.284 min residence time. The P_{Max} values were used as the target for initial P saturation in regeneration experiments.	101

Table	Page
3.3 Experimental sequence for sorption and desorption cycles for the regeneration of Al/Fe-rich P sorption materials (PSMs). The same cycles were tested at both low level (0.5 mg P L^{-1}) and high level (50 mg P L^{-1}) P treatments. All experiments were conducted in duplicate.	102
4.1 Calculated P sorbed to P sorption materials (PSMs) in flow-through experiments at 40% cumulative removal of P input (figure 4.2 at 40% [$P_{40\%}$]) and corresponding P concentrations added in batch isotherms to reach $P_{40\%}$ using a solid:solution ratio of 1:15.	133
4.2 Chemical composition of tile drainage used in incubations. The reported concentrations are the average among three replicates, except for nitrogen (duplicates). Standard deviation is listed in parenthesis.	133
4.3 Chemical characterization of the non-treated and P-treated P sorption materials. Average and standard deviation are reported.	134
4.4 Pre-incubation analysis: total concentrations of trace metals in phosphorus sorption materials (PSMs). \bar{X} is the average among the two replicates of each non-treated PSM and S the standard deviation.	135
4.5 Redox potentials and experimental time required for reaching the target (Eh_{-200}) and final Eh values among P-treated and non-treated PSMs during incubation with no oxygen. “Reference” treatments refer to those that did not receive glucose addition.	136
4.6 Ferrozine analysis of post-incubation solution samples for Fe(II) and (III), conducted under conditions of no oxygen for P-treated and non-treated P sorption materials. “Reference” treatment refer to those that did not receive glucose addition.	137
4.7 Post-incubation analysis: chemical composition of filtered and acidified solution samples collected after the respective incubation period. \bar{X} is the average among the three replicates in each treatment and S the standard deviation. No replicates exist for “tile drainage reference”, which contains no P sorption material. “Reference” treatments refer to those that did not receive glucose addition. . . .	138
4.8 Cumulative P removal under flow-through conditions for pre- and post-incubation samples for each PSM after cumulative addition of 700 mg kg^{-1} . Values are average of all replicates.	139
B.1 Pairwise comparison of cumulative P removal between slag samples: estimates of difference between groups, confidence intervals and level of significance of comparison.	149
C.1 pH of randomly selected flow-through samples.	158

Table	Page
C.2 Micro-constituents of steel slag samples: concentrations of Boron (B), Chromium (Cr), Cobalt (Co), Manganese (Mn), Sodium (Na), Nickel (Ni), Lead (Pb), Sulfur (S), Silica (Si) and Zinc (Zn) as measured in the digestions.	159
E.1 Alcan phosphorus (P) sorption and desorption results. Each row represents one regeneration treatment. The first ten rows refer to 0.5 mg L ⁻¹ P, the second ten are 50 mg L ⁻¹ P experiments.	162
E.2 Biomax phosphorus (P) sorption and desorption results. Each row represents one regeneration treatment. The first ten rows refer to 0.5 mg L ⁻¹ P, the second ten are 50 mg L ⁻¹ P experiments.	163
E.3 PhosRedeem phosphorus (P) sorption and desorption results. Each row represents one regeneration treatment. The first four rows refer to 0.5 mg L ⁻¹ P, the following six are 50 mg L ⁻¹ P experiments.	164

LIST OF FIGURES

Figure	Page
1.1 Percentage of river miles with a nutrient-related impairment in the U.S. Darker shades represent a greater impairment of rivers.	34
1.2 Example of a ditch P removal structure.	35
1.3 Example of a confined bed P removal structure. Downward flow.	35
2.1 Example phosphorus (P) removal expressed as a function of cumulative P added per unit slag mass. Two replicates and their respective fitted curves are being shown (the fitted curves equations are shown in the upper-right corner). Intersection of fitted line with vertical line at $60 \text{ mg}\cdot\text{P kg}^{-1}$ slag indicates cumulative P removal values used for statistical comparisons.	73
2.2 Heterogeneity of cumulative P removal by different steel slag samples. Each datum represents the P removal performance of steel slag samples in each of the flow-through experiments, and is colored according to the level of coating. . . .	74
2.3 Data distribution analysis: cumulative P removal (%) according to the parameters: (a) Steelmaking plant, (b) slag production process, (c) particle size range, (d) minimum particle size, (e) Coating and (f) Residence time.	75
2.4 Comparison of marginal means of groups: O.B. (overband magnet) had a mean significantly different in comparison to the other four sources, which were not significantly different amongst themselves. Open circles represent the means and the respective line the confidence interval.	76
2.5 Phosphorus cumulative removal versus main variables of interest for uncoated slags: (a) Calcium content and (b) EC.	76
2.6 Coated and uncoated slags: cumulative P removal according to evaluated variable: (a) Aluminum content (digestion analysis), (b) Al content in the oxalate fraction and (c) pH.	77
3.1 Experimental conditions and phosphorus (P) regeneration treatments tested. PV = pore volume; RT = residence time; RC = recirculation.	102
3.2 Preliminary evaluation of phosphorus (P) removal ability of Alcan in flow-through experiments conducted at a residence time (RT) of 0.28 min and inflow P concentrations of (a) 0.5 mg L^{-1} and (b) 50 mg L^{-1} . Cumulative P removal is plotted as a function of cumulative P added.	103
3.3 Preliminary evaluation of phosphorus (P) removal ability of Biomax in flow-through experiments conducted at a residence time (RT) of 0.28 min and inflow P concentrations of (a) 0.5 mg L^{-1} and (b) 50 mg L^{-1} . Cumulative P removal is plotted as a function of cumulative P added.	104

Figure	Page
3.4 Preliminary evaluation of phosphorus (P) removal ability of PhosRedeem in flow-through experiments conducted at a residence time (RT) of 0.28 min and inflow P concentrations of (a) 0.5 mg L ⁻¹ and (b) 50 mg L ⁻¹ . Cumulative P removal is plotted as a function of cumulative P added.	105
3.5 Effects of regeneration residence time on phosphorus (P) recovery from P sorption materials (PSM). Phosphorus recovery is shown after the first sorption cycle (S0-D0) only, treated with 20 pore volumes of 1 M KOH and no recirculation. Treatments separated based on PSM type and P concentration used during the sorption phase.	106
3.6 Effects of regenerative solution pore volume (PV) on phosphorus (P) recovery from P sorption materials (PSMs). Phosphorus recovery is shown after the first sorption cycle (S0-D0) only, treated with 1 M KOH at a residence time of 0.5 min with no recirculation. Treatments separated based on PSM type and P concentration used during the sorption phase.	106
3.7 Effects of the number of recirculation of regenerative solution on phosphorus (P) recovery from P sorption materials (PSMs). Phosphorus recovery is shown after the first sorption-desorption cycle (S0-D0) only, treated with five pore volumes of 1 M KOH at a residence time of 0.5 min. Treatments separated based on PSM type and P concentration used during the sorption phase.	107
3.8 Phosphorus (P) recovery across all evaluated cycles and treatments for Alcan. The treatments identified on the x-axis follow the notation: AX.PV.RC.RT, with X being the level of P concentration (L for low or 0.5 mg L ⁻¹ and H for high or 50 mg L ⁻¹), PV: pore volume (5 or 20), RC: number of recirculations (0,6 or 24) and RT: residence time used in the desorption phase. Phosphorus recovery in the S1-D1 cycle was omitted for the treatment AL.5.0.05, which showed an average of 3233% with standard deviation (S_x) of 2997.	108
3.9 Phosphorus (P) recovery across all evaluated cycles and treatments for Biomax. The treatments identified on the x-axis follow the notation: PX.PV.RC.RT, with X being the level of P concentration (L for low or 0.5 mg L ⁻¹ and H for high or 50 mg L ⁻¹), PV: pore volume (5 or 20), RC: number of recirculations (0, 6, or 24) and RT: residence time used in the desorption phase.	109
3.10 Phosphorus (P) recovery across all evaluated cycles and treatments for PhosRedeem. The treatments identified on the x-axis follow the notation: PX.PV.RC.RT, with X being the level of P concentration (L for low or 0.5 mg L ⁻¹ and H for high or 50 mg L ⁻¹), PV: pore volume (5 or 20), RC: number of recirculations (0, 6, or 24) and RT: residence time used in the desorption phase.	110

Figure	Page
4.1 Examples of different flow direction in phosphorus (P) removal structures: the top-down or downward flow requires larger structures, because they are limited to the depth at the point of discharge (exemplified as a ditch in the figure). Phosphorus removal structures built with upward flow can be deeper and contain the same amount of PSM, having a smaller footprint.	139
4.2 Phosphorus (P) removal curve for P sorption materials (PSMs) under flow-through conditions: (a) Alcan, two replicates, (b) AMDR, five replicates and (c) Metal shavings, two replicates. X-axis scale is different for each PSM illustrating the long-term P removal ability of metal shavings and Alcan.	140
4.3 The biogeochemical reactor is composed of a (1) gas tank containing CO ₂ and N ₂ , followed by a 2-stage gas regulator (2) and a pressure regulator (3). The gas is delivered to a water container (4) and is then distributed to the incubator cells through a manifold (5). The gas flow is controlled by flow regulators (6). The inset shows the incubator vessels in detail.	140
4.4 pH and pe data of Alcan incubated with no oxygen: (a) reference samples receiving no glucose, (b) non-treated samples and (c) P-treated samples. The range of pe and the duration of experiment differ for the different incubations.	141
4.5 pH and pe data of AMDR incubated with no oxygen: (a) reference samples receiving no glucose, (b) non-treated samples and (c) P-treated samples. The range of pe and the duration of experiment differ for the different incubations.	141
4.6 pH and pe data of metal shavings incubated with no oxygen: (a) reference samples receiving no glucose, (b) non-treated samples and (c) P-treated samples. The range of pe and the duration of experiment differ for the different incubations.	142
4.7 Phosphorus (P) removal expressed as a function of cumulative P added under flow-through conditions conducted on pre and post anoxic-incubated P sorption materials (PSMs): (a) non-treated Alcan (UAL), (b) non-treated AMDR (UAM) and (c) non-treated metal shavings (UMS). The graphs contain all pre- and post-incubation replicates and they are identified. For each incubated non-treated replicate (replicates 1,2,3), two flow-through experiments were conducted (replicates A and B). In all graphs, the pre-incubation results are shown in shades of black and gray. For the complete P removal curve for metal shavings, see Figure 4.2.	142
A.1 Schematic describing the elements in the flow-through experiments, a tool that was utilized in all studies in this research for measuring the P removal capacity of diverse PSMs.	148
B.1 Normal probability plots showing the lack of normality of the (a) low residence time and (b) high residence time datasets.	152

Figure	Page
B.2 Residuals distribution according to the different classes of coating: (a) shows the non-constant variance of the original residuals and (b) shows the residuals after transforming the data.	152
B.3 Histograms for checking normality of data. (a) and (c) are respectively the original and the transformed low RT data ($\lambda = 0.8156$) and (b) and (d) show the distribution of the original and transformed high RT data ($\lambda = 2.8256$).	153
B.4 Means and confidence intervals of transformed cumulative P removal of each combined treatment. Y-axis describe each combination of factors, with slag number first and level of Al-coating second. 100% coated slag 9 (in blue) had a superior performance and 18 groups (in red) showed population marginal means significantly different from Slag=9, Coating=100. The groups in gray had similar performance to 100% coated slag 9.	154
B.5 Coating Levels: group means represented by circle and the confidence interval represented by the line. All groups were statistically different from each other ($\alpha = 0.05$).	155
B.6 Evaluating multicollinearity of explanatory variables of cumulative P removal by uncoated steel slags: particle density and bulk density showed a significant correlation.	156
D.1 Phosphorus (P) removal by PhosRedeem in flow-through experiments using different residence times (RT). Experiments were performed with input solution of 0.5 mg P L^{-1}	160
D.2 Box plot: effect of residence time (RT) on P removal performance of PhosRedeem.	160

ABBREVIATIONS

BMPs	Best management practices
BOF	Basic oxygen furnace
EAF	Electric arc furnace
DP	Dissolved phosphorus
DI	Deionized
EC	Electrical conductivity
Eh	Redox Potential
HABs	Harmful Algal Blooms
MLR	Multiple linear regression
PSM	Phosphorus Sorption Materials
PV	Pore volume
RT	Residence time
S	Standard deviation
SLR	Simple linear regression
SRP	Soluble reactive phosphorus
VIF	Variance inflation factor
\bar{X}	Mean

NOMENCLATURE

Al	Aluminum
$\text{Al}_2(\text{SO}_4)_3$	Aluminum sulfate
B	Borum
Ca	Calcium
$\text{CaHPO}_4 \cdot 2 \text{H}_2\text{O}$	Brushite
CaCO_3	Calcite
CaCl_2	Calcium Chloride
CaO	Free lime
$\text{Ca}(\text{OH})_2$	Portlandite
$3 \text{CaO} \cdot \text{MgO} \cdot 2 \text{SiO}_2$	Merwinite
$2 \text{CaO} \cdot \text{SiO}_2$	Dicalcium silicate
CAS	Chemical abstracts service
Co	Cobalt
CO_2	Carbon dioxide
Cr	Chromium
Fe	Iron
FeO	Iron oxide
KH_2PO_4	Potassium phosphate
KOH	Potassium Hydroxide
Mg	Magnesium
MgO	Magnesium oxide
$2 \text{MgO} \cdot 2 \text{FeO} \cdot \text{SiO}_2$	Olivine
$\text{MgNH}_4 \text{PO}_4 \cdot 6 \text{H}_2\text{O}$	Struvite
$\text{MgHPO}_4 \cdot 3 \text{H}_2\text{O}$	Newberryite
Mn	Manganese
N	Nitrogen
NaOH	Sodium hydroxide
OH	Hydroxyl

P	Phosphorus
PO ₄	Phosphate
S	Sulfur
Si	Silicon
SiO ₂	Silicon dioxide
V	Vanadium
Zn	Zinc

ABSTRACT

Excessive phosphorus (P) is a threat to water quality and aquatic life, and one of the governing causes of eutrophication in water systems. It has been the object of much research that led to the implementation of P best management practices, aimed at curbing P export from agricultural and urban landscapes. However, these efforts are somewhat insufficient to mitigate and control dissolved P transport, a P pool 100% bioavailable for aquatic biota. Recent developments in nutrient management research highlight the ability of P removal structures to sequester dissolved P from flowing water, e.g., runoff and subsurface drainage, before it reaches water bodies. Phosphorus removal is accomplished through the use of reactive filter media, which are either manufactured, mined, or industrial by-products. These media, also referred to as P sorption materials (PSMs), vary in P removal ability, due to their origin, chemical and physical properties, or the conditions under which they operate. Consequently, there is a need to fully distinguish the characteristics of PSMs and their behavior in P removal structures that result in a superior P removal performance. In this study, six different types of PSMs were characterized according to their chemical and physical nature, and PSM-P interactions. To evaluate the variability of P removal capacity of steel slag, a series of flow-through experiments were conducted, using 18 different samples from different origins and generation processes. Phosphorus removal was evaluated on uncoated and aluminum(Al)-coated steel slag samples under two residence times. After chemically characterizing the samples, we found that, for the uncoated steel slags, electrical conductivity (EC), bulk density, particle density and magnesium (Mg) content could explain around 70% of the variability of P removal. Steel slags showed a high variability in their P removal ability, but such variability could be considerably decreased when coating the slags with Aluminum (Al). The Al-coating also allowed a significantly better P removal performance under shorter residence times. Flow-through experiments were also conducted to evaluate the ability to regenerate the P removal capacity of iron(Fe)- and Al-rich PSMs across two cycles of sorption-desorption with potassium hydroxide (KOH). This study found an average P recovery of 81%, 79% and 7% for Alcan, Biomax and PhosRedeem, Fe/Al-rich PSMs commercialized for contaminant removal. The most effective regeneration treatment was

characterized by the largest KOH volume (20 pore volumes) and no recirculation, with up to 100% reported P recovery, although a more economical/feasible use of 5 pore volumes of 1M KOH with recirculation was also found to perform well. The results suggested that the use of Al/Fe-dominated PSMs in P removal structures can be extended through the demonstrated regeneration technique. Iron-rich PSMs were further evaluated in regards to their behavior under anoxic conditions, a scenario that can be found in P removal structures with bottom-upward flow regimes. To evaluate the interference of redox-induced changes on P removal, PSM samples were incubated in a biogeochemical reactor in the presence of tile drainage water. Measurements of Eh throughout the incubation period indicated that PSMs, similar to soils, developed anoxic conditions. After incubation, the dissolved P concentrations in P-loaded and original PSMs were equally low, demonstrating the stability of P retention of PSMs under anoxic conditions. Additionally, the P removal ability of the original PSMs was not significantly altered by undergoing anoxic conditions, as determined from flow-through experiments following incubation. Anoxic-induced changes did not result in any limitations to the implementation of P removal structures with bottom-upward flow. These studies demonstrated the variability in P removal capacity of PSMs as a function of chemical and physical properties, the dominant P removal mechanism, and the operational characteristics of the P removal structure. The experimental data suggests that P removal structures are an effective and environmentally safe best management practice (BMP) that, in conjunction with traditional BMPs, are critical for the mitigation of dissolved P export to water systems.

1. INTRODUCTION

1.1 Rationale

Excessive dissolved phosphorus (P) has been reported in many agricultural, suburban and urban watersheds. In the U.S., the Environmental Protection Agency (EPA) estimated that 46% of the nation’s rivers and streams and 40% of the lakes are in poor conditions with regards to P [1], [2]. The agency reported that in water bodies where nitrogen (N) and P are high, biological communities are twice as likely to be in poor condition. Because P is frequently the limiting nutrient in aquatic ecosystems, excessive levels of P lead to water quality problems, such as eutrophication and harmful algal blooms. Consequently, reducing P concentrations is essential to attain satisfactory water quality. For instance, if P levels are reduced in the U.S. areas where levels are currently high, EPA predicts that 30% of the nation’s rivers and streams will improve to “good to fair” biological conditions, a recovery of 170,000 miles of impaired rivers [1]. However, traditional practices of control and mitigation of nonpoint P pollution have not been able to sustain P levels within acceptable ecological limits. These practices are focused on preventing particulate P delivery to water bodies, rather than dissolved P, which is 100% bioavailable to aquatic biota and the most challenging problem in many of the affected watersheds. Effective management of both P pools, particulate and dissolved P, is critical for attaining safe P levels in aquatic environments.

Freshwater inputs of P are primarily derived from (I) agricultural runoff and subsurface drainage, often due to P losses following fertilizer and manure applications, (II) “legacy” P losses from soils containing excessive P concentrations, and (III) discharge of wastewater treatment effluent [3]. Agriculture is often the main nonpoint P source,¹ for which several *Best management practices* (BMPs) and mitigation strategies have been developed. Still, P and N are currently the third highest reported cause of water pollution in the US; in fact, in all contiguous U.S. states, P-impaired rivers are present (Figure 1.1).

Therefore, despite continuous efforts for mitigating nonpoint P pollution in surface waters, the frequent application of fertilizers and manure-P beyond plant needs resulted - and continues to result - in P accumulation in soils [4]. Legacy-P soils inevitably lead to more

¹Depending on the watershed, horticulture, golf courses and residential lawns can also be significant nonpoint sources of P.

P being transported by runoff and subsurface drainage, constituting a long-term source of this nutrient. The effects can be seen for example in Lake Erie, where harmful algal blooms (HAB) that occur almost annually threaten drinking water supply, public health and the regional economy. In 2019, nearly 2,000 km² in the western basin of Lake Erie were covered by a potentially HAB [5]. The severity of these blooms has been rapidly progressing throughout the last two decades, with (I) springtime P losses following fertilizer and manure applications, and (II) long-term cumulative P loading as key drivers of bloom intensity [6]. Moreover, recent studies point out that eutrophication will potentially increase during the 21st century, mainly as a result of changes in precipitation patterns [7].² This scenario presents a need to develop new techniques and to improve the current conservation practices for overcoming the challenges imposed by changes in climate and increasingly intensive agriculture. Phosphorus removal structures, a technology that aims to intercept dissolved P in runoff and subsurface drainage, can help prevent and attenuate P-enrichment of water bodies. The use and behavior of *phosphorus sorption materials* (PSMs), the core component of P removal structures, are the object of this study.

1.2 State of the science on phosphorus (P) removal structures and P sorption materials

1.2.1 Definitions

Phosphorus Removal Structures

Phosphorus removal structures are a preventive and remedial measure focused on minimizing transport of dissolved P to water bodies. Upon arrival in a water body, dissolved P is essentially immediately available for algal uptake in aquatic environments [8], and because of this, BMPs targeting dissolved P are paramount to limit the emergence of eutrophic water bodies. Historically, particulate P has often been considered the most concerning P pool in regards to losses, for two main reasons: first, because particulate P is soil-bound and its transport is associated with the transport of sediments by erosion, a major transport path in agricultural soils; second, because the natural concentrations of dissolved P in soils are ex-

²The authors focus on the increase of nitrogen export due to changing patterns in precipitation; here, the same is assumed for P loading, which is also controlled by precipitation amount, frequency and intensity.

tremely low. However, because of accumulation of P in agricultural soils beyond plant needs, they become a long-term source of this nutrient for aquatic environments. In P-enriched soils, P solubility is elevated, resulting in higher concentrations in runoff [9]. Incidental losses of recently applied fertilizers and manure are also associated with higher P concentrations in runoff, including in urban watersheds [10]. An additional pathway, previously considered marginal, is P transport by subsurface drainage. Recent studies point out that subsurface transport of P can be significant in watersheds, particularly in the presence of high-P soils, low P sorption capacity, and artificial drainage [11].

Phosphorus removal structures serve as an immediate dissolved P removal strategy, that in conjunction with adequate traditional BMPs and long-term P removal strategies (e.g., phytoremediation) can prevent P losses in the short-term and long-term scenarios. Examples of P removal structures are shown in Figures 1.2 and 1.3. These structures can take many forms, such as drainage ditch filters (e.g., [12]–[14]), blind/surface inlets (e.g., [15], [16]) and bio-retention cells (e.g., [17], [18]), and are adaptable for treating agricultural, urban, and wastewater P sources. They are essentially characterized by four main properties [19]:

1. The structure contains an effective and unconsolidated PSM in a sufficient amount;
2. The structure is located in an area that receives runoff (or subsurface drainage) with high dissolved P concentrations;
3. The structure design allows the inflow water to flow through the PSM at sufficient flow rates and residence time (RT);
4. The PSM can be removed and substituted with relative ease or be regenerated when deemed appropriate.

As long as these criteria are met, P removal structures will remove variable amounts of P. Examples of cumulative P removal by P removal structures in the literature range from 0.4% [20] to 99% [21]. There are also examples of ineffective P removal structures, that due to a design flaw (e.g., poor choice of PSM, low incoming P concentrations, i.e., less than 0.2 mg P L⁻¹; [19]) do not function well. For instance, Agrawal *et al.* [22] reported a -150% cumulative P removal in a P removal structure installed in a golf course, meaning that the

chosen media contributed P to the outflow. The study illustrated the importance of an adequate design, and of choosing effective PSMs: the quantity, P sorption capacity and type of interaction between PSM and P are crucial aspects for successful P removal.

Phosphorus Sorption Materials

Phosphorus removal structures are partly designed around the PSM, specifically their P removal characteristics and physical properties that dictate flow. The necessary mass of PSM required for a given structure is a function of the PSM P removal ability, site characteristics (e.g., incoming P concentrations and flow rates), and P removal goals (desired P removal and lifetime). Choice of PSM will greatly impact the final design and cost of the structure, as this will dictate the necessary PSM mass and area of the structure. An inadequate choice of PSM can translate into overly-expensive structures or insufficient P removal.

Phosphorus sorption materials can be natural, manufactured, or industrial by-products. Examples in the literature include aluminum and iron oxides [23], iron ochre [24], limestone [25], acid mine drainage residual (AMDR) [26], steel slag [27] and waste products from oil-shale industry [28]. These media are rich in one or more of the following elements: calcium (Ca), magnesium (Mg), aluminum (Al) and iron (Fe), which are responsible for their chemical affinity to dissolved P. Phosphorus sorption materials can be classified in two categories according to the P sorption mechanism: (I) Ca/Mg-based PSMs remove P through precipitation, and (II) Al/Fe-based PSMs remove P through ligand exchange reactions. Precipitation-based reactions are dominant in alkaline environments in the presence of readily available Ca and/or Mg. Circumneutral pHs, on the other hand, favor the adsorption reaction of phosphate onto Al/Fe oxides, given the availability of positive surface sites (pH is lower than point of zero charge). The main practical difference between these mechanisms is the time of reaction: precipitation reactions are dependent on time and, therefore, on the incoming flow rates and structure design. Consequently, Al/Fe-dominated media are preferable for P removal structures that are designed to receive higher incoming flow rates through use of a smaller PSM mass and area.

The choice of PSM will greatly influence the efficacy and lifetime of the structure, since it partly determines the potential P removal. Other factors found to strongly influence the

degree of P sorption and associated mechanisms are pH, buffer capacity, ionic strength, common ion effects [29], and major elemental composition of PSMs (e.g., Ca content, as reported by Piatak *et al.* [30]).

1.3 Knowledge gaps and research needs

Several studies support the use of P removal structures as a BMP. Penn *et al.* [10] and many others have shown that they can be a valuable tool to mitigate and prevent dissolved P pollution in water systems. However, given the variability of the P removal ability of P removal structures and their use in diverse settings, there is still a need to explore the conditions under which they will operate at an optimum.

Because P removal structures can be adapted to the location settings and PSM type, there are several sources of variability in P removal, and can be divided into two main categories (assuming adequate structure design): (I) PSM-P interactions and (II) PSM intrinsic characteristics. The first category includes, for example, contact time, incoming P concentrations and direction of flow; the second category defines the mechanisms of P removal and the P sorption capacity of the media, which in turn will indicate the potential P removal by the P removal structure. More research is needed to determine which sources of variability are more influential and which ones can be modified to favor greater P removal.

1.3.1 Variability of the use of steel slags as PSMs

Designing a P removal structure requires a reasonable understanding of the chosen PSM. However, the behavior of PSMs is often oversimplified by generalizing the chemical and physical properties of the material, leading to the design of inadequate P removal structures.

Steel slag, a by-product from integrated steel mills, is a commonly used PSM [31]–[33]. Throughout the literature, its efficacy significantly varies. For instance, in a literature review, Penn *et al.* [10] found cumulative P removal by steel slag varying from -150% to 89%, which includes the treatment of wastewater and non-point drainage. Because steel slags can be generated through different processes of the steel industry, they show different chemical and physical characteristics. For instance, Navarro *et al.* [34] studied the chemical

and mineralogical composition of steel slag samples, and described slag as a crystalline heterogeneous material, composed of particle aggregates of different sizes and nature.

It is still unclear how the different nature of steel slags affects the PSMs P sorption ability. As a Ca-based PSM, it is intuitive to hypothesize that the Ca content in slag will dictate P removal. Piatak *et al.* [30] described a 50% correlation between Ca content and P removal capacity of steel slag, suggesting that a higher Ca content will result in a higher P removal. Bowden *et al.* [35] identified a positive effect of pH on P removal, while clast size showed a negative correlation. It is clear that the intrinsic characteristics of steel slags are influential on its P sorption capacity, but further investigating the most influential factors will distinguish the preferable slags to use in P removal structures.

Extrinsic characteristics can also affect the performance of steel slag as a PSM. For instance, Bowden *et al.* [35] identified a positive relationship between incoming P concentrations and P removal. Several studies identified the dependence of P removal on residence time (RT). However, the range of RT used in the literature is frequently much longer than the RTs observed in P removal structures. This is problematic because P export in many watersheds is highest during storm events [36], when discharge rate is highest. For instance, Drizo *et al.* [37] observed a greater P removal capacity of slag in experiments conducted with 24 hours in comparison to 8 hours of RT. In contrast, Penn & McGrath [27] observed 34 and 36% of cumulative P removal by slag in a P removal structure with RT = 10 minutes, a considerably lower RT. More research is needed to comparatively evaluate lower RTs and their effect on P removal.

Qin *et al.* [38] stated that Fe/Al-based PSMs should be preferred when RT is limited, as their mechanism of P removal (adsorption) occurs more quickly in comparison to Ca-based PSMs. Adding an Al-coating to the slags can aid the P sorption capacity of steel slags under lower RTs. This method was presented and tested by Penn & McGrath [27] as a rejuvenation strategy, but it requires further testing as a treatment for fresh slag before being recognized as a valuable aid to steel slags.

1.3.2 Development of a regeneration technique for Fe/Al-based PSMs

Aluminum/Iron-rich media, such as Al/Fe (hydr)oxides, zero-valent iron, Al/Fe-coated materials and drinking water treatment residuals, are a well-researched category of PSMs. In the literature, their use has been reported in wetlands, wastewater treatment, non-point drainage and groundwater treatment [23], [24], [26], [39], [40]. Aluminum-based chemicals are also popular, and have been historically used in wastewater treatment and lake restoration as a P coagulation agent [41], [42]. Both Al/Fe-based media retain dissolved P primarily through (pH-dependent) adsorption reactions, characterized as being a more rapid removal mechanism [38]. Because these are reversible reactions, once the media is P-saturated, regeneration is a possible route for recovering the P sorption ability of the PSM (without the need to replace the material), and the previously retained P.

In the literature, a few studies have proposed regeneration methodologies. Sibrell & Kehler [26] tested a regeneration treatment on granular ferric hydroxide media samples after an extensive P removal trial to remediate trout wastewater. The treatment was composed of three steps: (1) a rinse with softened tap water, (2) a rinse of 0.5% sodium hypochlorite, and (3) a recirculation of 5 bed volumes of 0.5 M sodium hydroxide (NaOH) through the PSM column for 24 hours, continuously sparging CO₂ to contain the pH increase. The treatment resulted in 45% of reactive P desorbed from the granular ferric hydroxide. The regeneration treatment was ineffective after a second sorption-desorption cycle. Allred *et al.* [39] conducted a regeneration treatment on P-saturated Fe hydroxides, using a 4 pore volume flush of a 4% by weight sodium hydroxide solution, followed by rinsing with 27 pore volumes of deionized (DI) water. The regenerated material was ineffective in a field test, although in column experiments, it was able to remove 34% of P, less than half of the P removal by the original material. Kunaschk *et al.* [43] also developed a NaOH-based regeneration, adding a prior rinse with hydrochloric acid, and a later rinse with DI water. The authors repeated the sorption-desorption cycles 8 times, observing no signs of decline in the P sorption capacity of the Fe-rich media. While these regeneration treatments have been tested with various degrees of success, there is no methodology accepted as standard

for regeneration of PSMs in P removal structures. More work is needed to propose a simple technique able to effectively recover the P sorption capacity of Al/Fe-based PSMs.

1.3.3 Behavior of PSMs under anaerobic conditions

The direction of flow within P removal structures is often downward (“top-down”), with filtered runoff or subsurface drainage exiting at the bottom of the structure through perforated pipe. This flow regime is considered a limitation for a wider adoption of P removal structures, particularly for buried confined beds that treat tile drainage, because PSM thickness is limited to the freeboard depth, resulting in larger footprints (freeboard depth is simply the depth between the outlet of a tile drain pipe and the bottom of the ditch in which it is located). Upward-flow P removal structures, with the water inlet at the bottom of the structure (“bottom-up”), are an alternative to this scenario, and can be especially advantageous where there is little freeboard, e.g., flat landscapes and shallow ditches [19]. However, using bottom-up flow creates an intrinsic complication: water will remain in the structure, submerging the media for prolonged periods of time between flow events. Such a scenario might promote anoxic conditions, which in turn, may result in redox-induced changes both in the solution and in redox-sensitive components of the PSMs. It is still unclear how PSMs behave in anoxic environments, particularly in regards to their P-sorption capacity and P retention.

There is extensive literature on soils and sediments under reduced conditions. De-Campos *et al.* [44] observed that strongly reducing conditions resulted in higher solution concentrations of redox-sensitive metals, Manganese (Mn) and Fe, and alkali and alkaline earth metals, specifically potassium (K), Ca and Mg. An increase in soluble P concentrations was also observed in high-P soils, attributed to the P dissolution associated with Fe-oxides. Similarly, the redox-induced release of P was the object of a few studies concerning the dynamics of P in wetlands [45], [46] that suggested that a low redox potential may have induced high concentrations of P. In the context of P filtration media, redox-induced P release has been observed in using steel slag in a constructed wetland, attributed to the transformation of crystalline Fe and Al minerals to amorphous forms [47]. Contrary to Drizo *et al.* [47], Pratt *et al.* [48] indicated an insignificant release of P by steel slag under low redox potential (-

400 mV) and neutral pH values ($\text{pH} = 6.7$). More research is needed to better understand if anoxic conditions will develop with Fe-rich PSMs and whether it will promote similar redox-induced changes on the media.

1.4 Dissertation focus and organization

The objective of this dissertation is to improve the understanding of the use and behavior of PSMs as a way to improve the operational ability of P removal structures. Key advances on the use of PSMs were developed through this work.

In Chapter 1 of this dissertation, a brief introduction provided the scientific background and relevance of this work to the literature of P removal practices. Chapter 2 deals with the quantification of the variability of steel slag samples and whether physical and chemical properties of the media can be used to predict their P sorption capacity. In that chapter, steel slags were evaluated in light of their generation processes, P-PSM interactions, and enhancement of P sorption capacity.

Chapter 3 presents a technology developed to regenerate P-saturated PSMs. It uses different volumes and contact times between the P-desorption solution and the P-saturated PSM to establish a feasible standard procedure to recover the P sorption capacity of P-saturated PSMs.

In Chapter 4, a different configuration of P removal structures was proposed. The novelty derives from changing the flow direction, which allows for implementation of P removal structures on shallow-ditch areas and flat landscapes with little freeboard. Different Fe-based PSMs were incubated under anaerobic conditions; P sorption capacity after incubation and P retention were evaluated. By establishing the behavior of PSMs under these conditions, the goal was to determine whether P removal structures could be effective in the presence of standing water between flow events, a consequence of inverting the flow direction.

Finally, Chapters 5 summarizes the main conclusions and key findings of this research, offering insights for future applications.

References

- [1] Office of Water and Office of Research and Development, “National rivers and streams assessment 2008-2009: A collaborative survey (epa/841/r-16/007),” U.S. Environmental Protection Agency, Tech. Rep., 2016.
- [2] Office of Water, “National lakes assessment 2012 (epa 841-r-16-11),” U.S. Environmental Protection Agency, Tech. Rep., 2016.
- [3] U.S. Geological Survey. (2020). “Phosphorus and water.” Accessed on September 20th, 2020, [Online]. Available: https://www.usgs.gov/special-topic/water-science-school/science/phosphorus-and-water?qt-science_center_objects=0#qt-science_center_objects.
- [4] A. N. Sharpley, S. Chapra, R. Wedepohl, J. Sims, T. C. Daniel, and K. Reddy, “Managing agricultural phosphorus for protection of surface waters: Issues and options,” *Journal of environmental quality*, vol. 23, no. 3, pp. 437–451, 1994.
- [5] National Centers for Coastal Ocean Science. (2019). “Lake erie harmful algal blooms 2019 retrospective: Bloom severity was 7.3, as predicted by seasonal forecast.” Accessed on September 20th, 2020, [Online]. Available: <https://coastalscience.noaa.gov/news/lake-erie-hab-2019-retrospective-bloom-severity-was-7-3-as-predicted-by-the-seasonal-forecast/>.
- [6] J. C. Ho and A. M. Michalak, “Phytoplankton blooms in lake erie impacted by both long-term and springtime phosphorus loading,” *Journal of Great Lakes Research*, vol. 43, no. 3, pp. 221–228, 2017.
- [7] E. Sinha, A. Michalak, and V. Balaji, “Eutrophication will increase during the 21st century as a result of precipitation changes,” *Science*, vol. 357, no. 6349, pp. 405–408, 2017.
- [8] A. N. Sharpley, S. Smith, O. Jones, W. Berg, and G. Coleman, “The transport of bioavailable phosphorus in agricultural runoff,” *Journal of environmental quality*, vol. 21, no. 1, pp. 30–35, 1992.
- [9] P. Vadas, P. J. Kleinman, A. Sharpley, and B. Turner, “Relating soil phosphorus to dissolved phosphorus in runoff: A single extraction coefficient for water quality modeling,” *Journal of Environmental Quality*, vol. 34, no. 2, pp. 572–580, 2005.
- [10] C. Penn, I. Chagas, A. Klimeski, and G. Lyngsie, “A review of phosphorus removal structures: How to assess and compare their performance,” *Water*, vol. 9, no. 8, p. 583, 2017.

- [11] K. W. King, M. R. Williams, M. L. Macrae, N. R. Fausey, J. Frankenberger, D. R. Smith, P. J. Kleinman, and L. C. Brown, "Phosphorus transport in agricultural sub-surface drainage: A review," *Journal of environmental quality*, vol. 44, no. 2, pp. 467–485, 2015.
- [12] C. Penn, J. Bowen, J. McGrath, R. Nairn, G. Fox, G. Brown, S. Wilson, and C. Gill, "Evaluation of a universal flow-through model for predicting and designing phosphorus removal structures," *Chemosphere*, vol. 151, pp. 345–355, 2016.
- [13] R. B. Bryant, A. R. Buda, P. J. Kleinman, C. D. Church, L. S. Saporito, G. J. Folmar, S. Bose, and A. L. Allen, "Using flue gas desulfurization gypsum to remove dissolved phosphorus from agricultural drainage waters," *Journal of Environmental Quality*, vol. 41, no. 3, pp. 664–671, 2012.
- [14] V. S. Shedekar, C. J. Penn, L. Pease, K. W. King, M. M. Kalcic, and S. J. Livingston, "Performance of a ditch-style phosphorus removal structure for treating agricultural drainage water with aluminum-treated steel slag," *Water*, vol. 12, no. 8, p. 2149, 2020.
- [15] J. M. Gonzalez, C. J. Penn, and S. J. Livingston, "Utilization of steel slag in blind inlets for dissolved phosphorus removal," *Water*, vol. 12, no. 6, p. 1593, 2020.
- [16] C. Penn, J. Gonzalez, M. Williams, D. Smith, and S. Livingston, "The past, present, and future of blind inlets as a surface water best management practice," *Critical Reviews in Environmental Science and Technology*, vol. 50, no. 7, pp. 743–768, 2020.
- [17] W. Zhang, G. O. Brown, D. E. Storm, and H. Zhang, "Fly-ash-amended sand as filter media in bioretention cells to improve phosphorus removal," *Water Environment Research*, vol. 80, no. 6, pp. 507–516, 2008.
- [18] G. H. LeFevre, K. H. Paus, P. Natarajan, J. S. Gulliver, P. J. Novak, and R. M. Hozalski, "Review of dissolved pollutants in urban storm water and their removal and fate in bioretention cells," *Journal of Environmental Engineering*, vol. 141, no. 1, p. 04014050, 2015.
- [19] C. J. Penn and J. M. Bowen, *Design and construction of phosphorus removal structures for improving water quality*. Springer, 2017.
- [20] H. Pant, K. Reddy, and E. Lemon, "Phosphorus retention capacity of root bed media of sub-surface flow constructed wetlands," *Ecological Engineering*, vol. 17, no. 4, pp. 345–355, 2001.
- [21] C. J. Penn, R. B. Bryant, P. J. Kleinman, and A. L. Allen, "Removing dissolved phosphorus from drainage ditch water with phosphorus sorbing materials," *Journal of Soil and Water Conservation*, vol. 62, no. 4, pp. 269–276, 2007.

- [22] S. G. Agrawal, K. W. King, J. F. Moore, P. Levison, and J. McDonald, "Use of industrial byproducts to filter phosphorus and pesticides in golf green drainage water," *Journal of environmental quality*, vol. 40, no. 4, pp. 1273–1280, 2011.
- [23] R. Wood and C. McAtamney, "Constructed wetlands for waste water treatment: The use of laterite in the bed medium in phosphorus and heavy metal removal," *Hydrobiologia*, vol. 340, no. 1-3, pp. 323–331, 1996.
- [24] K. Dobbie, K. Heal, J. Aumonier, K. Smith, A. Johnston, and P. Younger, "Evaluation of iron ochre from mine drainage treatment for removal of phosphorus from wastewater," *Chemosphere*, vol. 75, no. 6, pp. 795–800, 2009.
- [25] C. M. Hill, J. Duxbury, L. Geohring, and T. Peck, "Designing constructed wetlands to remove phosphorus from barnyard runoff: A comparison of four alternative substrates," *Journal of Environmental Science & Health Part A*, vol. 35, no. 8, pp. 1357–1375, 2000.
- [26] P. L. Sibrell and T. Kehler, "Phosphorus removal from aquaculture effluents at the northeast fishery center in lamar, pennsylvania using iron oxide sorption media," *Aquacultural Engineering*, vol. 72, pp. 45–52, 2016.
- [27] C. J. Penn and J. M. McGrath, "Predicting phosphorus sorption onto steel slag using a flow-through approach with application to a pilot scale system," *Journal of Water Resource and Protection*, vol. 3, no. 4, p. 235, 2011.
- [28] C. Vohla, E. Poldvere, A. Noorvee, V. Kuusemets, and Ü. MANDER, "Alternative filter media for phosphorous removal in a horizontal subsurface flow constructed wetland," *Journal of Environmental Science and Health*, vol. 40, no. 6-7, pp. 1251–1264, 2005.
- [29] C. Penn, R. B. Bryant, M. Callahan, and J. McGrath, "Use of industrial by-products to sorb and retain phosphorus," *Communications in Soil Science and Plant Analysis*, vol. 42, no. 6, pp. 633–644, 2011.
- [30] N. M. Piatak, R. R. Seal, D. A. Hoppe, C. J. Green, and P. M. Buszka, "Geochemical characterization of iron and steel slag and its potential to remove phosphate and neutralize acid," *Minerals*, vol. 9, no. 8, p. 468, 2019.
- [31] C. Penn, J. McGrath, J. Bowen, and S. Wilson, "Phosphorus removal structures: A management option for legacy phosphorus," *Journal of Soil and Water Conservation*, vol. 69, no. 2, 51A–56A, 2014.
- [32] C. Barca, S. Troesch, D. Meyer, P. Drissen, Y. Andres, and F. Chazarenc, "Steel slag filters to upgrade phosphorus removal in constructed wetlands: Two years of field experiments," *Environmental science & technology*, vol. 47, no. 1, pp. 549–556, 2013.

- [33] S. C. Bird and A. Drizo, “Eaf steel slag filters for phosphorus removal from milk parlor effluent: The effects of solids loading, alternate feeding regimes and in-series design,” *Water*, vol. 2, no. 3, pp. 484–499, 2010.
- [34] C. Navarro, M. Díaz, and M. A. Villa-García, “Physico-chemical characterization of steel slag. study of its behavior under simulated environmental conditions,” *Environmental science & technology*, vol. 44, no. 14, pp. 5383–5388, 2010.
- [35] L. I. Bowden, A. P. Jarvis, P. L. Younger, and K. L. Johnson, “Phosphorus removal from waste waters using basic oxygen steel slag,” *Environmental science & technology*, vol. 43, no. 7, pp. 2476–2481, 2009.
- [36] A. N. Sharpley, P. J. Kleinman, A. L. Heathwaite, W. J. Gburek, G. J. Folmar, and J. P. Schmidt, “Phosphorus loss from an agricultural watershed as a function of storm size,” *Journal of Environmental Quality*, vol. 37, no. 2, pp. 362–368, 2008.
- [37] A. Drizo, C. Forget, R. P. Chapuis, and Y. Comeau, “Phosphorus removal by electric arc furnace steel slag and serpentinite,” *Water research*, vol. 40, no. 8, pp. 1547–1554, 2006.
- [38] Z. Qin, A. L. Shober, K. G. Sheckel, C. J. Penn, and K. C. Turner, “Mechanisms of phosphorus removal by phosphorus sorbing materials,” *Journal of environmental quality*, vol. 47, no. 5, pp. 1232–1241, 2018.
- [39] B. J. Allred, L. R. Martinez, and D. L. Gamble, “Phosphate removal from agricultural drainage water using an iron oxyhydroxide filter material,” *Water, Air, & Soil Pollution*, vol. 228, no. 7, p. 240, 2017.
- [40] T. D. McCobb, D. R. LeBlanc, and A. J. Massey, “Monitoring the removal of phosphate from ground water discharging through a pond-bottom permeable reactive barrier,” *Groundwater Monitoring & Remediation*, vol. 29, no. 2, pp. 43–55, 2009.
- [41] I. de Vicente, H. S. Jensen, and F. Ø. Andersen, “Factors affecting phosphate adsorption to aluminum in lake water: Implications for lake restoration,” *Science of the total environment*, vol. 389, no. 1, pp. 29–36, 2008.
- [42] E. Galarneau and R. Gehr, “Phosphorus removal from wastewaters: Experimental and theoretical support for alternative mechanisms,” *Water Research*, vol. 31, no. 2, pp. 328–338, 1997.
- [43] M. Kunaschk, V. Schmalz, N. Dietrich, T. Dittmar, and E. Worch, “Novel regeneration method for phosphate loaded granular ferric (hydr) oxide—a contribution to phosphorus recycling,” *Water research*, vol. 71, pp. 219–226, 2015.

- [44] A. B. De-Campos, C.-h. Huang, and C. T. Johnston, “Biogeochemistry of terrestrial soils as influenced by short-term flooding,” *Biogeochemistry*, vol. 111, no. 1-3, pp. 239–252, 2012.
- [45] C. Vohla, R. Alas, K. Nurk, S. Baatz, and Ü. Mander, “Dynamics of phosphorus, nitrogen and carbon removal in a horizontal subsurface flow constructed wetland,” *Science of the Total Environment*, vol. 380, no. 1, pp. 66–74, 2007.
- [46] K. M. Johannesson, J. L. Andersson, and K. S. Tonderski, “Efficiency of a constructed wetland for retention of sediment-associated phosphorus,” *Hydrobiologia*, vol. 674, no. 1, pp. 179–190, 2011.
- [47] A. Drizo, Y. Comeau, C. Forget, and R. P. Chapuis, “Phosphorus saturation potential: A parameter for estimating the longevity of constructed wetland systems,” *Environmental science & technology*, vol. 36, no. 21, pp. 4642–4648, 2002.
- [48] C. Pratt, A. Shilton, S. Pratt, R. G. Haverkamp, and I. Elmetri, “Effects of redox potential and pH changes on phosphorus retention by melter slag filters treating wastewater,” *Environmental science & technology*, vol. 41, no. 18, pp. 6585–6590, 2007.

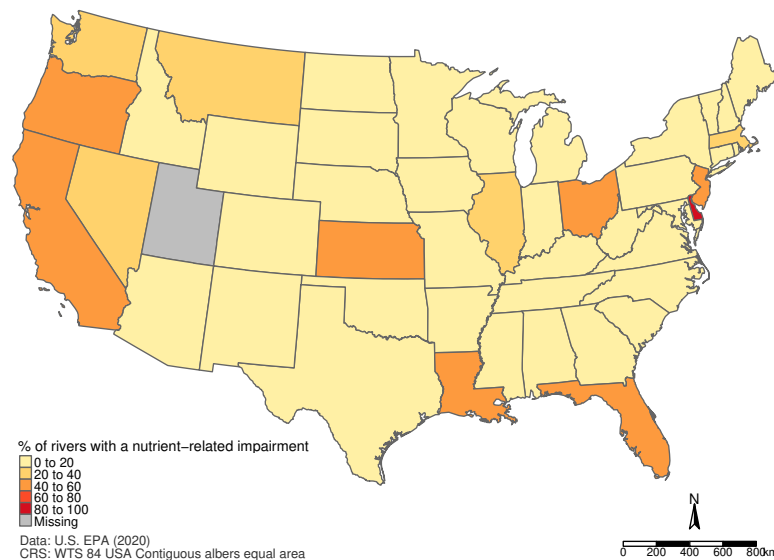


Figure 1.1. Percentage of river miles with a nutrient-related impairment in the U.S. Darker shades represent a greater impairment of rivers.



Figure 1.2. Example of a ditch P removal structure.



Figure 1.3. Example of a confined bed P removal structure. Downward flow.

2. ESTIMATING THE VARIABILITY OF STEEL SLAG PROPERTIES AND THEIR INFLUENCE IN PHOSPHORUS REMOVAL ABILITY

2.1 Abstract

Steel slag has been proven to be an effective phosphorus (P) removal media, and a potential aid to mitigate point and nonpoint P pollution in freshwater systems. However, the behavior of steel slag as a P sorption material (PSM) is often oversimplified through the generalization of its chemical and physical properties, preventing proper design of P removal structures. In this work, we tested eighteen steel slag samples from different batches, production processes, and steel-making plants, for the purpose of relating slag origin and chemical and physical properties to P removal ability, under two different flow regimes. Slag samples were also coated with aluminum (Al) and tested for P removal. Characterization included elemental composition, particle density, buffer capacity, and P removal ability. There was great variability in the evaluated properties across slag sources and origin, compelling the individual characterization of steel slag samples, since their intrinsic characteristics were key variables in determining their potential P removal capacity. Specifically, electrical conductivity (EC), bulk density, particle density and magnesium (Mg) content could explain around 70% of the variability of P removal by uncoated steel slags. Increasing residence time (RT) always increased P removal for uncoated slags. Steel slags showed a high variability in their P removal ability, but such variability was considerably decreased by coating the slags with Al. Additionally, the Al-coating process significantly improved P removal performance under more rapid flows (lower RT).

2.2 Introduction

Phosphorus (P) is a ubiquitous element in natural waters. It participates in the life cycle of aquatic organisms, and plays a vital role in both aquatic and terrestrial ecosystems [1]. However, excessive amounts of P, mainly derived from human activities, have been shown to be a key driver of eutrophication in freshwater systems, especially dissolved P (DP) or

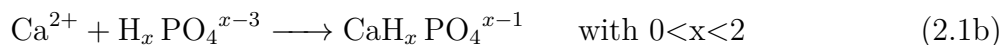
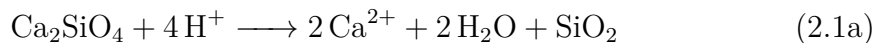
soluble reactive P (SRP), which is 100% bioavailable to aquatic biota [2]. Lake Erie is an example of a freshwater body with consistently high loadings of P, particularly from nonpoint sources [3]. As a result of increasing inputs of DP, more frequent and intense algal blooms have been occurring in the lake, despite the continuous efforts for reducing internal and external P loads [4]. In order to reduce or eliminate harmful algal blooms, the Ohio Task Force recommended an average loading reduction of 41% of DP for Lake Erie [5]. The use of steel slag in P removal structures can be a valuable aid to achieve this target.

Steel slag is an effective P sorption material (PSM) and has been proven useful in P removal structures, intercepting surface and subsurface P-rich waters. However, the P sorption ability of steel slags varies considerably, with an extensive range of P removal described in the literature [6]. This paper investigates the possible sources of this variability and whether the P removal ability of steel slags can be associated with the inherent characteristics of the media. More specifically, this work addresses the question: is P removal capacity of steel slag significantly impacted by its inherent chemical and physical properties, source, and production process?

Steel slag is a by-product from integrated steel mills, originating from (I) the conversion of iron to steel in basic oxygen furnace (BOF), (II) the melting of scrap to make steel in an electric arc furnace (EAF), or (III) the further refinement of the metal in the ladle [7]. Despite these being different processes of the steel industry, most steel slags are composed primarily of the following mineral phases: merwinite ($3\text{CaO} \cdot \text{MgO} \cdot 2\text{SiO}_2$), olivine ($2\text{MgO} \cdot 2\text{FeO} \cdot \text{SiO}_2$), dicalcium silicate ($2\text{CaO} \cdot \text{SiO}_2$), calcite (CaCO_3), portlandite ($\text{Ca}(\text{OH})_2$), CaO (free lime), MgO, SiO_2 and FeO [8]. The properties and proportion of these minerals vary, as well as the presence of other minor components depending on the facility, raw materials, type of steel, and furnace conditions [7].

The primary use of steel slag in the United States is as aggregate in civil engineering applications, including road construction; excess steel slag is usually sent to landfills for disposal [9]. Recently, there has been an increasing interest for using steel slag in other applications, particularly in water and wastewater treatment, due to their low cost and wide availability. Because of the predominance of Ca minerals, steel slag is able to remove DP

from surface and subsurface flows through a dissolution followed by a precipitation reaction, as illustrated in reactions 2.1a and 2.1b:



Given the dependence of the precipitation reaction (and, therefore, of P removal) on readily available soluble Ca, one possible approach to assess and predict the P removal ability of a steel slag sample is to investigate the impact of Ca content on P removal. Piatak *et al.* [10] observed a positive (linear) correlation between total Ca content and P removal capacity of steel slag ($R^2 = 0.5$; 12 samples), and argued that Ca content can be used to provide an initial assessment of usable slag materials. Similarly, Zuo *et al.* [11] attributed a higher P removal by steel slag to the dissolution of dicalcium silicate, suggesting that the presence of this mineral may indicate a superior P removal ability.

Navarro *et al.* [12] reported a significant heterogeneity of the chemical and physical nature of steel slag samples, which suggests that other variables may also interfere with P sorption capacity. Bowden *et al.* [13] found a positive correlation between P removal and equilibrium pH, as well as between P removal and initial P concentration, a recognized characteristic of precipitation reactions. A negative correlation was reported between P removal and clast size, i.e., the finest size fraction has an increased reactivity and higher P removal. Although this finding may imply that finer fractions should be preferred, their use in P removal structures can be problematic, as it interferes with the hydraulic conductivity and the longevity of the structure, due to clogging [6].

These works show that not only do chemical and physical properties of steel slag impact its P removal ability, but also the nature of the interactions between P and the media, e.g., input P concentrations and residence time. Drizo *et al.* [14] observed a significant effect of residence time on P removal by comparing two experiments conducted at 24 hours and 8 hours of residence time. The authors discussed that the longer residence time resulted in a greater P removal capacity, indicating that interaction time between slag and P have a

significant effect on P removal. This finding suggests that longer residence times should be preferred. However, these aforementioned residence times are rarely feasible in field-scale P removal structures, as they operate under much shorter residence times, especially during heavy storm events [15]–[19]. In this paper, we evaluated the effect of residence times on P removal by steel slag, simulating conditions normally found in P removal structures.

For steel slag samples that show an insufficient P removal, we proposed an Aluminum (Al) coating treatment. The ability of Al-coating to enhance P removal is due to adsorption reactions in which the phosphate ion replaces hydroxyl ions (OH^-) on the surfaces of the Al-(hydr)oxides. Essentially, the Al treatment aims to create a new path for P removal by the addition of terminal hydroxide groups. Specifically for slag, Al-coating and its impacts on P sorption has not yet been amply investigated. Penn & McGrath [20] used Al-coating as a rejuvenation strategy, treating the media after its sorption capacity was saturated. The authors observed a cumulative removal of 59 and 54 $\text{mg}\cdot\text{P}\cdot\text{kg}^{-1}\cdot\text{slag}$ for original and rejuvenated slag, respectively. In this work, we use Al-coating treatment not as a rejuvenation strategy, but rather as an enhancement methodology, aiding sorption capacity to poorer slags. There are examples of this approach in the literature. For instance, Shedekar *et al.* [17] constructed a field-scale P removal structure using Al-coated slag for treating tile drainage. Similarly, Penn *et al.* [16] reported a 58% cumulative P removal ($54\text{ mg P} \cdot \text{kg}^{-1}\text{ PSM}$) in a surface bed structure that treated runoff from around poultry barns, using Al-coated slag. In a study using solid-state spectroscopy on several spent PSMs, Qin *et al.* [21] discovered that P-saturated Al-coated slag contained both Al- and Ca-related P, illustrating the efficacy of the Al-coating technique. Arias *et al.* [22] identified that the flow rate used in wastewater column experiments with Al-coated quartz particles had negligible effect on the removal efficiency. This is an advantage of Al- and Fe-based removal in comparison to Ca-based removal, e.g., in uncoated slags. Due to the intrinsic differences in the removal mechanisms, Ca-rich media is more dependent on residence time in comparison to Al- or Fe-rich materials. Coating slags may minimize this limitation, allowing their use in P removal structures that operate predominantly under lower residence times.

An additional aspect of steel slag investigated in this paper pertains to environmental safety. Steel slag is not considered a hazardous material and its excess has been disposed in

landfill sites for long periods of time [10], [12]. Nevertheless, because it is a by-product, there may be risks associated with its use in environmental settings due to the presence of minor metal constituents, such as Chromium (Cr). Because of that, there has been interest in studying the environmental suitability of steel slag. For instance, Piatak *et al.* [10] identified Al, Cr and Mn exceeding water quality guidelines in a leaching procedure mimicking leaching of contaminants from weathering. In terms of elemental composition, the authors reported that Cr and Mn barely exceeded soil guidelines. Navarro *et al.* [12] studied the leaching of toxic trace elements during exposure of slags to dry and wet air currents and carbonated water. The authors reported that leaching levels from Cr and vanadium (V) were not significant and would not lead to a significant environmental impact. After washing ground samples of steel slag with DI water, the authors established that the chemical composition of the washed samples (as determined by X-ray fluorescence spectroscopy) was unaltered in comparison to the raw samples, indicating that no significant dissolution of major or minor constituents occurred. Bowden *et al.* [13] conducted both leaching and desorption tests, after using steel slag samples in continuous flow columns and no potentially toxic elements were released, indicating that slags can be used as a long-term removal mechanism for P. Penn *et al.* [19] reported that trace metals were identified in the slag used in a P removal structure, however, concentrations in the effluent were below detection limits. Hedström *et al.* [23], to the contrary, identified leakage of sulfuric compounds in a pilot-scale blast furnace slag filter, with concentrations reaching 1200 mg L⁻¹ of sulfur (S) initially, and stabilizing after two weeks of operation to 80-150 mg·S L⁻¹.

The objectives of this study were to determine (I) the P sorption ability and environmental suitability of steel slag produced from different processes and sources; (II) the impacts of RT and Al-coating on P removal, and (III) if observed differences in P removal (if any) could be explained by the slag chemical and physical properties and their origin.

2.3 Material and methods

Eighteen steel slag samples were obtained from Edw. C. Levy Co. (Dearborn, MI), from three different steel-making plants and five different slag-making processes. Table 2.1

describes the samples and their specific origins. All samples were produced in integrated steel mills and were collected at the plants from stockpiles in 20-L buckets.

A few aspects of the materials are worth mentioning. First, regarding the material type. Head pulley and overband magnets separate the remaining metal portions from the slag and therefore, these samples are expected to have a lower iron (Fe) content. Kish is the denomination of a slag resulting from the process of iron desulfurization of steel and is expected to contain higher concentrations of sulfur in their composition. The “iron metallics” denomination refers to samples that were segregated using magnets and, therefore, are expected to contain higher Fe concentrations. Basic oxygen furnace (BOF) slags are the residue of the basic-oxygen-furnace process of steelmaking [8]. They are the final product of blowing oxygen into a furnace containing steel scrap and molten iron. Intense oxidation reactions occur, removing the impurities of the charge. Lime or dolomite is then charged into the furnace with fluxing agents, and combine with the impurities, forming slag. The separation process is density-based as slag floats on top of the molten steel [8]. Second, regarding the particle size range. The slag samples were screened twice: first, to select the particle sizes using a mechanical shaker, and second, to exclude fine particles. The category “fines” is defined by the American Society for Testing and Materials (ASTM) as containing particle sizes less than 4.76 mm.

The experimental characterization of the samples was completed in two main phases: (I) quantification of physical and chemical characteristics of steel slag samples and (II) estimation of the P removal capacity of the PSMs under various flow-through conditions. Prior to these analyses, we produced Al-coated steel slag samples by coating each of the original samples with two concentrations of aluminum sulfate ($\text{Al}_2(\text{SO}_4)_3$) solutions as described in Penn & McGrath [20]: 95 g L^{-1} (100% coating solution) and 66.5 g L^{-1} (70% coating solution). Slag samples were immersed for 48 hours in the coating solutions. The supernatant was then collected and pH was measured. All chemical and physical analyses were then conducted on uncoated, 70% Al-coated and 100% Al-coated slags.

2.3.1 Analysis of steel slags: chemical and physical characterization

Phase I of steel slag characterization consisted of several techniques, all of which are described in Table 2.2, together with the specific instruments used in each analysis, and are further detailed below. All analyses were conducted in duplicate, unless noted otherwise.

For measurements of both pH and EC, a 1:5 solid to deionized (DI) water ratio was used. The samples were shaken for 1 minute and equilibrated for 20 minutes. Regarding buffer capacity, uncoated samples were prepared by adding 2 g of PSM to 200 mL of DI water and shaking for 5 minutes. The samples were then centrifuged for 10 min at 5000 rpm. An aliquot of 40 mL was titrated (MetroHM 906 Titrando) to pH 6 using 0.01 M or 0.1 M HCl; pH buffer index was calculated as follows:

$$\text{Buffer Index} = \frac{TC \times V \times 5}{m} \quad (2.2)$$

where TC is the titrant concentration (mg L^{-1}), V is the volume of titrant (mL) and m is the mass of the PSM in grams. The multiplier of five is to account for the aliquot volume (i.e., $\frac{1}{5}^{th}$ of the original extraction volume).

The EPA 3050-B methodology was used for total elemental analysis [24]. In total, 18 elements were analyzed, including Ca, Mg, Al, Fe, K, Mn, B, Si, P, Na, Mn, S, Zn and heavy metals (Cr, Co, Ni and Pb). Ammonium oxalate extractions were conducted according to Penn & Bowen [25]. Digestion and extraction solutions were analyzed in an inductively coupled plasma - optical emission spectrometry (ICP-OES). A check soil sample was included in each set of samples in all experimental methods as well as a blank. The analysis of the micro-components and potential pollutants was used to evaluate the environmental safety of steel slags. To this end, we also analyzed randomly selected flow-through samples on the ICP-OES (n=22 samples).

2.3.2 Analysis of steel slags: P removal ability

For the second phase of slags characterization, flow-through sorption experiments were used to estimate the P sorption capacity of samples. A summary of this technique is further detailed in Penn & Bowen [25]. This is a dynamic sorption experiment, in which a continuous

flow of a P-rich solution (0.5 mg L^{-1}) passes through a cell containing a known mass of PSM. By collecting samples at predetermined sampling intervals and analyzing for dissolved P concentrations, the total amount of P removal is determined. Each experiment was conducted for 4 to 20 hours, aiming to reach a target of 40% of cumulative P removal, corresponding to the 40% P removal goal established by the Great Lakes Water Quality Agreement [26].

Steel slags were tested in duplicates in the flow-through system with constant input phosphorus (P) concentrations of 0.5 mg L^{-1} . For the uncoated slags, we tested two residence times (RTs): 0.284 min and 9.85 min, representing a typical range for field-scale P removal structures [17]–[19]. The duration of the experiments depended on the residence time used, with the longer duration (20 h) used for the lower RT. For the Al-coated samples, we conducted all flow-through experiments with $\text{RT}=0.284 \text{ min}$, as the phosphorus removal mechanism by Al is less dependent on RT [20], [27]. The specific parameters tested and their respective levels are detailed in Table 2.3.

2.3.3 Data analysis: effects of the variability of steel slag samples on P removal ability

Phosphorus removal under flow-through conditions was normalized based on PSM mass and expressed as the cumulative mass of P removed ($\text{mg}\cdot\text{P kg}^{-1}\cdot\text{slag}$) as a function of cumulative P added ($\text{mg}\cdot\text{P kg}^{-1}\cdot\text{slag}$). Figure 2.1 shows an example of the data produced during these experiments (Slag 12, uncoated, $\text{RT} = 0.28 \text{ min}$). Figure 2.1 also illustrates the response variable used to compare the different materials and conditions: percentage cumulative removal corresponding to the addition of $60 \text{ mg}\cdot\text{P kg}^{-1}\cdot\text{media}$ (indicated by the vertical line). This value was chosen because it is the maximum amount of P added for which all slags had observed data. A significance level (α) of 0.05 was employed for all tests in this study.

To investigate the impact of residence time on P removal, we compared the data obtained in 72 flow-through experiments among uncoated slag samples: 36 experiments conducted with residence time (RT) of 0.28 minutes and 36 with RT of 9.85 minutes. All experiments were conducted in duplicates (except for slag 17, for which there were three observations. The results of two replicates were averaged to maintain a balanced design). A two-sample

non-parametric test, the Wilcoxon rank-sum test (due to the lack of normality of the dataset, as shown in Figure B.1), was used to test the null hypothesis that modifying the RT did not result in a different P removal. The Wilcoxon rank-sum test tests whether one group tends to produce larger observations than the second group, more specifically, the null hypothesis is that the datasets come from continuous distributions with equal medians. The non-normal distribution of the data was confirmed by a Kolmogorov-Smirnoff test ($n=18$; low RT: $p\text{-value} = 2.96 \times 10^{-11}$, $KS = 0.82$; high RT: $p\text{-value} = 2.13 \times 10^{-16}$, $KS = 1$). Prior to conducting the nonparametric test, the datasets were transformed using Box-Cox transformation to evaluate whether a power transformation could approximate the data to a normal distribution. However, the transformation was unsuccessful for normalizing the data and we proceeded with the non-parametric option. The failure of the power transformation was attributed to the heavy-tails of the data distribution.

Then, we analyzed whether the Al-coating procedure was effective in enhancing the P removal ability of steel slags under low RT (RT=0.28 min). The hypothesis was that the Al-coating would reduce the dependence of P removal on RT, and thus allow for acceptable P removal under short RT. In order to analyze whether this hypothesis was supported by observational data, an analysis of variance (ANOVA) was conducted, considering two experimental factors: coating level and slag sample. The experimental design was factorial, with replicates for all combinations of treatments. The statistical model is described below:

$$y_{ij} = \mu + \tau_i + \beta_j + (\tau\beta)_{ij} + \epsilon_{ijk} \quad (2.3)$$

where the response y_{ij} is the cumulative P removal (%) observed when 60 mg·P kg⁻¹·slag were added to the PSM; μ is the grand mean, τ_i is the i th effect of coating treatment ($i=0, 70$ and 100), β_j is the j th effect of slag sample ($j=1, 2, \dots, 12$)¹ and ϵ_{ijk} is the error, assumed to be independent and normally distributed - $N(0, \sigma^2)$. There are two replicates per treatment, resulting in a balanced design, with equal number of samples per treatment. The null hypothesis stated that all treatments were equal. Because 2 factors (coating level and slag sample) together defined a treatment, it was necessary to first evaluate whether the

¹Slags 13 to 18 are not being considered in this analysis because there were no observations for coating level 100% for those slags.

interaction between the factors was significant. A Tukey’s test for non-additivity, with null hypothesis that the interaction term coefficient is 0 ($H_0: \tau\beta_{ij} = \gamma = 0$) confirmed that the interaction term was significant ($p\text{-value} < 0.0001$; $F = 24.80$, $df=1$). Based on that finding, the complete ANOVA model was conducted, checking for normality, independence and constant variance of residuals, and did find an issue of heteroscedasticity. For normality, we plotted the probability plot of the residuals and conducted the Anderson-Darling goodness-of-fit test for normal distribution (fail to reject H_0 of normal distribution with $p\text{-value}>0.25$). For constant variance, the residuals were plotted against each factor and a decreasing pattern was found when observing the coating levels 0, 70 and 100. The Bartlett’s test confirmed the inconstant variance of the residuals according to the coating levels (Bartlett’s statistic = 18.39, $df = 2$, $p\text{-value} = 0.0001$). Figure B.2 in the appendix shows the residuals distribution according to the coating level before and after the Box-Cox transformation. Because this is a balanced design, it is expected that the F-test is only slightly affected by the heteroscedasticity violation [28]. Nevertheless, we performed a Box-Cox transformation (after subtracting the minimum observation from all values and adding 1, accounting for the negative observations) and conducted an ANOVA using the transformed data. The Box-Cox power (λ) identified in this procedure was 1.4915. The transformation did result in significant change, as confirmed by the Bartlett’s test (Bartlett’s statistic = 2.69, $df = 2$, $p\text{-value} = 0.2638$).

Finally, since there was remarkable variability on the cumulative removal of P among the different samples of steel slag, we investigated whether we could explain the sources of this variability. For this analysis, a multiple linear regression (MLR) was used, with the goal to explain as much variation observed in P removal as possible (i.e., the response variable y). This analysis was conducted separately for uncoated (using the data produced under $RT=9.85$ minutes only; $n=18$ datapoints) and coated slags ($n=30$, with 12 100% Al-coated samples and 18 70% Al-coated samples), because we understood that different variables would be more influential in each case (e.g., we hypothesized that Al content would be more influential on the P removal by coated slags than by uncoated slags). The predictors for the multiple linear regression (i.e., independent variables x ’s) were defined based on the relationship between the residuals of a simple linear regression between P removal and one of the variables of interest, and each of the other variables, examining whether the residuals

showed a pattern as a function of these variables. The simple linear regression (SLR) model can be denoted as:

$$y = \beta_0 + \beta_1 x_1 + \varepsilon_i \quad (2.4)$$

where β_0 is the intercept and β_1 is the slope coefficient for the explanatory variable. ε_i is the error term, assumed to be independent with $\varepsilon_i \sim N(0, \sigma^2)$. For the SLR model, we used EC as the dependent variable for both coated and uncoated analysis. After defining the variables to include in the MLR model (variables are specified in sections 2.4.4 and 2.4.5), we determined whether any of them were closely related to one or more of the others. There was significant evidence of multicollinearity in both MLR models (coated and uncoated slags) and ridge regression was used to account for that issue. Ridge regression is a machine learning application that drops the requirement of unbiased β_i 's, making the variance of the coefficients smaller, with a penalizing increase on the residual sum of squares. We first confirmed the presence of multicollinearity using the variance inflation factor (VIF) for each term in the model and then conducted the ridge regression analysis for obtaining a more reliable estimation of the regression coefficients and potentially a better prediction accuracy.

2.4 Results and Discussion

2.4.1 Analyses of P sorption ability of steel slags in flow-through experiments

Figure 2.2 shows the cumulative P removal observed in each of the flow-through experiments (n=133), including all coated and uncoated samples. There is a remarkable heterogeneity on the behavior of steel slag. Cumulative P removal (after 60 mg·P kg⁻¹·slag was added) varied from -55 to 100%. This variability agrees with the wide range of P removal ability reported by Penn *et al.* [6], with reference to several works in the literature. Still, Figure 2.2 shows a distinct grouping of the two Al-coated groups, with 100% coated slags visually appearing to remove more P than the 70% coated slag samples. The uncoated steel slags, on the other hand, appear more random.

Figure 2.3 offers insights about some of the possible causes of this variability, based on a subset of the selected variables being investigated in this work. For instance, it is clear that

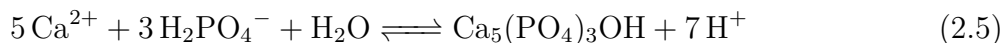
coating had an impact on the variability of P removal, and that the effect of residence time on P removal may be significant.

In the next section, the causes for P removal variability were investigated by first examining the effect of RT on P removal. Then, the P removal performances of coated and uncoated steel slag samples under low RT were compared. Finally, we investigated whether the selected variables (chemical and physical properties of steel slag samples) could explain the variability of P removal. If so, the expectation was that we could use the developed model as an assessment of the potential P removal for new slag samples.

Impact of residence time on P removal by uncoated steel slags

For analyzing the effect of residence time on P removal, the null hypothesis (H_0) that modifying RT did not improve the (mean) P removal response was tested. Under the assumption that H_0 is true, if RT is changed from 0.284 min to 9.85 minutes, no change in P removal would occur. For the same slag sample, the difference in P removal under 0.284 minutes and 9.85 minutes ranged from 8% and 86%, indicating a higher efficiency of the longer RT. To confirm the impact of the longer RT, we performed a Wilcoxon rank-sum test, a nonparametric test.² The null hypothesis of equal medians ($n=18$; $p\text{-value} = 1.039 \times 10^{-5}$, $Z_{rs} = 4.408$) was rejected, meaning that the experiments conducted with $RT = 9.85$ min showed a superior P removal performance in comparison to the $RT = 0.284$ min. The conclusion is that RT has a significant impact on P removal by steel slag, and because of that, the PSM will potentially remove more P in structures that are designed for allowing a longer contact time between the slag and the incoming high-P flow.

This result is supported by the chemistry of precipitation reactions. Claveau-Mallet *et al.* [29] discusses that hydroxyapatite ($\text{Ca}_5(\text{PO}_4)_3\text{OH}$) is the main phosphate phase precipitated in slag filters. Then, we can represent the precipitation of calcium phosphate as follows:



²The histograms for the original and transformed distributions are shown in Figure B.3. The normal probability plots and Kolmogorov-Smirnoff test indicated that both original and transformed data were non-normal.

Precipitation of ionic crystals from solution can be characterized by a general pattern in which a period of very slow precipitation (i.e., induction period) is followed by a rapid removal, and then by another slow period as the reactant concentration decreases towards an equilibrium level (i.e., crystal growth period) [30]. The induction period is the period of nucleation of calcium phosphate and is time-dependent, and the primary reason why RT has a significant effect on P removal.

The dependence of P removal on RT is supported by the existing literature [14], [29], [31], [32]. For instance, Claveau-Mallet *et al.* [29] investigated P removal by electric arc furnace (EAF) slag in columns tests, testing 3 levels of RT: 16.3 h, 3.8 h and 1.5 h. They reported a better performance of the filter under longer RTs, and attributed the dependence on RT to the rate of dissolution of slag minerals and to the crystal accumulation and organization. They argued that a low inflow velocity (and, therefore, a longer RT in the column) allows phosphorus to completely precipitate over short distances, favoring a more compact crystal organization. However, if the flow rate is too low, it will result in excessive calcium carbonate formation, limiting the effectiveness and lifetime of the structure as clogging may occur.³

Most of the previous research examines P removal under longer retention times, representative of wastewater treatment plants. The current study differs through testing much shorter RTs that are normally observed in P removal structures. For instance, Penn *et al.* [19] observed significant P removal in a field-scale P removal structure with RTs varying between 12 and 110 minutes. Wang *et al.* [33] inferred that P removal structures must provide sufficient RT to accommodate the precipitation of calcium phosphate. This study confirms that longer RTs should be preferred, and RT=10 minutes is sufficient to produce satisfactory P removal by steel slags.

2.4.2 Differences between uncoated and coated steel slags under low RTs

When the incoming flows and/or the structure design do not allow for longer RTs, we proposed that Al-coating could aid the P removal ability of steel slags. The results of the ANOVA testing that proposition are shown in Table 2.4.

³Excessive clogging is also likely among influent containing appreciable bicarbonate, such as tile drainage water [19].

Although the non-constant variance was a violation of the ANOVA model (and data was transformed to address it), this characteristic of the data revealed an aspect of the coating process: by coating steel slag samples, the P removal ability of the samples is homogenized. In practical terms, we can predict the behavior of 100% Al-coated slags with an increased precision in comparison to uncoated slags.

The ANOVA indicated that the variance components due to coating and due to the slag sample were significant, as well as their interaction. The significance of the interaction indicates that the coating effect depends on the slag sample being coated. The highest mean P removal was observed for 100% Al-coated slag 9, but that mean was not significantly different from 17 out of the 36 combined treatments, including all but one (slag 4) 100% Al-coated slags (Figure B.4).

Overall, a higher level of coating resulted in a superior P removal performance, as shown by the comparison among the marginal means (Tukey’s Studentized Range test for levels of coating) in Table 2.5 and Figure B.5. The test indicated that all coating levels are significantly different from each other and the 100% coating level had the highest means among the Al-treatments.

The coated steel slag had their chemical properties altered through the Al-coating process. Most prominently, the pH of the coated slags was relatively lower in comparison to the original material. Uncoated slags showed a mean pH of 10.52 (standard deviation $[S] = 1.55$), 70% and 100% coated slags had mean pHs of 7.37 ($S = 1.55$) and 7.80 ($S = 1.22$). Aluminum content reported in digestates did not vary considerably among the coating levels, however the Al content in ammonium oxalate extractions reflect the higher amount of Al in the coated samples, with the 70% and 100% coated samples registering a higher mean Al content. Because ammonium oxalate solution dissolves the Al and Fe of amorphous fractions, it was expected that this fraction would reflect the Al addition. Penn & McGrath [20] also cited changes on water soluble Ca after coating a saturated steel slag. The authors observed an increase on dissolution of Ca hydroxide and calcite minerals and a decrease on water soluble Al, both as a result of the lower pH. At near-neutral pH, Al is precipitated as Al-hydroxide minerals on the surface of slags, providing a new path for P removal: adsorption,

which is not as dependent on time of contact. The pH observed in flow-through samples support this finding, as it varied between 4.7 and 8.7.

Based on these findings, the additional P removal mechanism provided by the Al-coating did in fact result in a superior P removal performance by steel slag under low RTs. This suggests that Al-coated slags should be utilized over non-coated slags for P removal structures that are designed to receive more rapid flows. Consider that the majority of dissolved P is transported during the events with the greatest discharge [15], [34], and this is expected to intensify with climate-change-induced precipitation [35].

2.4.3 Phosphorus removal capacity and origin of slag samples

In the ANOVA analysis described in the previous section, we could also identify the uncoated slag samples that showed a higher marginal P removal mean (Table 2.6). The highest means were identified for slags 7, 8, 9, 10, 11 and 12. All of them were originated from the same steel-making plant (Plant 3), but they are the residue of different slag-making processes as described in Table 2.1. Based on this finding, we were interested in determining whether a specific steel plant or steel-making process could be identified as producing superior steel slags with regards to P removal ability. A one-way ANOVA was conducted to investigate if the steel-making process had an impact by comparing the P removal of the uncoated slags under RT=9.85 min among the processes: BOF, H.P. blend, iron metallics, O.B. blend and kish. This subset of data was chosen because it represented the raw slag operating under prime conditions, which attenuates any confounding factors.

The F-statistic indicated that not all groups have equal means ($df=4$, $F=\text{statistic} = 17.5$, $p\text{-value} = 1.06 \times 10^{-7}$). The model assumptions of normality of residuals, independence and constant variance of observations were adequate.⁴ Upon further investigation, the O.B. blend, correspondent to slag samples 3 and 4, was identified as the only significantly different group, with a mean cumulative P removal of 21.62% and standard deviation of 13.4%. Based on the chemical and physical analysis of the slag samples, bulk density and particle density

⁴Shapiro-Wilk test was used to check normality of residuals (SW-statistic = 0.9433, $p\text{-value} = 0.06$). Constant variance per treatment group was checked through Bartlett's test ($df = 4$, Bartlett's statistic = 8.31, $p\text{-value} = 0.08$). No issues of serial correlation were identified in the plot of residuals versus the predictor variable.

in these samples are higher than in the others, resulting in a lower porosity of slags 3 and 4. This finding may explain in part the low P removal capacity of O.B. slags. The Al-coating was able to significantly aid the P removal ability of these slags: the 100% Al-coated slags 3 and 4 had a mean P removal of 63% and 44%. Another aspect to be considered is that O.B. slags showed the lowest values of pH buffer index, which can be a hindrance for Ca-phosphate precipitation [25].

The one-way ANOVA also indicated that a third of the P removal variation (as measured by the sum of squares) could be attributed to the error, i.e., variation within the different slag-making processes. Therefore, further discriminating the causes of variability of P removal was necessary to identify other factors able to explain high-performance slags.

2.4.4 Factors explaining P sorption capacity of steel slags

Calcium content was chosen as the initial explanatory variable because a greater degree of Ca-phosphate precipitation is expected with higher Ca concentrations in solution, assuming constant and sufficient phosphate concentrations. For instance, Piatak *et al.* [10] observed a positive correlation between Ca content and phosphate removal capacity ($n=12$; reported $R^2=0.5$), as measured in column experiments. This analysis included only the uncoated slag samples, because they rely solely on Ca-phosphate precipitation for P removal. Calcium phosphate precipitation is a process that involves various parameters, including calcium and phosphate concentrations, supersaturation, ionic strength, temperature, pH, and time [36], as noted in the previous analysis of RTs.

Overall, the levels of pH found in the collected outflow samples during the flow-through experiments demonstrate favorable conditions for Ca-PO_4 precipitation to occur. Additionally, it is notable that the pH of the collected samples decreased with time of experiment, which is consistent with the fact that precipitation of the solid phase is accompanied by a decrease in pH, as formation of Ca-P can release protons [37].

The linear model between Ca content and cumulative P removal (%) was fitted ($n=18$; uncoated slags, $\text{RT}=9.85$ min), and we found that the Ca term was not significant ($t\text{-statistic}=1.49$, $p\text{-value}=0.15$). Based on the pattern of the Ca content versus P removal curve (Figure 2.5(a)), we tested a polynomial model, denoted by:

$$y = \beta_1 \times x^2 + \beta_2 \times x + \beta_3 + \varepsilon_i \quad (2.6)$$

where β_1 , β_2 and β_3 are the model coefficients, x is the explanatory variable Ca content and ε_i the error. The model was also not significant (F-statistic versus constant model: 2.34, $p\text{-value} = 0.146$). This finding indicated that the Ca content of steel slag samples is overall irrelevant as an explanatory factor, and P removal will occur with sufficient solution Ca and P concentrations, and the experimental conditions allow for supersaturation. Total Ca content is then a poor predictor for steel slag P removal ability.

The next step was to choose a better predictor for the simple linear regression analysis. Because electrical conductivity (EC) measures the ionic content of a solution, it could be a proxy for dissolved Ca in solution that precipitates with P. The linear model between EC and cumulative P removal was significant (F-statistic: 5.65, $p\text{-value} = 0.03$); the next step was to analyze the residuals and their relation to the other variables. Table 2.7 shows the variables of interest and the significance of the models produced between each variable and the residuals of the EC and P removal relationship.

The variables that were included in the multiple regression model were: EC, total magnesium, bulk density and particle density. It is notable that although pH is a key variable in Ca-PO₄ precipitation reactions, the relationship between slag pH and P cumulative removal was not significant. One possible explanation is that most of the pH values were sufficiently high to offer favorable conditions for precipitation reactions to occur and, as such, P removal ability of steel slag could not be explained by this variable.

Prior to conducting the multiple linear regression, the explanatory variables were examined in regard to multicollinearity. Figure B.6 shows the matrix plot, and it illustrates a positive linear relationship between particle density and bulk density. The linear correlation was confirmed through a Pearson's correlation test ($\rho = 0.89$, $p\text{-value} = 5.70 \times 10^{-7}$). The presence of multicollinearity can have serious effects on the least-squares estimates of the regression coefficients, threatening the predicting ability of the model.

Multicollinearity was confirmed for particle density and bulk density using the variance inflation factor (VIF) for each term in the model (VIFs were 5.30 and 5.54, respectively),

indicating that the regression coefficients were poorly estimated [38]. Table 2.8 shows the original and ridge estimators (ridge trace[k]=0.28). As previously discussed, the ridge estimators are a stable set of parameter estimates with decreased variance and serve as a regulation for multicollinearity.

Therefore, the final model that best explains the variation of P cumulative removal by steel slag is:

$$\begin{aligned} \text{Cumulative P removal}[y] = & 130.73 + 0.005 \times EC - 48.96 \times \text{Bulk Density} \\ & + 0.85 \times \text{Particle density} + 0.0004 \times \text{Total Mg} \end{aligned} \quad (2.7)$$

These four parameters were able to explain 67% of the variability of the existing data, as measured by the adjusted R^2 . The root mean square error (RMSE) of the ridge regression model was 11.13, in comparison to 10.87 of the original model, evidence that the increase in bias exceeded the decrease in variance of the ridge regression estimator, probably as a result of the small sample size. Electrical conductivity, as mentioned before, serves as a proxy for dissolved Ca, and is a better predictor of P removal than total Ca content, because it describes readily available Ca for precipitation reactions.

Magnesium showed a positive correlation with P removal. Total Mg content varied from 22,000 to 89,000 mg kg⁻¹ in the slag samples, as indicated by the digestions. This suggests that dissolved Mg was likely produced in the flow-through cells, and available for precipitation with P in variable degrees. Abbona *et al.* [39] demonstrated that in the presence of Ca and Mg ([Ca] + [Mg] = [P]; pH ranging from 5.44 to 8.65), phosphate reacted with both elements, and among the precipitated phases, there were brushite (CaHPO₄ · 2 H₂O), struvite (MgNH₄ PO₄ · 6 H₂O) and newberryite (MgHPO₄ · 3 H₂O). Struvite is not possible in this case due to the lack of Nitrogen (N). For the Mg-rich slag samples, the Mg-PO₄ precipitation becomes significant, and because of that, Mg content can explain part of the variability of P removal by steel slags. Both Abbona *et al.* [39] and Pant *et al.* [40] cited the low stability of Mg-associated P observed in batch experiments, mixing solutions of ammonium phosphate, Ca and Mg chlorides, and in wetlands constructed with Lockport dolomite, respectively. Nevertheless, for the Mg-rich slag samples, the solubility of the Mg-phosphate precipitates

is expected to be low, due to the potentially large supply of soluble Mg, and even if low-stability Mg-PO₄ minerals are formed, they transform into metastable phases. Stoner *et al.* [27] also found a significant influence of total Mg on the model coefficients relating discrete P removal and P added in flow-through experiments with several industrial by-products, including slag.

The presence of bulk density and particle density in the final model indicates the significance of particle size and surface area. Porosity is the variable that relates bulk density and particle density,⁵ and it shows a positive correlation with P removal. The lowest values of porosity (0.40 and 0.42), observed for the O.B. slag samples, corresponded to the lowest P removal observed.

2.4.5 Coated slags

Figure 2.6 shows the differences in P removal for the uncoated and coated slags, as a function of total Al, oxalate extractable Al and pH. Oxalate extractable Al was higher in coated than uncoated samples, while the total Al content in digestates was similar for both. pH of coated samples were considerably lower, ranging from 4.75 to 10, while pH among uncoated slags ranged from 8 to 12.

Based on the exploratory analysis of this data, oxalate-Al was chosen to build a simple regression model whose residuals were used to investigate whether the other variables could explain variability in cumulative P removal among coated slags. However, the model was not significant (n=30; F-statistic vs. constant model: 2.23, *p-value* = 0.147); therefore, the explanatory variable EC was tested against P removal, which resulted in a significant relationship (F-statistic: 4.46, *p-value* = 0.0438). Table 2.9 shows the individual models, relating the residuals from the EC vs. cumulative P removal model and each of the variables of interest (n=30).

Following the same procedure described for the uncoated slags, a multiple linear regression was conducted using the significant explanatory variables shown in Table 2.9 (N=30;

5

$$Porosity = 1 - \frac{\text{Bulk Density}}{\text{Particle Density}} \quad (2.8)$$

n=18 70% coated and n=12 100% coated slags). Although the 2-way interactions were found to be significant (in comparison to the simpler model), most of them did not have a theoretical backing (e.g., interaction between Fe content and coating level). The interactions that had a theoretical significance (e.g., interaction between EC and coating level) did not improve the explanatory power of the model and therefore, were excluded from the final model. Total Fe and Ca contents displayed aspects of multicollinearity; VIF was 11.77 and 10.17. A ridge regression was then conducted to account for the multicollinearity. A ridge trace of 3.52 was found and the final estimators are shown in Table 2.10.

The final model that can best explain the variability of P removal of coated slags is shown in Equation 2.9:

$$\begin{aligned} \text{Cumulative P removal}[y] = & 64.39 + 0.014 \times EC + 4.73 \times 10^{-5} \times \text{Total Ca} \\ & - 1.95 \times 10^{-5} \times \text{Total Fe} - 15.96 \times \text{Coating Level 70\%} \end{aligned} \quad (2.9)$$

The RMSE of the ridge regression model was 10.33 in comparison to 9.95 of the original model. Again, the appearance of EC in the model shows the influence of dissolved solutes on the P removal potential of a sample. For coated slags, EC serves as a proxy for both dissolved Al and Ca, elements that actively participate in P removal, depending on the pH of the medium. Coating level was expected to explain part of the variability of P removal, since a significant difference between the coating levels was previously detected. The ability of this variable to explain part of the variability of P removal by coated slags is further evidence that the 100% coating level is preferred. The fact that Al did not show a significant effect illustrates that this variable was unable to capture the differences between the coating levels. Iron content had a significant effect on P removal, possibly because of the lower pH range of the coated samples that allowed for P adsorption to Fe to occur, as this mechanism can be considerable in circumneutral pHs [41]. Consequently, the samples with a greater content of Fe were able to remove more P, once the environmental conditions were appropriate for the reaction to occur. Li *et al.* [41] demonstrated that the P adsorption capacity of Fe (hydr)oxides tends to increase with decreasing pH at pH 2-12.

Calcium content was a significant explanatory variable, potentially due to residence time. Because the coated slag experiments were conducted under rapid flow rates, i.e., sub-optimal conditions for Ca dissolution [29], the greater the Ca content of the sample, the higher probability of Ca-PO_4 precipitation to occur.

Uncoated and coated steel slags showed different behavior during the flow-through experiments and in regards to their chemical properties. These differences are reflected in the models developed for each media, as different explanatory variables were able to explain P removal capacity of coated and uncoated slags. Electrical conductivity is present in both models, and as discussed earlier, serve as a proxy for Ca, Al, Mg and Fe, the active elements in the P removal mechanisms. Additionally, it is an easily-measurable attribute that can be used for a preliminary evaluation. More slag samples are necessary for testing the prediction accuracy of the models.

2.4.6 Environmental safety of steel slags

Because steel slag is a by-product, there may be risks associated with its use in environmental settings due to the presence of minor metal constituents. The content of trace and heavy metals (as established in the digestions) was low in all the analyzed slag samples (Tables 2.11 and C.2), except for Manganese (Mn) and Chromium (Cr). Slags 9 to 18 had Mn equal or greater than 15 g kg^{-1} ·slag. These slags were BOF or iron metallics. The other material types had Mn concentrations below that threshold. The same categories also had higher Cr concentrations. Although the Mn and Cr content of these slag samples were high, the concentrations of Mn found in the flow-through samples were significantly lower than the levels of Mn commonly found in freshwater ($1\text{-}200 \mu\text{g L}^{-1}$ [42]) and no Cr was identified in the water samples. These observations demonstrate how some slags have elevated levels of total Mn and Cr, but they do not reflect the concentrations found in the treated water, i.e., these elements are not soluble. Additionally, the concentrations of Cr in the material were still lower than the maximum concentration allowed for biosolids application to soils, a reference level shown in Table 2.11; there is no restriction for Mn in the soil amendments regulations [43]. Maghool *et al.* [44] have also found higher values of Cr in EAF and ladle

slag samples, and after leachate tests, concluded that the slags posed no threat for water systems beyond the regulations for fill materials and solid inert waste.

Other potential contaminants in freshwater systems, such as Sulfur (S) and Silicon (Si) were also evaluated. As expected, kish slags (slags 5, 6, 7 and 8) showed a higher S content as well as slags 1 and 2, generated from the head-pulling magnetic separation. Sulfur is of low toxicity and it is generally not considered a hazard in terms of ecological effects [45]. The higher contents of Si (in comparison to normal soil levels) were expected, as Ca is associated with this element in slags, and studies indicate Ca-silicates as the dominant mineral phases, for example, in electric arc furnace slags [11].

Nutrient level and toxic criteria can vary depending on the ecoregions of the U.S. At a federal level, the National Pollutant Discharge Elimination System (NPDES) provides water quality standards for the receiving water body. Table 2.11 shows the most recent water quality criteria for the chemicals of interest. The Clean Water Act considers Cr, Ni, Pb, and Zn toxic pollutants (33 U.S.C. §401.15). Because of that, there are clear federal regulations only for these elements. For the other elements, only state regulations or maximum concentrations for river and lake samples could be identified.

Regarding road construction, the alkaline pHs of slags can be problematic as the pH of leachate from steel slag can exceed 11, which can be corrosive to aluminum or galvanized steel pipes placed in direct contact with the slag, according to the U.S. Department of Transportation [9]. However, for treating runoff and drainage, the higher pH of the media is not as concerning as the alkalinity of the material. The alkalinity indicates the ability of the receiving water body to buffer the pH of the incoming solution. Penn *et al.* [25] described drainage water that after being filtered through an alkaline media did not result in an increase of pH on the receiving pond, as it was not sufficiently alkaline.

Alkalinity can be considered an expression of buffer capacity. In this study, the pH buffer index of slags ranged between 0.007 and 0.11 eq·acid kg⁻¹ required to decrease solution pH to 6.0. Highly buffered slags favor Ca-phosphate precipitation, but in terms of environmental safety, water bodies generally lack alkalinity and most regulations indicate a minimum alkalinity for effluent discharge, rather than a maximum. Overband slags (Slags 3 and 4)

showed the lowest values of buffer index, in contrast to the higher pH buffer indices for the iron metallics slags (Slags 9 and 10).

2.5 Conclusions

The steel slags evaluated in this work showed distinct P removal, highlighting the variability of P removal ability of different samples. The average P removal after adding 60 mg·kg⁻¹ slag in flow-through experiments varied between 12% and 96%, depending on slag source, residence time (RT) and level of Al-coating. The heterogeneity of P removal ability by steel slags indicates a need to individually characterize each sample, rather than classify them in a general category of Ca-rich PSMs. In this work, the operational conditions and slag properties able to promote a higher efficiency of P removal were investigated, and models were developed to explain the variation of P removal of steel slags.

Residence time (RT) was found to influence P removal. Phosphorus removal at RT=9.85 minutes was significantly superior to RT = 0.28 minutes. The design of P removal structures using steel slags must allow at least ten minutes of contact time between the incoming P-rich solution and the PSM. This result is supported by the chemistry of Ca-PO₄ precipitation reactions, in which there is an induction period followed by a rapid removal. When a long RT is not possible, we recommended the use of Al-coated slags. By coating the PSM, a new path for P removal was added to the samples, less dependent on time and consequently with a superior performance under the low RT (0.28 min). The Al-coating technique allows a structure to receive more rapid flows, and P removal effectiveness will not be inhibited as much. A 95 g L⁻¹ of Al₃(SO₄)₂ solution should be used to coat the materials, providing a coating level equivalent to the 100% level used in this study. Another consequence of Al-coating was the homogeneity of P removal performance, as the variability of P removal of the coated slags is lower in comparison to the uncoated media. That finding indicates that predicting the behavior of coated slags is easier than uncoated slags, since the performance of the former is more uniform.

The investigation of the different steel slag types revealed that the O.B. slag was the least effective in terms of P removal. The poor performance of that uncoated slag was attributed to the low pH buffer index and to the low porosity of this media. The Al-coating was able

to improve the P removal ability of O.B. slags. Phosphorus removal by BOF slag, H.P. slag, iron metalics and kish slag was not significantly different. However, the material types could not explain all of the variability in P removal, and based on that finding we developed models to define the chemical and physical characteristics that could better explain the P removal. The most influential characteristics for the uncoated slags were EC, total Mg content, particle density, and bulk density. Together, these properties were able to explain 67% of the variability of P removal. For coated slags, the most influential characteristics were EC, total Ca content, Fe content, and coating level. Both models can be used to predict the P removal capacity of unknown slag samples. Future work may include evaluating the models developed for both coated and uncoated slags, and assess their accuracy using new slag samples. Finally, no environmental risks were identified in the analysis of minor and trace components of steel slags.

References

- [1] D. L. Correll, “The role of phosphorus in the eutrophication of receiving waters: A review,” *Journal of environmental quality*, vol. 27, no. 2, pp. 261–266, 1998.
- [2] C. Penn, J. McGrath, J. Bowen, and S. Wilson, “Phosphorus removal structures: A management option for legacy phosphorus,” *Journal of Soil and Water Conservation*, vol. 69, no. 2, 51A–56A, 2014.
- [3] J. C. Ho and A. M. Michalak, “Phytoplankton blooms in lake erie impacted by both long-term and springtime phosphorus loading,” *Journal of Great Lakes Research*, vol. 43, no. 3, pp. 221–228, 2017.
- [4] P. Kleinman, A. Sharpley, A. Buda, R. McDowell, and A. Allen, “Soil controls of phosphorus in runoff: Management barriers and opportunities,” *Canadian Journal of Soil Science*, vol. 91, no. 3, pp. 329–338, 2011.
- [5] Ohio Phosphorus Task Force, *Ohio lake erie phosphorus task force - final report*, 2013.
- [6] C. Penn, I. Chagas, A. Klimeski, and G. Lyngsie, “A review of phosphorus removal structures: How to assess and compare their performance,” *Water*, vol. 9, no. 8, p. 583, 2017.

- [7] C. Shi, “Steel slag - its production, processing, characteristics, and cementitious properties,” *Journal of Materials in Civil Engineering*, vol. 16, no. 3, pp. 230–236, 2004.
- [8] I. Z. Yildirim and M. Prezzi, “Chemical, mineralogical, and morphological properties of steel slag,” *Advances in Civil Engineering*, vol. 2011, 2011.
- [9] United States Department of Transportation, *User guidelines for waste and byproduct materials in pavement construction*, Accessed on July 28, 2020, Washington DC, 2016. [Online]. Available: <https://www.fhwa.dot.gov/publications/research/infrastructure/structures/97148/ssa1.cfm>.
- [10] N. M. Piatak, R. R. Seal, D. A. Hoppe, C. J. Green, and P. M. Buszka, “Geochemical characterization of iron and steel slag and its potential to remove phosphate and neutralize acid,” *Minerals*, vol. 9, no. 8, p. 468, 2019.
- [11] M. Zuo, G. Renman, J. P. Gustafsson, and W. Klysubun, “Phosphorus removal by slag depends on its mineralogical composition: A comparative study of aod and eaf slags,” *Journal of Water Process Engineering*, vol. 25, pp. 105–112, 2018.
- [12] C. Navarro, M. Díaz, and M. A. Villa-García, “Physico-chemical characterization of steel slag. study of its behavior under simulated environmental conditions,” *Environmental science & technology*, vol. 44, no. 14, pp. 5383–5388, 2010.
- [13] L. I. Bowden, A. P. Jarvis, P. L. Younger, and K. L. Johnson, “Phosphorus removal from waste waters using basic oxygen steel slag,” *Environmental science & technology*, vol. 43, no. 7, pp. 2476–2481, 2009.
- [14] A. Drizo, C. Forget, R. P. Chapuis, and Y. Comeau, “Phosphorus removal by electric arc furnace steel slag and serpentinite,” *Water research*, vol. 40, no. 8, pp. 1547–1554, 2006.
- [15] A. N. Sharpley, P. J. Kleinman, A. L. Heathwaite, W. J. Gburek, G. J. Folmar, and J. P. Schmidt, “Phosphorus loss from an agricultural watershed as a function of storm size,” *Journal of Environmental Quality*, vol. 37, no. 2, pp. 362–368, 2008.
- [16] C. Penn, J. Bowen, J. McGrath, R. Nairn, G. Fox, G. Brown, S. Wilson, and C. Gill, “Evaluation of a universal flow-through model for predicting and designing phosphorus removal structures,” *Chemosphere*, vol. 151, pp. 345–355, 2016.
- [17] V. S. Shedekar, C. J. Penn, L. Pease, K. W. King, M. M. Kalcic, and S. J. Livingston, “Performance of a ditch-style phosphorus removal structure for treating agricultural drainage water with aluminum-treated steel slag,” *Water*, vol. 12, no. 8, p. 2149, 2020.
- [18] J. M. Gonzalez, C. J. Penn, and S. J. Livingston, “Utilization of steel slag in blind inlets for dissolved phosphorus removal,” *Water*, vol. 12, no. 6, p. 1593, 2020.

- [19] C. Penn, S. Livingston, V. Shedekar, K. King, and M. Williams, “Performance of field-scale phosphorus removal structures utilizing steel slag for treatment of surface and subsurface drainage,” *Water*, vol. 12, no. 2, p. 443, 2020.
- [20] C. J. Penn and J. M. McGrath, “Predicting phosphorus sorption onto steel slag using a flow-through approach with application to a pilot scale system,” *Journal of Water Resource and Protection*, vol. 3, no. 4, p. 235, 2011.
- [21] Z. Qin, A. L. Shober, K. G. Sheckel, C. J. Penn, and K. C. Turner, “Mechanisms of phosphorus removal by phosphorus sorbing materials,” *Journal of environmental quality*, vol. 47, no. 5, pp. 1232–1241, 2018.
- [22] M. Arias, J. Da Silva-Carballal, L. Garcia-Rio, J. Mejuto, and A. Nunez, “Retention of phosphorus by iron and aluminum-oxides-coated quartz particles,” *Journal of colloid and interface science*, vol. 295, no. 1, pp. 65–70, 2006.
- [23] A. Hedström and L. Rastas, “Methodological aspects of using blast furnace slag for wastewater phosphorus removal,” *Journal of Environmental Engineering*, vol. 132, no. 11, pp. 1431–1438, 2006.
- [24] EPA, “Method 3050b. acid digestion of sediments, sludges, and soils. revision 2,” *Test Methods for Evaluating Solid Wastes: Physical/Chemical Methods*, EPA SW-846Section a, 3050B–1e3050B, 1996.
- [25] C. J. Penn and J. M. Bowen, *Design and construction of phosphorus removal structures for improving water quality*. Springer, 2017.
- [26] USEPA, Environment and Climate Change Canada, *Annex 4 objects and targets task team, 2015: Recommended phosphorus loading targets for lake erie*, May 2015. [Online]. Available: <https://www.epa.gov/sites/production/files/2015-06/documents/report-recommended-phosphorus-loading-targets-lake-erie-201505.pdf>.
- [27] D. Stoner, C. Penn, J. McGrath, and J. Warren, “Phosphorus removal with by-products in a flow-through setting,” *Journal of environmental quality*, vol. 41, no. 3, pp. 654–663, 2012.
- [28] D. C. Montgomery, *DESIGN AND ANALYSIS OF EXPERIMENTS*. John Wiley and Sons, Inc. New Jersey, 2012.
- [29] D. Claveau-Mallet, S. Wallace, and Y. Comeau, “Model of phosphorus precipitation and crystal formation in electric arc furnace steel slag filters,” *Environmental science & technology*, vol. 46, no. 3, pp. 1465–1470, 2012.

- [30] J. F. Ferguson, D. Jenkins, and J. Eastman, "Calcium phosphate precipitation at slightly alkaline ph values," *Journal (Water Pollution Control Federation)*, pp. 620–631, 1973.
- [31] A. Shilton, S. Pratt, A. Drizo, B. Mahmood, S. Banker, L. Billings, S. Glenney, and D. Luo, "'active' filters for upgrading phosphorus removal from pond systems," *Water Science and Technology*, vol. 51, no. 12, pp. 111–116, 2005.
- [32] C. Barca, S. Troesch, D. Meyer, P. Drissen, Y. Andres, and F. Chazarenc, "Steel slag filters to upgrade phosphorus removal in constructed wetlands: Two years of field experiments," *Environmental science & technology*, vol. 47, no. 1, pp. 549–556, 2013.
- [33] L. Wang, C. Penn, C.-h. Huang, S. Livingston, and J. Yan, "Using steel slag for dissolved phosphorus removal: Insights from a designed flow-through laboratory experimental structure," *Water*, vol. 12, no. 5, p. 1236, 2020.
- [34] C. Penn, J. Gonzalez, M. Williams, D. Smith, and S. Livingston, "The past, present, and future of blind inlets as a surface water best management practice," *Critical Reviews in Environmental Science and Technology*, vol. 50, no. 7, pp. 743–768, 2020.
- [35] E. Sinha, A. Michalak, and V. Balaji, "Eutrophication will increase during the 21st century as a result of precipitation changes," *Science*, vol. 357, no. 6349, pp. 405–408, 2017.
- [36] L. Montastruc, C. Azzaro-Pantel, B. Biscans, M. Cabassud, and S. Domenech, "A thermochemical approach for calcium phosphate precipitation modeling in a pellet reactor," *Chemical Engineering Journal*, vol. 94, no. 1, pp. 41–50, 2003.
- [37] M. Van Kemenade and P. De Bruyn, "A kinetic study of precipitation from supersaturated calcium phosphate solutions," *Journal of Colloid and Interface Science*, vol. 118, no. 2, pp. 564–585, 1987.
- [38] D. C. Montgomery, E. A. Peck, and G. G. Vining, *Introduction to linear regression analysis*. John Wiley & Sons, 2012, vol. 821.
- [39] F. Abbona, H. L. Madsen, and R. Boistelle, "The initial phases of calcium and magnesium phosphates precipitated from solutions of high to medium concentrations," *Journal of crystal Growth*, vol. 74, no. 3, pp. 581–590, 1986.
- [40] H. Pant, K. Reddy, and E. Lemon, "Phosphorus retention capacity of root bed media of sub-surface flow constructed wetlands," *Ecological Engineering*, vol. 17, no. 4, pp. 345–355, 2001.

- [41] M. Li, J. Liu, Y. Xu, and G. Qian, “Phosphate adsorption on metal oxides and metal hydroxides: A comparative review,” *Environmental Reviews*, vol. 24, no. 3, pp. 319–332, 2016.
- [42] World Health Organization, “Manganese in drinking water,” World Health Organization, Geneva, Switzerland, Tech. Rep., Apr. 2011, Accessed on Oct 7th 2020. [Online]. Available: https://www.who.int/water_sanitation_health/dwq/chemicals/manganese.pdf?ua=1.
- [43] Natural Resources Conservation Service, “Heavy metal soil contamination,” Soil Quality Institute, Auburn, AL, Tech. Rep., Sep. 2000. [Online]. Available: https://www.blogs.nrcs.usda.gov/Internet/FSE_DOCUMENTS/nrcs142p2_053279.pdf.
- [44] F. Maghool, A. Arulrajah, Y.-J. Du, S. Horpibulsuk, and A. Chinkulkijniwat, “Environmental impacts of utilizing waste steel slag aggregates as recycled road construction materials,” *Clean Technologies and Environmental Policy*, vol. 19, no. 4, pp. 949–958, 2017.
- [45] U.S. Environmental Protection Agency, “Pesticide and toxic substances: R.e.d. facts - sulfur,” U.S. Environmental Protection Agency, Washington, DC, Tech. Rep., May 1991. [Online]. Available: <https://archive.epa.gov/pesticides/reregistration/web/pdf/0031fact.pdf>.

Table 2.1. Origin and particle sizes of steel slag samples.

Sample ID	Production	Material type	Particle size range (mm)	Minimum particle size (mm)
1	Plant 2	H.P ¹ , slag blend	fines	1.19
2	Plant 2	H.P., slag blend	fines	0.595
3	Plant 2	O.B. ² , slag blend	fines	1.19
4	Plant 2	O.B., slag blend	fines	0.595
5	Plant 2	Kish	fines	1.19
6	Plant 2	Kish	fines	0.595
7	Plant 3	Kish	6.35 x 0	1.19
8	Plant 3	Kish	6.35 x 0	0.595
9	Plant 3	Kish, iron metalics	6.35 x 0	1.19
10a	Plant 3	Kish, iron metalics	6.35 x 0	0.595
11	Plant 3	BOF ³	12.7 x 0	1.19
12	Plant 3	BOF	12.7 x 0	0.595
13	Plant 3	BOF	19.0 x 12.7	1.19
14	Plant 3	BOF	19.0 x 12.7	0.595
15	Plant 6	BOF	12.7 x 0 (Coarse)	1.19
16	Plant 6	BOF	12.7 x 0 (Coarse)	0.595
17	Plant 6	BOF	19.1 x 12.7	1.19
18	Plant 6	BOF	19.1 x 12.7	0.595

¹Head pulling magnet²Overband magnet³Basic oxygen furnace

Table 2.3. Characterization of steel slag samples: specific parameters tested and their respective levels.

Uncoated Slags <i>RT</i> : 0.284 and 9.85 minutes; <i>Slag source</i> : 3 steel-making plants; 5 production processes <i>Mesh sizes (cm)</i> : fines, 0.64, 1.28, 1.91 and 1.28-coarse; <i>Particle size</i> : 16 or 30; <i>Chemical properties assessed</i> : pH, EC, buffer capacity and calcium (Ca) content. <i>Physical properties</i> : Bulk density and particle density.	Coated Slags <i>Level of Coating</i> 70% and 100%; <i>Slag source</i> : 3 steel-making plants; 5 production processes; <i>Mesh sizes (cm)</i> : fines, 0.64, 1.28, 1.91 and 1.28-coarse; <i>Particle size</i> : 16 or 30; <i>Chemical properties assessed</i> : pH, EC, Ca content and aluminum (Al) content.
-----------------------------------------------------------------------------------------------------------------------------------------------------------------------------------------------------------------------------------------------------------------------------------------------------------------------------------------------------------------------------------------------------------	-------------------------------------------------------------------------------------------------------------------------------------------------------------------------------------------------------------------------------------------------------------------------------------------------------------------------------------

Table 2.2. Methods for characterization of steel slag properties.

Experimental Method	Evaluated parameters
pH in water	pH
EC in water	Electrical conductivity
Acid titration	Buffer index
Total digestion	Total Ca, Al and Fe content
Ammonium oxalate extraction	Amorphous Al and Fe
Mass of PSM in container of known-volume	Bulk density
PSM water displacement	Particle density

Table 2.4. Analysis of variance: the effect of slag sample and level of coating on the cumulative P removal response (data was previously transformed due to heteroscedasticity).

Source of Variation	Sum of Squares	Degrees of freedom	Mean square	F ₀	Prob>F
Slag ¹	1,008,710	11	91,700	7.06	3.33×10 ⁻⁶
Coating ²	2,855,270	2	1,427,635	109.89	4.70×10 ⁻¹⁶
Interaction	734,529	22	33,387	2.57	0.006
Error	467,710	36	12,991		
Total	5,066,221	71			

¹Factor has 12 levels, each representing a slag sample.

²Factor has 3 levels, each representing a Al-coating level: 0, 70 and 100.

Table 2.5. Mean estimates of cumulative P removal (%) for the coating groups and comparison between the marginal means of coating levels.

Level of Coating		Mean (original data)	Mean (transformed data) ¹		
0		22.89	486.52		
70		51.56	738.00		
100		74.01	974.23		
Groups ²		Difference ³	Lower limit ⁴	Upper limit ⁴	p-value
0%	70%	-251	-332	-171	1.52 × 10 ⁻⁸
0%	100%	-487	-568	-407	9.57 × 10 ⁻¹⁰
70%	100%	-236	-316	-1.56	5.78 × 10 ⁻⁸

(1) $\frac{data^\lambda - 1}{\lambda}$; $\lambda = 1.4915$;

²Groups refer to the levels of coating being compared;

³Difference between the estimated transformed group means;

⁴95% confidence intervals for the true mean difference.

Table 2.6. Mean estimates of cumulative P removal for the slags and comparison between the marginal means of different slag samples.¹

Slag Sample	Mean (original data [%])	Mean (transformed data) ²	Tukey's groups ³
Slag 1	49.13	727.20	bcd
Slag 2	44.79	683.23	bcd
Slag 3	33.39	573.67	cd
Slag 4	27.86	521.24	d
Slag 5	37.44	667.42	bcd
Slag 6	41.96	657.23	bcd
Slag 7	58.49	810.99	ab
Slag 8	56.15	786.76	abc
Slag 9	74.57	981.46	a
Slag 10	59.93	839.64	ab
Slag 11	54.51	768.07	abc
Slag 12	55.45	778.05	abc

¹Pairwise comparison shown in the appendix (Table B.1).

⁽²⁾ $\frac{data^\lambda - 1}{\lambda}$; $\lambda = 1.4915$.

³Means with same letter are not significantly different
($\alpha = 0.05$).

Table 2.7. Single linear regression models (uncoated steel slags): each of the variables was tested against the residuals of the EC versus P cumulative removal model (data shown in Figure 2.5b). We also show the variables for which the model was significant (indicated by the asterisk), i.e., variables that were able to explain the variability of the residuals.

Variables	F-statistic ⁴	<i>p-value</i>	Adj. R ²
Total calcium ¹	2.37	0.14	0.08
Total magnesium ^{1*}	4.49	0.05	0.17
Total iron ¹	1.24	0.28	0.02
Total aluminum ¹	3.34	0.09	0.12
Oxalate iron ²	0.10	0.75	-0.06
Oxalate aluminum ²	0.20	0.66	-0.05
pH	0.805	0.38	-0.01
Buffer Index	4.24×10^{-4}	0.98	-0.06
Bulk Density (mg L ⁻¹)*	15.70	0.001	0.46
Particle Density (g mL ⁻¹)*	9.99	0.006	0.346
Particle size range ³	1.45	0.275	0.118
Min. particle size	0.08	0.778	-0.0571

¹ mg kg⁻¹; concentration in digestates;

² mg kg⁻¹; ammonium oxalate extraction;

³ Categorical variable;

⁴ F-statistic vs. constant model.

Table 2.8. Summary of multiple linear regression predicting cumulative P removal of uncoated steel slags: original and corrected (ridge estimators) parameter estimates.

Variable	DF	Estimate	Standard error	t-stat	p-value	Ridge Estimate
Intercept	1	124.71	29.10	4.28	0.000887	130.73
EC	1	0.0048	0.00283	1.72	0.109	0.005
Bulk Density	1	-69.22	26.42	-2.62	0.021	-48.96
Particle Density	1	12.95	16.87	0.77	0.46	0.85
Total magnesium	1	0.00045	0.0002	2.25	0.042	0.0004
Number of observations: 18;						
Adjusted R squared: original regression: 0.69 / ridge regression: 0.68.						

Table 2.9. Single linear regression models (Al-coated steel slags): each of the variables were tested against the residuals of the EC versus P cumulative removal model. We show the variables for which the model were significant (indicated by the asterisk), i.e., variables that were able to explain the variability of the residuals.

Variables	F-statistic ⁴	<i>p-value</i>	Adj. R ²
Total calcium ^{1*}	4.16	0.05	0.10
Total magnesium ¹	3.05	0.09	0.07
Total iron ^{1*}	4.69	0.04	0.11
Total aluminum ¹	0.01	0.912	-0.04
Oxalate iron ²	0.90	0.35	-0.004
Oxalate aluminum ²	0.977	0.332	8×10^{-4}
pH	0.943	0.34	-0.002
Bulk Density (g mL ⁻¹)	1.3	0.264	0.01
Particle Density (g mL ⁻¹)	0.0813	0.78	-0.03
Particle size range ³	1.2,	0.34	0.03
Min. particle size	0.066	0.8	-0.03
Coating Level ^{3*}	12.8	0.001	0.30

¹ mg kg⁻¹; concentration in digestates;

² mg kg⁻¹; ammonium oxalate extraction;

³ Categorical variable;

⁴ F-statistic vs. constant model.

Table 2.10. Summary of multiple linear regression predicting cumulative P removal of coated steel slags: original and corrected (ridge estimators) parameter estimates.

Variable	Estimate	Standard error	t-stat	p-value	Ridge Estimate
Intercept	17.90	34.86	0.514	0.612	64.39
EC	0.02	0.0071	2.83	0.009	0.014
Total calcium	0.0004	9.67×10^{-5}	1.412	0.17	4.73×10^{-5}
Total iron	1.49×10^{-5}	4.805×10^{-5}	0.312	0.7578	-1.95×10^{-5}
Coating Level 70%	-19.86	4.268	-4.654	9.14×10^{-5}	-15.96
Number of observations: 30;					
Adjusted R squared: original regression: 0.55 / ridge regression: 0.52.					

Table 2.11. Range of micro-constituents of steel slag samples and water quality criteria for freshwater systems and for heavy metals applied to soils: evaluating the environmental safety of steel slag according to drinking water and soil amendments standards.

Element	Measured range	Maximum	Measured range ²	CMC ³
		allowable		
		concentration in biosolids ¹		
	$(mg\ kg^{-1})$		$(mg\ L^{-1})$	
B	0 - 44	-	0.16-1.42	5 ⁽⁵⁾
Cr	150 - 1840	3000	0	0.57
Co	0 - 6	25 ⁽⁴⁾	0.003 - 0.01	0.01 ⁽⁸⁾
Mn	415 - 23140	-	0 - 0.02	0.1 ⁽⁶⁾
Na	3 - 1045	-	1.60 - 2.30	*
Ni	8 - 530	75	0	0.47
Pb	72 - 440	420	0 - 0.006	0.082
S	400 - 16500	-	0 - 15.63	250 ⁽⁷⁾
Si	340 - 728	-	0.50 - 2.11	2
Zn	7 - 446	7500	0 - 0.15	0.12

¹ Maximum allowable concentration of heavy metals applied to soils [1];

² Measured from random flow-through samples;

³ Criterion maximum recommendation [2], unless noted otherwise;

⁴ Rules of Georgia DNR, EPD, Hazardous Site Response (Adapted from Sonon *et al.* [3]);

⁵ Maximum concentration found in 1,546 samples of river and lake waters from various parts of the U.S.[4];

⁶ Drinking water quality criteria from the World Health Organization [5];

⁷ Secondary maximum contaminant levels [6];

⁸ Max. concentration in surface waters of populated areas [7];

* No drinking-water based threshold [5] and no environmental-based criteria was found.

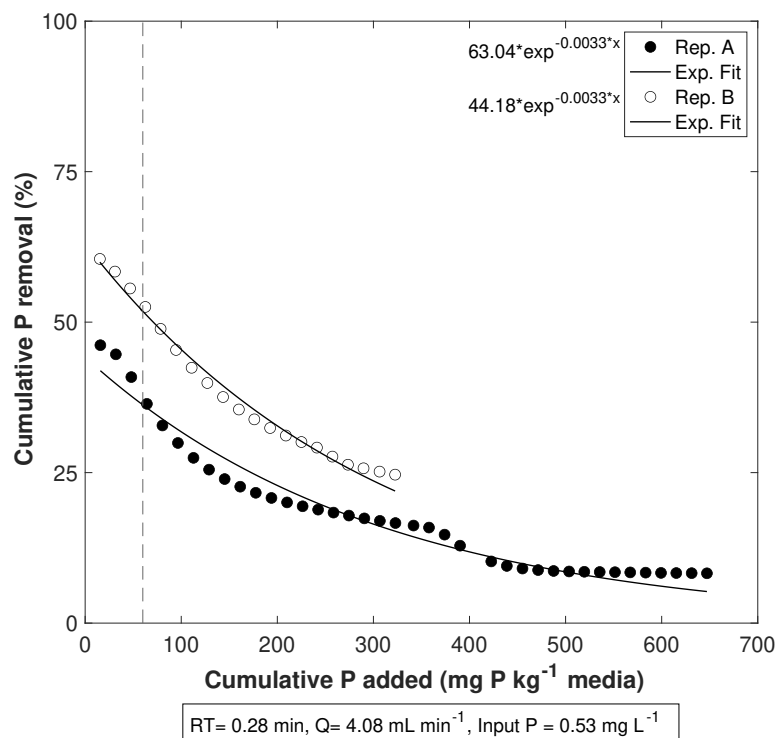


Figure 2.1. Example phosphorus (P) removal expressed as a function of cumulative P added per unit slag mass. Two replicates and their respective fitted curves are being shown (the fitted curves equations are shown in the upper-right corner). Intersection of fitted line with vertical line at 60 mg·P kg⁻¹·slag indicates cumulative P removal values used for statistical comparisons.

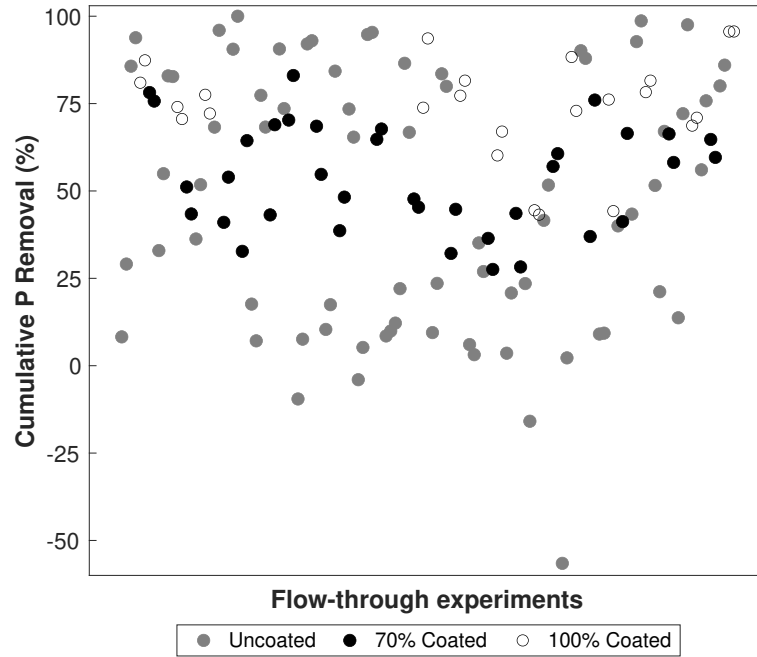


Figure 2.2. Heterogeneity of cumulative P removal by different steel slag samples. Each datum represents the P removal performance of steel slag samples in each of the flow-through experiments, and is colored according to the level of coating.

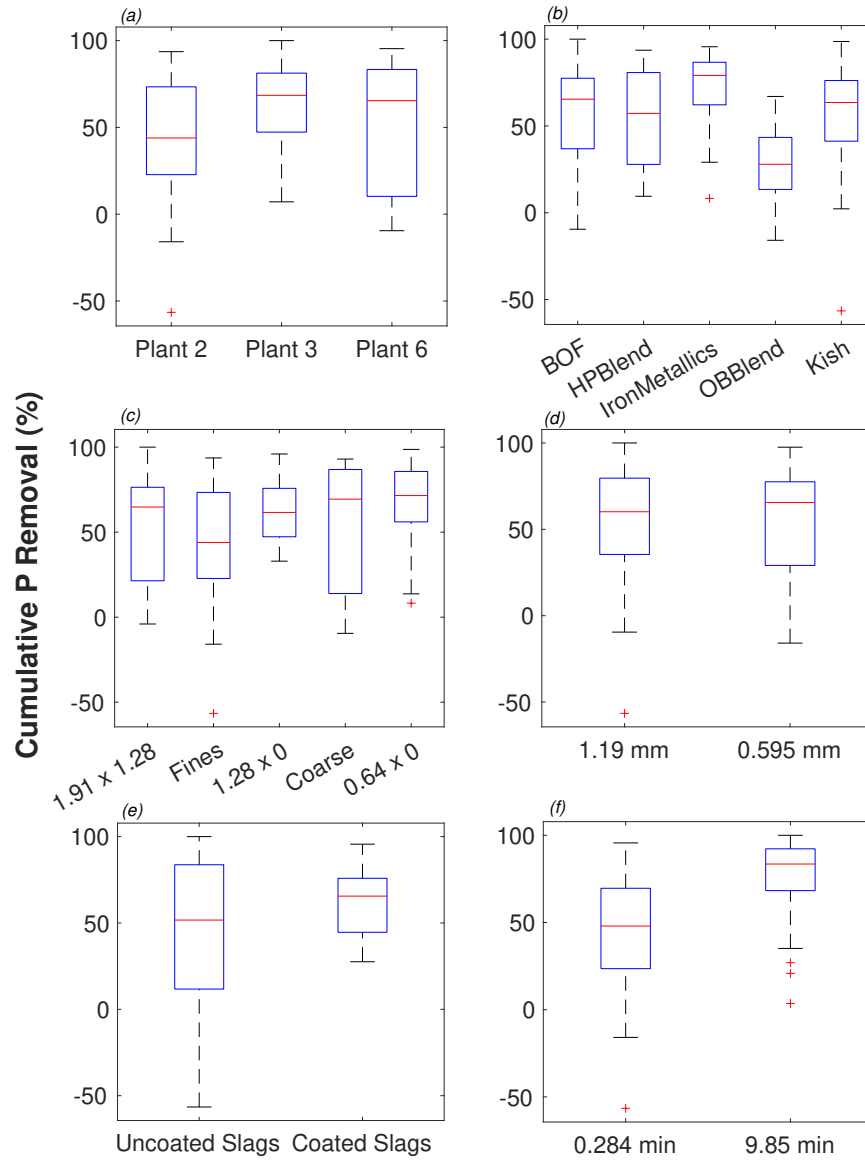


Figure 2.3. Data distribution analysis: cumulative P removal (%) according to the parameters: (a) Steelmaking plant, (b) slag production process, (c) particle size range, (d) minimum particle size, (e) Coating and (f) Residence time.

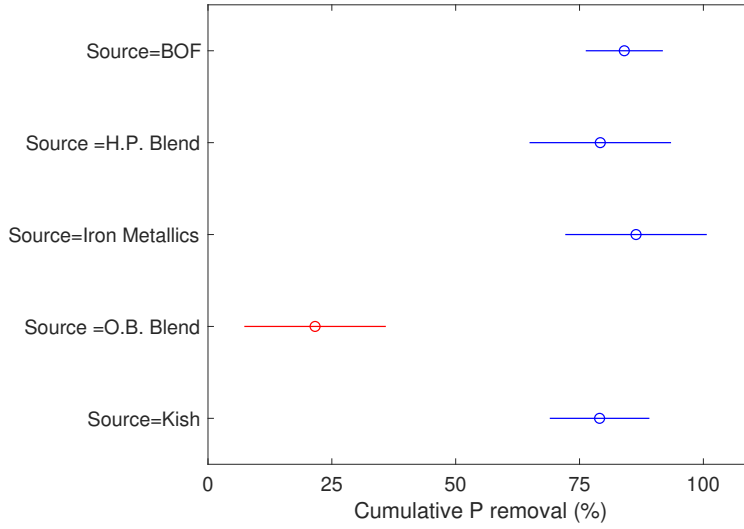


Figure 2.4. Comparison of marginal means of groups: O.B. (overband magnet) had a mean significantly different in comparison to the other four sources, which were not significantly different amongst themselves. Open circles represent the means and the respective line the confidence interval.

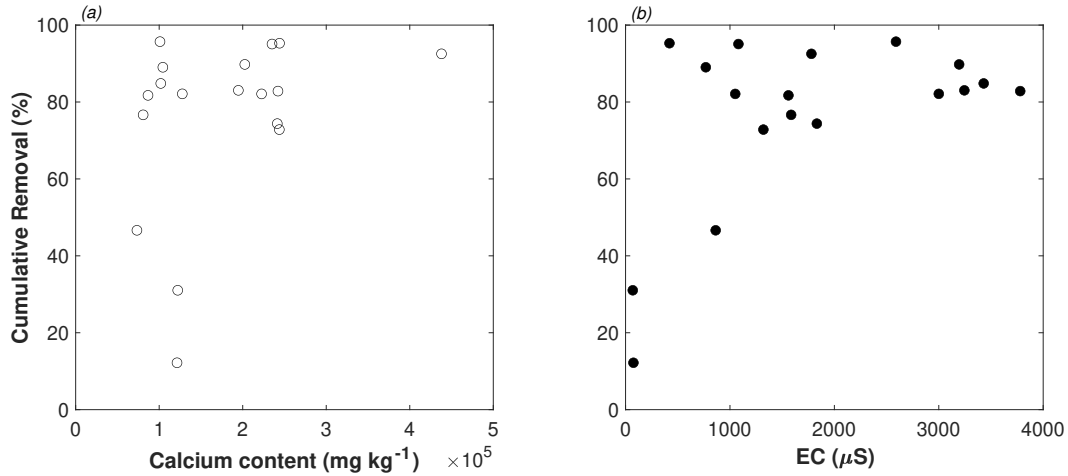


Figure 2.5. Phosphorus cumulative removal versus main variables of interest for uncoated slags: (a) Calcium content and (b) EC.

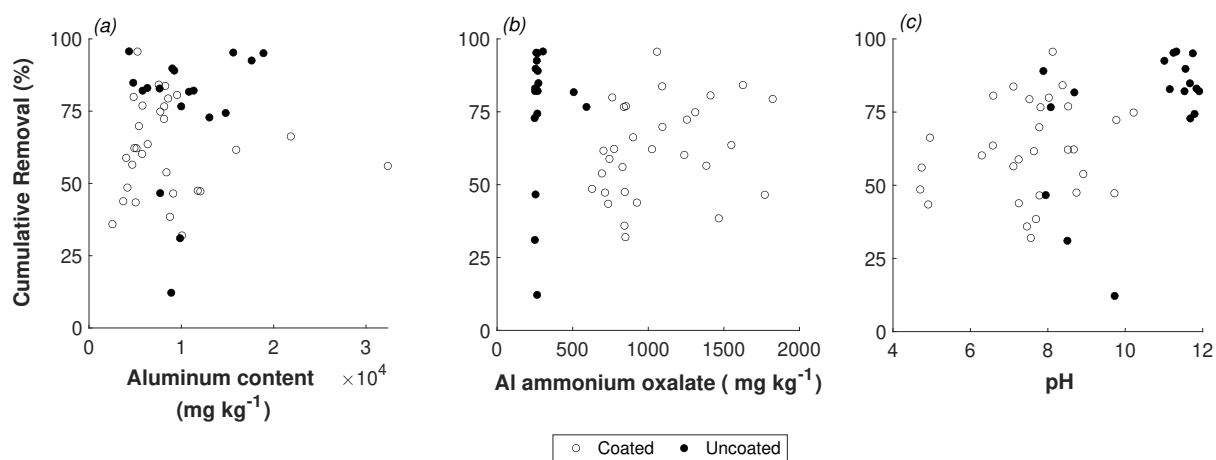


Figure 2.6. Coated and uncoated slags: cumulative P removal according to evaluated variable: (a) Aluminum content (digestion analysis), (b) Al content in the oxalate fraction and (c) pH.

3. DEVELOPMENT OF A REGENERATION TECHNIQUE FOR ALUMINUM-RICH AND IRON-RICH PHOSPHORUS SORPTION MATERIALS

3.1 Abstract

The reduction of dissolved phosphorus (P) transport to water systems is of critical importance for water quality. Phosphorus sorption materials (PSMs) are media with high affinity for dissolved P, and serve as the core components of P removal structures. These structures can intercept dissolved P in surface and subsurface flows, before discharge into water bodies. While the P removal ability of PSMs has been extensively studied, lesser is known about the capacity to regenerate and recover P from P-saturated PSMs. This article evaluates a methodology to recover the P removal ability of aluminum- and iron-rich P-saturated PSMs. A series of flow-through experiments were conducted, alternating between P sorption (0.5 and 50 mg L⁻¹ P) and desorption with potassium hydroxide (KOH; 5 or 20 pore volumes [PV]), varying residence times (0.5 min and 10 min), and number of recirculations (0, 6 and 24). Across two cycles of sorption-desorption, Alcan, Biomax and PhosRedeem showed an average P recovery of 81%, 79%, and 7%, with standard deviation of 10%, 21% and 6%, respectively. The most effective regeneration treatment was characterized by the largest KOH volume (20 PV) and no recirculation, with up to 100% reported P recovery. Although KOH at 5 PV was less effective, the use of recirculation did increase P recovery. The lifetime of Al/Fe-dominated PSMs in P removal structures can be extended through feasible regeneration techniques demonstrated in this study, for both high and low P concentration scenarios.

This study has been published in *Water*: SPC Scott, I., J Penn, C., Huang, C. H. (2020). “Development of a regeneration technique for aluminum-rich and iron-rich phosphorus sorption materials,” *Water* , 12(6), p.1784, 2020.

3.2 Introduction

Phosphorus Sorption Materials (PSMs) are media with a high affinity for phosphorus (P) and the core of P removal structures, i.e., landscape-scale filters able to intercept surface and subsurface P-rich water. Phosphorus sorption materials can be broadly categorized as (1) natural materials; (2) manufactured materials; or (3) industrial residuals. Their ability to bind with dissolved P has been amply studied and several media have been tested to that end, including steel slag, acid mine drainage residuals, limestone, and gypsum [1], [2]. A common characteristic among PSMs is their high affinity for dissolved P due to their calcium (Ca), magnesium (Mg), iron (Fe), or aluminum (Al) contents. These elements are responsible for actively retaining P from flowing waters through different mechanisms. Calcium- or Mg-rich media remove dissolved P primarily by precipitation, forming solid Mg/Ca-phosphates when pH is sufficiently high [3]. Aluminum- or Fe-rich materials retain P mainly through ligand exchange adsorption reactions on their surface hydroxyl sites. The practical difference between these mechanisms is reaction time: ligand exchange is a rapid reaction, while precipitation of phosphate compounds can have a much slower rate of reaction [4]. Another difference involves the ability to regenerate the media once they become saturated with P; for adsorption-based removal, the P sorption reaction can be reversed by favoring the desorption of P through shifts in chemical equilibrium conditions. However, for precipitation-based removal, the loss of Ca/Mg as P-precipitates prevents the recovery of the original sorption material.

The choice of PSM for a P removal structure is partly a function of the P removal mechanism, either precipitation or adsorption, as well as the characteristics of the incoming flow, especially peak flow rate and residence time. Other factors that will influence the choice of PSM and the potential efficacy of a P removal structure are incoming P concentration, volume, and direction of flow. These factors will also define the longevity of the PSM; once saturated, it will require replacement, or regeneration of the media.

The purpose of this study was to develop and evaluate a methodology to recover the P removal ability of P-saturated Al/Fe-based PSMs using potassium hydroxide (KOH). If

successful, this would prevent the need for frequent physical replacement of PSMs, decreasing costs and further simplifying the use of P removal structures.

3.2.1 Sorption of P by Al/Fe-Rich Materials

In the context of P removal technologies, Al/Fe-rich media, such as Al/Fe oxides, iron mine tailings, Al/Fe-coated materials and alum residuals, have been evaluated as sorbents for phosphate, demonstrating varying degrees of efficiency of P sorption. In the literature, there are examples of applications in wetlands, wastewater, non-point drainage and ground-water treatment [4]–[9]. For example, Wood *et al.* [7] reported a 93% P removal by using laterite—a material rich in hydrous oxides of Fe and Al, in a newly constructed wetland. Dobbie *et al.* [5] investigated the use of iron ochre ($\text{Fe}(\text{OH})_3$ and $\text{FeO}(\text{OH})$) for removing P from a secondary-treated wastewater effluent. The authors observed a 50% removal of total P mass, indicating a significant efficacy of the media to remove P from wastewater. Clayton *et al.* [10] observed that iron mine tailings significantly reduced P release from lake sediments to solution, suggesting the formation of hydrous ferric oxide complexes or precipitates containing P. Coated materials have also been reported in the literature. For example, Ayoub *et al.* [11] evaluated the performance of Al/Fe hydroxy(oxide) coated sand and olivine, showing a removal of 70% to 90% depending on the source of P, i.e., either water or wastewater, with outflow concentrations of 0.05 mg L^{-1} .

Phosphorus adsorption by metal (hydr)oxides is a well-understood process. As Fe is a ubiquitous component of soils (especially tropical and highly weathered soils), the mechanisms of P adsorption by metal oxides has been amply studied and can be applied to the context of Al- and Fe-rich PSMs. Phosphate (PO_4) sorption onto Al/Fe-rich PSMs can be accomplished through three different mechanisms: (1) precipitation of metal-phosphates through dissolution of Fe^{2+} , Fe^{3+} or Al^{3+} , (2) ligand exchange on particle surfaces, and (3) anion exchange at low pH range [4], [12].

Both ferric (Fe^{3+}) and ferrous (Fe^{2+}) iron react with phosphate, forming precipitates, hydrous ferric oxide and phosphate compounds, depending on pH and Eh. Most Fe^{3+} minerals are insoluble, but under acidic conditions, they dissolve and can then react with PO_4 . In wastewater treatment, Mao *et al.* [13] claimed that to remove P using ferric salts, the

most efficient route is to form the precipitate $\text{FePO}_{4(s)}$, due to the 1:1 molar ratio of Fe and P. However, at circumneutral pHs, this precipitation reaction is unlikely to occur, and P removal is dominated by phosphate adsorption to ferric oxides [13], according to the reaction:



Aluminum hydroxide is also a popular chemical for phosphorus removal in wastewater and it has been used in lake restoration as a P coagulant agent [14]. The P adsorption mechanism onto Al-rich PSMs is similar to the process described in Equation (3.1), the ligand exchange between $\text{H}_x(\text{PO}_4)^{x-2}$ and the hydroxide groups on the surface of the minerals.

Essentially, the metal (Al/Fe) beneath the surface hydroxyl acts as a Lewis acid and exchanges the surface OH groups for phosphates, resulting in an inner-sphere complex (no water in between). The exact type of complex being formed depends on the type of Al/Fe (hydr)oxides, pH and initial P concentration, and determines the strength with which P is bound [15]. Equation (3.1) also illustrates the determinant role of pH in P adsorption. In general, as pH decreases, $\text{H}_x(\text{PO}_4)^{x-2}$ adsorption increases, whereas solubility of the metal-phosphate complex decreases [16]. Siwek *et al.* [16] stated that the optimal pH range for the formation of durable Fe-P compounds is between 5 and 7. In this range, the electrostatic attraction between P and the Fe-rich PSM is optimum (pH of solution is lower than its point of zero charge and P is in its anionic form). For Al, Tanada *et al.* [17] reported a maximum P adsorption capacity by aluminum oxyhydroxide at pH = 4.

3.2.2 Desorption of P from Al/Fe-Rich Materials

Once the Al/Fe-rich PSMs are saturated and are not able to sequester additional dissolved P, there are two options for the P removal structure to continue functioning: (1) replacement, or (2) regeneration of the media. Due to a relatively high cost of Al/Fe-rich PSMs and labor-intensive processes of replacing the material after exhaustion, regeneration is of great interest. Few studies on regeneration of PSMs at bench-scale and pilot-scale have been reported in the literature. A standard treatment able to be performed at the field scale is yet to be determined. In particular, most studies do not use a feasible volume of regenerative

solution able to be scaled up to field conditions (i.e., the solid-solution ratio established at the laboratory scale must be maintained for providing the same proportion between available OH^- and surface sorption sites).

An example of existing regeneration treatments is reported by Sibrell *et al.* [18], in which they tested a regeneration treatment on granular ferric hydroxide media samples, after an extensive P removal trial to remediate trout wastewater. The authors used 0.5 M NaOH solution in a 24-h recirculation. Prior to the addition of NaOH, the media was washed with softened tap water, followed by a rinse with 0.5% sodium hypochlorite. At the conclusion of the regeneration sequence, the media was again washed with tap water and the authors continuously sparged CO_2 to maintain an optimal pH in the interstitial solution. They reported a 45% desorption of P. Although the volume of regenerative solution was not reported in this study, the authors mention prior research that resulted in 70–80% of recovery by using up to 60 bed volumes of 0.5 M NaOH solution [19].

Allred *et al.* [4] tested desorption/dissolution cycles after a P sorption saturated column experiment. The methodology consisted of a 3-pore volume flush with a 4% by weight NaOH solution followed by a 27 pore volume distilled water rinse. The authors reported that around 80% of the adsorbed P was remobilized in the regeneration process tested in columns. In column experiments, the regenerated material exhibited the same effectiveness of P removal when compared to the original media (>98%). When tested in a field-scale filtering system, the regenerated material was able to remove 34% of incoming phosphate in comparison to 75% removal by the original iron oxyhydroxide. However, in the field-scale system, the authors used 195 L of 4% by weight NaOH solution, while the pore volume of the PSM in the field system was 229 L; to reproduce the laboratory conditions, 687 L would be required for a 3 pore volume flush. The lesser volume used for regeneration may have contributed to the inferior performance of the field system as compared to the results obtained from the laboratory trial.

In another study, Kunaschk *et al.* [20] successfully tested a regeneration method on a granular hydrated ferric oxide using three steps: (1) Fe-rich adsorbent was rinsed with diluted hydrochloric acid, (2) desorption of P using 80 to 100 bed volumes of 1 M NaOH solution and (3) adsorbent was rinsed with deionized (DI) water until reaching a near-neutral

pH. The authors reported that the adsorbent was nearly restored to its initial state after six regeneration cycles.

The regeneration research cited above share one common notion: pH manipulation forcing P from the surface adsorption sites. Ligand exchange is a pH-sensitive mechanism, and the affinity between the media and P is directly affected by the addition of OH^- . The added anion competes with the adsorbed phosphate and the equilibrium in Equation (3.1) is reversed.

In this research, the degree of reversibility of P adsorption by Al/Fe compounds was evaluated, and based on that, a regeneration strategy for Al/Fe-rich PSMs was developed, in order to improve cost and longevity of P removal structures. Specifically, the objectives for this work were to (1) evaluate P removal by three different Al/Fe-rich media at two different inflow P concentrations under flow-through conditions; (2) test the efficiency of different pore volumes, residence time, and number of recirculations on stripping P from PSMs; (3) quantify the ability of the regenerated media to remove P; and (4) determine if regeneration is repeatable. This study differs from previous research on PSM regeneration in that it uses simpler regeneration sequences and feasible pore volumes, residence time, and number of recirculations that can be translated to manageable techniques when scaling up to field P removal structures.

3.3 Materials and Methods

3.3.1 Characterization of PSMs

ActiGuard AAFS50 (henceforth referred to as Alcan), Biomax and PhosRedeem are the objects of this research. Alcan and Biomax are manufactured media, while PhosRedeem is a naturally occurring mined mineral; all three are commercialized as media for contaminant removal. Alcan (Axens Solutions, Rueil-Malmaison, France) is an iron-enhanced activated alumina, marketed for arsenic removal, but also proven useful in phosphate and nitrate reduction [21]. Biomax is a product of ABS Materials (Wooster, OH), marketed as a solution for stormwater treatment [22], and PhosRedeem (US Iron LLC Mines, Miramar Beach, FL, USA) is an iron oxide-based mineral, marketed specifically for P removal of surface waters.

Table 3.1 shows the major elemental composition of the tested PSMs, obtained through acid digestion (Method USEPA 3050B Acid digestion of sediments, sludges and soils; six replications). The Al, Ca, Fe and Mg concentration in digestates was determined by inductively coupled plasma optical emission spectroscopy (ICP-OES). Media pH (two replications) was determined with an ion-selective electrode in deionized (DI) water (1:5 solid:solution ratio) after equilibration for 15 min.

Prior to the experiments, PhosRedeem was sieved to obtain between 0.5–2 mm particle diameter. Alcan was washed with DI water and filtered through a geotextile fabric (ADS Geosynthetics 0401T, Advanced Drainage Systems, Hilliard, OH, USA), typically used in the field for constructing P removal structures and blind inlets, in order to remove very fine particles.

3.3.2 Preliminary Evaluation: Flow-Through Experiments and Batch Isotherms

To evaluate the P removal capacity of the PSMs under flowing conditions, flow-through sorption experiments were conducted. A summary of the flow-through technique and setup is further detailed in Penn *et al.* [23]. Essentially, this method is characterized as a dynamic sorption experiment, in which a continuous flow of a P-rich solution passes through a cell containing a known mass of PSM. By collecting samples at predetermined intervals and analyzing for dissolved P concentrations, the total amount of sorbed P is calculated and presented as a function of the cumulative amount of added P. The experiment is ideally conducted until PSM saturation, and duration depends on the sample, incoming concentrations and flow rate. In this work, the objective of the flow-through experiments was to estimate the total P removal capacity of the PSM (in terms of mg P per kg of PSM; “ P_{Max} ”) under the flow-through conditions given below. At this target, the PSMs are considered “saturated” and are no longer effective for removing P (i.e., inflow and outflow P concentrations are equal).

We conducted the flow-through experiments using two inflow P concentrations: 0.5 mg L⁻¹ and 50 mg L⁻¹, simulating typical agricultural drainage and wastewater P concentrations, respectively. The solutions were produced with potassium phosphate (KH₂PO₄) and DI water. The mass of PSM used in the experiments varied between 0.75 g and 3 g, and inert

pure quartz sand (Acros Organics, CAS: 14808-60-7) was added to complete 5 g of media in the flow-through cell, in order to achieve the desired pore volume. The theoretical hydraulic residence time (RT) was 0.28 min and the duration of the experiments varied between 360 and 720 min, depending on the materials and P inflow concentration. All flow-through experiments were conducted in duplicates.

The results from this preliminary evaluation allowed calculation of P_{Max} under the specified flow-through conditions, i.e., the target in the first sorption phase (S0) of the regeneration sequence. The P_{Max} value (Table 3.2) was calculated as the mean between the two replicates of each material.

Following the preliminary flow-through sorption experiments, batch isotherms were conducted to determine the P concentrations (mg L^{-1}) that corresponded to the target P_{Max} ($\text{mg P per kg of PSM}$) for each PSM at both inflow P concentrations (i.e., 0.5 and 50 mg L^{-1} ; Table 3.2). Using batch isotherms in the first sorption phase allowed for quickly saturating a large mass of PSM to the level of P_{Max} , in preparation for testing the first regeneration. The P concentrations tested in the isotherms (solid:solution ratio of 1:15 and 3 hours of equilibration) were 0, 0.5, 5, 25, 50, 100, 200, 500, 750 and 1000 mg L^{-1} . The isotherms revealed a linear behavior for all PSMs. After fitting the appropriate model, the P concentration that would be used for saturating the PSMs in order to achieve P_{Max} was established (individual P concentrations are listed below).

3.3.3 Sorption-Desorption Cycles: Testing Regeneration Treatments

The regeneration treatments were evaluated through sorption-desorption cycles (Table 3.3). The experiments were conducted on the flow-through system, except for the first sorption phase (S0). The objective of S0 was simply to load the PSM sample to achieve P_{Max} previously determined from the preliminary flow-through experiments, specific to each PSM and inflow P concentration. Using the same solid:solution ratio and equilibration time as the batch isotherm, a sufficient mass of each PSM was initially saturated to achieve their respective P_{Max} , for use in the subsequent regeneration experiments described below. Specifically, the value corresponding to the 0.5 mg P L^{-1} inflow P_{Max} was achieved by equilibrating 1000, 570, and 88 mg P L^{-1} with Alcan, Biomax, and PhosRedeem, respectively.

For the 50 mg L⁻¹ inflow P_{Max} value, samples were equilibrated with 1250, 1470, and 2800 mg P L⁻¹ with Alcan, Biomax, and PhosRedeem, respectively. The target P_{Max} values are listed in Table 3.2. The remaining phases were all conducted in the flow-through system with several adaptations for desorption, including the elimination of the Mariotte bottle, since specific pore volumes and recirculation number were being tested.

Every sorption phase was followed by a desorption phase, i.e., the regeneration step. 1 M KOH was used as the regenerative solution. Hydroxyl is the hardest Lewis base among common inorganic anions, therefore, KOH acts as an eluting reagent [24]. The use of KOH rather than NaOH was proposed to potentially increase the added value of the final extract, which would contain both potassium (K) and P.

We tested regeneration treatments at two different initial P_{Max} values by varying the volume of regenerative solution, RT and number of recirculations (Figure 3.1). The volume of regenerative solution tested was 5 and 20 pore volumes. The regeneration treatment consisted of adding the appropriate amount of KOH to the sample inside the adapted flow-through cell and adjusting the flow rate to achieve the desired RT: 0.5 min or 10 min. When recirculation was tested, the outflow tube of the cell was connected back into the inflow and the KOH solution was allowed to recirculate through the media to test the impact of 6 and 24 recirculations. For no-recirculation experiments, once the entire solution flowed through the PSM, it was immediately collected and not pumped back into the inflow of the cell. After desorption, the PSM samples were rinsed twice in a 60-mL vial to remove P remaining in pore water. The rinse involved using a 0.01 KCl solution at a ratio of 1:15 with 5 min equilibration. The same rinsing process was repeated after sorption cycles, but only once. The PSM samples were then air-dried before the next phase.

As described in Table 3.3 and Figure 3.1, 2 cycles of sorption-desorption were conducted. Table 3.3 specifies the terms “cycle” and “phase”, respectively, as the sorption-desorption sequence (cycle) and the individual sorption or desorption experiments (phase), e.g., cycle 0 refers to the first sorption-desorption phases jointly, while phase S0 refers to the first sorption run alone. By repeating the sorption-desorption cycle, the main purpose was to evaluate whether repeated regeneration would result in similar efficacy of P stripping. All collected samples from sorption and desorption phases were analyzed colorimetrically by the

Murphy–Riley method [25], using an automated analyzer (Gallery, Thermo Fisher Scientific, Waltham, MA USA).

3.4 Results and Discussion

This section consists of a discussion about the P removal ability of the tested PSMs as measured in the flow-through experiments (Section 3.4.1), followed by an evaluation of the proposed regeneration treatments (Section 3.4.2), assessing the effects of P concentration, residence time, volume of regenerative solution and recirculation. Still in Section 3.4.2, the efficacy of repeated desorption phases was examined.

3.4.1 Preliminary Experiments: Evaluation of P Removal Ability of Al/Fe-Rich PSMs

All PSMs possessed a high content of Fe; the differences among them are most evident regarding Ca and Al proportions. Alcan and Biomax are Al-dominated, while PhosRedeem is Fe- and Ca-dominated. Based on the pH measurements, Alcan and Biomax offer favorable conditions for P adsorption by Al/Fe, while pH of PhosRedeem is within the range that favors Ca precipitation. Nevertheless, as Fe and Al were predominant, the expectation was that P removal would be dominated by adsorption, a mechanism less dependent on RT. Based on that, the sorption experiments were conducted under a short RT (0.28 min) for all PSMs.

Cumulative P removal under flow-through conditions was measured as a function of total P added during the experiments. We tested two levels of P concentrations, as described in Section 3.3.2. The advantage of flow-through experiments over the more common batch isotherms is the ability to determine a more practical P_{Max} value that is specific to flow-through conditions, rather than an absolute maximum that occurs through saturating media with unrealistic P concentrations. The flow-through experiments simulate processes occurring in P removal structures, therefore, the estimated P removal potential can be scaled up to field installations. P removal potential is estimated with more realistic conditions. The P removal flow-through curves are shown in Figures 3.2–3.4, for both P concentration levels.

The shape of the curves provides information about P removal potential and longevity of PSMs. For instance, a steeper slope, such as the one observed in the PhosRedeem curves, is an indication of a short-lived PSM. On the contrary, Biomax and Alcan exhibited a gradual decay, indicating a longer lifetime in comparison to PhosRedeem, as quantified by the slope of the exponential model listed in Table 3.2 and Figures 3.2–3.4. Additionally, P removal curves for Biomax and Alcan were similar at both 0.5 and 50 mg P L⁻¹, as indicated by the slope and intercept of the exponential equations. However, Alcan demonstrated a greater longevity in the 0.5 mg L⁻¹ experiments. After adding 8000 mg P kg⁻¹ media, cumulative P removal by Alcan was still above 40%, which is considered the target P reduction for western Lake Erie as established by the Great Lakes Water Quality Agreement (GLWQA) [26].

The differences in P removal between the PSMs at 0.5 mg P L⁻¹ inflow were not observed during the 50 mg P L⁻¹ sorption experiments. In fact, for the 50 mg L⁻¹ experiments, Alcan, Biomax and PhosRedeem had a relatively similar behavior in terms of P removal, while the PhosRedeem had a much lower slope compared to Alcan and Biomax at 0.5 mg P L⁻¹ (Table 3.2). For Alcan and Biomax, the similarity in flow-through sorption slope and intercepts between the 0.5 and 50 mg P L⁻¹ experiments reveals that the P sorption mechanism is likely dominated by ligand exchange. Little difference in percent P removal with increasing P concentrations is a characteristic of ligand exchange that distinguishes it from precipitation [27], whereas precipitation increases percent P removal as the initial concentration is increased. Phosphorus removal by PhosRedeem improved with inflow concentrations of 50 mg P L⁻¹ compared to 0.5 mg P L⁻¹, suggesting precipitation as the dominant mechanism. Overall, all three PSMs tested would behave similarly in removing P from wastewater treatment plants; however, Alcan would be the most appropriate media to be used to treat non-point drainage water containing low P concentrations.

3.4.2 Regeneration Treatments

Overall, PhosRedeem had the lowest desorption efficacy when comparing the PSMs. In fact, during the 0.5 mg P L⁻¹ PhosRedeem treatments, none of the evaluated desorption phases were able to displace P. The unsuccessful desorption can be attributed to the fact that the dominant removal mechanism for PhosRedeem is likely Ca-phosphate precipita-

tion and not Fe adsorption. Because Ca-dominated PSMs with pH levels above 6, such as PhosRedeem (Table 3.1), favor the precipitation of Ca-phosphates [20], the proposed regeneration treatment would be ineffective for such products. The pH measured in treated water samples confirmed the prevalence of elevated pH. More specifically, the range of pH measured in random outflow samples collected from the PhosRedeem 0.5 mg L⁻¹ flow-through experiments was 8.98 to 10.19. For the same experimental conditions, pH range of Alcan and Biomax flow-through samples was 6.31-9.35 and 6.12-9.39, respectively, with the lower values reported towards the end of the experiment. Further evidence of P removal via precipitation is supported by the increase in P removal from increasing P inflow concentrations from 0.5 to 50 mg P L⁻¹, as previously discussed. Additionally, in order to illustrate the dependency of PhosRedeem P removal on Ca precipitation—and therefore, on RT, flow-through sorption experiments were conducted under various RT: 0.5, 2 and 5 min (Figure D.1). It is clear that P removal was dependent on RT (Figure D.2). For instance, consider the experiments conducted with a 5-minute RT compared to 0.5 min. The greater P removal at a RT of 5 min was confirmed by a Tukey Studentized Range Test; RT=5 min resulted in significantly greater P removal in comparison to the other RTs ($\alpha = 0.05$).

All tested regeneration treatments were successful on Biomax and Alcan, for samples produced from both 0.5 and 50 mg P L⁻¹ P sorption experiments. The differences in desorption capacity between the tested treatments are discussed in the sections below. We evaluated the efficacy of desorption as “P recovery”, a relative measurement calculated according to Equation (3.2):

$$\text{P recovery (\%)} = 100 \times \frac{\text{Total P desorbed (mg P kg}^{-1} \text{ media)}}{\text{Total P sorbed (mg P kg}^{-1} \text{ media)}} \quad (3.2)$$

P recovery was calculated per cycle and was used as the comparative measure for the different treatments and PSMs tested. Additionally, the net P sorbed after completing all cycles is also shown. The average P recovery across all treatments and sorption-desorption cycles was 81%, 79% and 7% for Alcan, Biomax and PhosRedeem, with standard deviations (S_x) of 10%, 21% and 6%, respectively.

Effect of P Concentration on Regeneration

As discussed in Section 3.3.2, two levels of P concentrations were tested, 0.5 and 50 mg P L⁻¹. Intuitively, there was an expectation that the PSM saturated with the greater P concentration (50 mg P L⁻¹) would result in more P being stripped in the subsequent desorption phase. It is known that the sorption of P is concentration-driven, the question here was whether the desorption would also exhibit similar behavior.

In absolute terms, 50 mg P L⁻¹ experiments did in fact result in a greater amount of desorbed P, but the increase in desorption was not proportional to the P concentration increase from 0.5 to 50 mg P L⁻¹. For instance, for Alcan, the first desorption phases (D0) exhibited a range of total desorbed P of 4380–10,900 and 5000–13,300 mg P per kg of media across the different treatments for the 0.5 mg P L⁻¹ and 50 mg P L⁻¹, respectively. For Biomax, the ranges were 1700–8000 and 7800–16,100 mg P kg⁻¹ PSM for the low and high levels of P concentration, respectively. However, when considering 0.5 mg P L⁻¹ and 50 mg P L⁻¹ in terms of the amount of P desorbed compared to the amount of P sorbed in the previous sorption phase, a certain proportionality in most of the tested treatments can be identified. The predicted amount of P to be desorbed in the 50 mg P L⁻¹ experiments was calculated based on the proportion of total adsorbed and desorbed in the 0.5 mg P L⁻¹ experiments. (A true proportional amount of P desorbed in the 50 mg P L⁻¹ experiments would be 100% of the expected amount of desorbed P, based on the results obtained in the 0.5 mg P L⁻¹ experiments.) The observed and predicted P desorbed were similar in 4 and 3 of the 5 desorption treatments with Alcan and Biomax, respectively (100% ± 10%). The remaining predictions showed a deviation of 55% or less compared to the actual results for both Alcan and Biomax.

Overall, the desorptions following the 0.5 mg L⁻¹ P and 50 mg L⁻¹ P sorption experiments showed similar P recovery for both Biomax and Alcan. For instance, Alcan exhibited an average P recovery across all treatments of 67% and 64% for low and high P concentrations, respectively, with standard deviations (S_x) of 26% and 16%. For the same experimental conditions, Biomax exhibited an average P recovery of 65% ($S_x = 20\%$) and 64% ($S_x = 21\%$).

For PhosRedeem, the 0.5 mg P L⁻¹ desorption treatments were virtually ineffective. For the 50 mg P L⁻¹ samples, however, D0 could remove a portion of P (9% to 16% of total P sorbed during previous P sorption phase). We do not attribute the P desorption to chemical regeneration via ligand exchange, but rather a result of dissolution of P minerals formed in the sample. This conclusion arises from the fact that both KOH and the KCl wash were equally effective in removing P from the PhosRedeem samples. The second desorption phase (D1) was again virtually ineffective for this PSM, at both P concentrations tested.

Thus far, the discussion regarding P concentration was based solely on cycle 0, the first sorption-desorption cycle, aiming to isolate the effect of input P concentrations on regeneration. For the second phase (D1), carry-over effects must also be considered. Overall, the results showed that Biomax and Alcan at both low and high P saturation levels can be regenerated to achieve similar P recovery. For PhosRedeem, regeneration treatments were ineffective at both P concentration levels.

Effect of Residence Time

We tested two residence times (RT) during the regeneration phases: 0.5 and 10 min. Our hypothesis was that a longer RT would allow for a greater contact between the KOH solution and media, resulting in a more effective P desorption.

Both RTs were tested using 20 pore volumes of KOH for each PSM and no recirculation. At this point, it had been already established that the regeneration treatment was not effective for PhosRedeem, and therefore this PSM was excluded from this discussion. Additionally, only D0 was used for the comparison between RTs, aiming to isolate the effect of this variable on the regeneration treatment.

For Alcan, P recovery in D0 using RT=10 min was moderately superior over 0.5 min, with 93% ($S_x = 2\%$) and 82% ($S_x = 6\%$), respectively. These values refer to the average P recovery of both inflow concentration levels. For the 0.5 mg P L⁻¹ experiments only, the average P recovery was 95% ($S_x = 1\%$) and 82% ($S_x = 5\%$), at a RT 10 min and 0.5 min, respectively. Phosphorus recovery for the 50 mg P L⁻¹ treatments was also in the same range: 91% ($S_x = 2\%$) and 82% ($S_x = 9\%$) for 10 and 0.5 min, respectively. The differences

in P recovery between RTs in D0 were statistically significant for Alcan (p -value = 0.01; Figure 3.5). (All statistical tests were conducted at a significance level of 0.05.)

Biomax exhibited similar P recovery for 0.5 min and 10 min for the 0.5 mg P L⁻¹: 88% (S_x = 20%) and 91% (S_x = 4%). The difference between RTs for Biomax was not statistically significant (p -value = 0.19). During the 50 mg P L⁻¹ experiments, however, RT=10 min showed a relatively better efficacy, with 92% (S_x = 0.5%) in comparison to 67% (S_x = 2%) using RT=0.5 min (Figure 3.5).

Based on this analysis, a RT of 10 min would be preferred in a regeneration treatment of PSMs, particularly when dealing with higher input P concentrations. The difference between all 10 min treatments in comparison to all 0.5 min proved to be statistically significant (p -value = 0.02). However, when comparing only the 0.5 mg L⁻¹ experiments, the difference between RTs was not significant (p -value = 0.28). These results indicate that a longer RT can improve the results of regeneration in heavily P loaded samples, perhaps because it allows for greater potential contact between P on the sorption sites and the OH⁻ in solution. For the 0.5 mg L⁻¹, the shorter RT is sufficient for a thorough contact between sorbed PO₄ and the regenerative solution. We chose to conduct the remaining treatments using RT = 0.5 min, aiming for establishing an effective yet simplest and most feasible regeneration methodology at the field scale.

Effect of Volume of Regenerative Solution

In this analysis, the 5 and 20 pore volumes (PV) treatments with no recirculation and RT = 0.5 min were compared with regards to P recovery. The expectation was that a larger volume of KOH would be able to desorb a larger amount of P, given the greater OH⁻ availability.

There was a clear improvement in P recovery for the first desorption phase (D0) using 20 PV rather than 5 PV, for both 0.5 and 50 mg P L⁻¹ treatments. According to a two-sample t-test, the difference in P recovery between 5 and 20 PV was significant (p -value = 9.69×10^{-6}) and that difference can be visualized in Figure 3.6. For D1, the relationship was not as clear. For instance, in Alcan 0.5 and 50 mg L⁻¹ experiments, 5 PV showed to be more efficient than 20 PV. However, other variables may be influencing P recovery in D1, due to

legacy effects from the previous phases. Therefore, the discussion regarding the effects of different volumes of KOH will be limited to the S0-D0 cycle.

Over all P treatments and PSMs in D0, 5 PV had an average P recovery of 39% ($S_x = 12\%$), in contrast with 80% ($S_x = 12\%$) for 20 PV treatments (Figure 3.6). A larger volume of regenerative solution clearly improves P recovery; however, there is a trade-off with increasing the volume of regenerative solution regarding feasibility, given the large amounts of PSMs typically used in P removal structures.

There is a lack of literature sources discussing the implementation of desorption of P from PSMs at a large scale. Most of the research is conducted in the laboratory, where there are no limitations regarding the amount of regenerative solution to be used, due to the small scale used. In this research, the goal was to evaluate solid:solution ratios that would be most feasible for large structures, especially regarding transport logistics and cost. This is one aspect that previous research overlooked, as some used up to 100 bed volumes of regenerative solution [18], [20]. Moreover, with satisfactory P recovery achieved through using 5 or 20 PV, the cost of regeneration can be decreased. Recovery of P in smaller volumes also contributes to the feasibility of recovering the nutrient for posterior use as fertilizer. The comparative analysis of the levels of PV without recirculation indicated that 20 PV is preferred.

Effect of Number of Recirculations

Number of recirculations (RC) was tested at $RT = 0.5$ min. For Alcan 0.5 mg P L^{-1} treatments, P recovery was 64% ($S_x = 6\%$) and 46% ($S_x = 0.5\%$) with 6 and 24 RC, respectively. At the same P concentration level, Biomax exhibited similar levels of P recovery on both RC tested: 64% ($S_x = 2\%$) and 60% ($S_x = 2\%$), for 6 and 24 RC, respectively. For the 50 mg P L^{-1} experiments, 6 and 24 RC showed equivalent efficacy, for both Alcan (58% and 55%, respectively, with $S_x = 1\%$ in both conditions) and Biomax (54% and 58%, with $S_x = 3\%$ and $S_x = 0.5\%$, respectively).

Overall, there was no effect of increasing the number of recirculations from 6 to 24, as the difference between these values was not significant ($p\text{-value} = 0.09$). However, when comparing P recovery between recirculation (6,24) and no-recirculation (0) for D0 only, a clearer advantage in using recirculation is observed, as shown in Figure 3.7. The average P

recovery in the 5 PV no recirculation treatment is 39% ($S_x = 12\%$), in contrast with 59% ($S_x = 5\%$) and 54% ($S_x = 6\%$) for 6 and 24 recirculations, respectively. These averages refer to both Alcan and Biomax.

There is an advantage in using recirculation during the desorption phases in comparison to no recirculation when using 5 PV and RT of 0.5 min. By recirculating KOH, a greater potential for contact between the sorbed P and the input solution was imposed, with a better use of the available OH^- . However, when evaluating all tested treatments, the efficacy of 20 PV with no recirculation is still higher (average P recovery is 80% across all 20 PV experiments, with $S_x = 12\%$) than a 5 PV with 6 recirculations (P recovery average of 60%, with $S_x = 6\%$). Thus, the data suggests that when using the larger PV of 20, recirculation does not have much of an impact, but at the smaller PV, recirculation improves P recovery. Recirculation likely improves P recovery at smaller PVs by increasing contact between the added hydroxide and surface-complexed phosphate.

Effect of Repeated Desorption Cycles

Based on previous research conducted on Fe oxides, there was a suspicion that each regeneration treatment would be less effective than the prior. Cabrera *et al.* [28] discussed that the difficulty in desorbing all P can be explained by its occlusion within the oxides and/or micropores. Our intention in conducting a rinse after each phase was to displace remaining P in interstitial water. However, desorption phases and their respective rinses were never able to remove 100% of the adsorbed P, perhaps due to occlusion of P within the Fe-oxide. As sorption phases were repeated, more P became occluded and the efficacy of the treatment decreased.

We observed that P recovery for D1 (i.e., the second desorption phase) was highly variable across the different treatments and PSMs, ranging from 0 to 6000% (Figures 3.8–3.10). This variability demonstrates the carry-over effects of previous sorption and desorption phases. In most of the treatments, D1 had a P recovery of more than 100%, meaning that the KOH regeneration was able to displace P from earlier P additions (i.e., sorption phases). After D1, another sorption phase (S2) was conducted, in which the PSMs were observed to retain more P than in the previous sorption (S1). The P removal capacity of the PSMs was successfully

recovered in that second desorption phase. (The total mass of sorbed and desorbed P per treatment, phase and cycle is shown in Tables E.1–E.3.)

Our hypothesis of decreasing efficacy of desorption with repeated regeneration treatment was confirmed. For instance, consider the 20 PV, $RT = 0.5$ min treatment on Alcan at the low level of P (0.5 mg P L^{-1}): $9700 \text{ mg P kg}^{-1}$ of PSM was desorbed in the first desorption phase (D0), in comparison to $2100 \text{ mg P kg}^{-1}$ of PSM in the second desorption phase (D1). Thus, regarding the actual mass of P desorbed in mg P kg^{-1} , D0 was more effective than D1. However, when comparing P recovery (Equation (3.2)), D1 (190%) was superior to D0 (85%), due to the reduced amount of P sorbed during S1. The same decrease in total desorbed P from D0 to D1 was observed for all tested treatments, except Alcan and Biomax 50 mg P L^{-1} , at 5 PV, with no recirculation (Tables E.1 and E.2). Despite this decrease, P recovery across all sorption-desorption cycles (S0-D0 and S1-D1) was substantial. For some of the tested treatments, the net P was 0, as 100% of the added P was recovered.

We conclude that regeneration cycles can be repeated and although the efficacy of the treatment decreased in absolute values (mg P kg^{-1}), P recovery (%) did not follow the same pattern due to legacy effects of previous cycles.

3.5 Conclusions and Implications

Low volumes of regenerative solution are effective for desorption treatments, which can enable the use of regeneration in field-scale P removal structures. Desorption treatments can be used under conditions where PSMs were saturated with P from either low or high P inflow concentrations, simplifying the use of PSMs for P removal. Residence time did not show a significant effect on the final P recovery, measured across all sorption and desorption cycles. In general, increasing the volume of regenerative solution from 5 to 20 PV increased P recovery. Pore volume was more influential than the number of recirculations. For example, the most effective regeneration treatment used 20 PV of 1 M KOH with no recirculation, as recirculation did not improve P recovery when 20 PV were used. Although the smaller PV of 5 was less effective than 20 PV, the use of recirculation (6 or 24 times) increased P recovery. This is important because increasing the PV of regeneration solution translates to greater chemical costs and the need for bigger equipment (tanks) to handle the larger

volume of solution, whereas increasing the number of recirculations can be achieved more easily as it simply results in a longer time required for regeneration.

For PhosRedeem, the analysis indicated that although it is a material that resembles a Fe-rich PSM and is commercialized as such, the dominant mechanism of removal is likely Ca-phosphate precipitation. Evidence for this conclusion is found in four observations: (1) the PSM contained a high Ca concentration and maintained an elevated solution pH, (2) P removal increased with increasing RT, (3) an increase in inflow P concentration from 0.5 to 50 mg P L⁻¹ dramatically increased percent P removal, and (4) regenerative treatment with KOH was virtually ineffective.

Regeneration was equally effective on Biomax and Alcan, with final P recovery ranging from 66–100%. Therefore, although these are manufactured PSMs with an appreciable higher cost (about 22 and 3.3 U.S. dollars per kg for Biomax and Alcan, respectively) in comparison to industrial by-products, their use can be effectively extended through the regeneration techniques demonstrated.

The costs of P desorption and PSM regeneration can be segmented into PSM, transportation, chemical solutions, required equipment, and labor. As a demonstration, consider an actual site located in Ohio, U.S., in which a 10 Ha field produces 0.2 mg L⁻¹ dissolved P from 16.3 ML of annual flow volume from a subsurface tile drain. Using the P removal curve shown in Figure 3.2a, it would require 2.1 Mg of Alcan to remove 40% of the 10-year dissolved P load. This mass of Alcan would cost approximately 6800 U.S. dollars. Assuming an additional US \$6000 for materials and labor, this would result in a P removal cost of US \$1000 per kg dissolved P removed, which is within the realm of the cost of P removal in wastewater treatment. However, consider that subsequent regeneration would decrease the cost of P removal nearly in half, for every regeneration cycle, since it would not involve any new expenses with PSM replacement. While it is tempting to consider the value of the recovered P in offsetting structure costs, it is important to keep in mind that the mass of dissolved P being lost to surface waters is very small compared to agronomic requirements. Considering current costs of P fertilizer (US \$1–2 per kg), the amount of P trapped after ten years with this theoretical structure (12.8 kg) is only worth US \$13–26, and not even enough P for fertilization of one ha for a single year. However, under situations where PSMs are

used to treat wastewater with high P concentrations, it may become economically favorable to recover the P in the regeneration solution. More research is needed in order to evaluate the feasibility of recovering the desorbed P.

Phosphorus losses to surface waters are considered one of the primary drivers of cultural eutrophication. Eutrophication and associated harmful algal blooms have been reported all over the world, and their occurrence has been increasing with growing anthropogenic pressures on the environment. Current field conservation practices will not be effective in reducing dissolved P in drainage waters, and P removal structures can be an important ally to control dissolved P transport before P enters ditches and channels. However, the construction and maintenance of these structures can be cost-limiting. Our work offered a cost-effective alternative to the replacement of PSMs, improving the longevity and, consequently, the potential ecological benefit of P removal structures.

Overall, the conclusions of this work were: (1) Al/Fe-rich materials can have their P removal ability recovered after the media is saturated with P, (2) the level of P concentration in the sorption phases did not significantly impact P recovery; (3) for higher input P concentrations, increasing RT of regeneration phase resulted in greater P recovery; (4) a larger volume of regenerative solution did result in more P being desorbed; (5) increasing the number of recirculations did significantly improve the efficacy of 5 PV desorptions, and (6) the regeneration treatment can be repeated, but with decreasing efficacy in absolute values of desorbed P.

References

- [1] C. Vohla, M. Kõiv, H. J. Bavor, F. Chazarenc, and Ü. Mander, “Filter materials for phosphorus removal from wastewater in treatment wetlands—a review,” *Ecological Engineering*, vol. 37, no. 1, pp. 70–89, 2011.
- [2] C. Penn, I. Chagas, A. Klimeski, and G. Lyngsie, “A review of phosphorus removal structures: How to assess and compare their performance,” *Water*, vol. 9, no. 8, p. 583, 2017.

- [3] D. Claveau-Mallet, S. Wallace, and Y. Comeau, "Model of phosphorus precipitation and crystal formation in electric arc furnace steel slag filters," *Environmental science & technology*, vol. 46, no. 3, pp. 1465–1470, 2012.
- [4] B. J. Allred, L. R. Martinez, and D. L. Gamble, "Phosphate removal from agricultural drainage water using an iron oxyhydroxide filter material," *Water, Air, & Soil Pollution*, vol. 228, no. 7, p. 240, 2017.
- [5] K. Dobbie, K. Heal, J. Aumonier, K. Smith, A. Johnston, and P. Younger, "Evaluation of iron ochre from mine drainage treatment for removal of phosphorus from wastewater," *Chemosphere*, vol. 75, no. 6, pp. 795–800, 2009.
- [6] T. D. McCobb, D. R. LeBlanc, and A. J. Massey, "Monitoring the removal of phosphate from ground water discharging through a pond-bottom permeable reactive barrier," *Groundwater Monitoring & Remediation*, vol. 29, no. 2, pp. 43–55, 2009.
- [7] R. Wood and C. McAtamney, "Constructed wetlands for waste water treatment: The use of laterite in the bed medium in phosphorus and heavy metal removal," *Hydrobiologia*, vol. 340, no. 1-3, pp. 323–331, 1996.
- [8] O. Bastin, F. Janssens, J. Dufey, and A. Peeters, "Phosphorus removal by a synthetic iron oxide–gypsum compound," *Ecological Engineering*, vol. 12, no. 3-4, pp. 339–351, 1999.
- [9] N. Boujelben, J. Bouzid, Z. Elouear, M. Feki, F. Jamoussi, and A. Montiel, "Phosphorus removal from aqueous solution using iron coated natural and engineered sorbents," *Journal of hazardous materials*, vol. 151, no. 1, pp. 103–110, 2008.
- [10] M. E. Clayton, S. Liegeois, and E. J. Brown, "Phosphorus sequestration in lake sediment with iron mine tailings," *Soil & Sediment Contamination*, vol. 13, no. 5, pp. 421–431, 2004.
- [11] G. M. Ayoub, B. Koopman, and N. Pandya, "Iron and aluminum hydroxy (oxide) coated filter media for low-concentration phosphorus removal," *Water Environment Research*, vol. 73, no. 4, pp. 478–485, 2001.
- [12] M. Li, J. Liu, Y. Xu, and G. Qian, "Phosphate adsorption on metal oxides and metal hydroxides: A comparative review," *Environmental Reviews*, vol. 24, no. 3, pp. 319–332, 2016.
- [13] Y. Mao and Q. Yue, "Kinetic modeling of phosphate adsorption by preformed and in situ formed hydrous ferric oxides at circumneutral pH," *Scientific reports*, vol. 6, p. 35 292, 2016.

- [14] I. de Vicente, H. S. Jensen, and F. Ø. Andersen, “Factors affecting phosphate adsorption to aluminum in lake water: Implications for lake restoration,” *Science of the total environment*, vol. 389, no. 1, pp. 29–36, 2008.
- [15] P. Wilfert, P. S. Kumar, L. Korving, G.-J. Witkamp, and M. C. van Loosdrecht, “The relevance of phosphorus and iron chemistry to the recovery of phosphorus from wastewater: A review,” *Environmental science & technology*, vol. 49, no. 16, pp. 9400–9414, 2015.
- [16] H. Siwek, A. Bartkowiak, and M. Włodarczyk, “Adsorption of phosphates from aqueous solutions on alginate/goethite hydrogel composite,” *Water*, vol. 11, no. 4, p. 633, 2019.
- [17] S. Tanada, M. Kabayama, N. Kawasaki, T. Sakiyama, T. Nakamura, M. Araki, and T. Tamura, “Removal of phosphate by aluminum oxide hydroxide,” *Journal of colloid and interface science*, vol. 257, no. 1, pp. 135–140, 2003.
- [18] P. L. Sibrell and T. Kehler, “Phosphorus removal from aquaculture effluents at the northeast fishery center in lamar, pennsylvania using iron oxide sorption media,” *Aquacultural engineering*, vol. 72, pp. 45–52, 2016.
- [19] P. L. Sibrell, G. A. Montgomery, K. L. Ritenour, and T. W. Tucker, “Removal of phosphorus from agricultural wastewaters using adsorption media prepared from acid mine drainage sludge,” *Water research*, vol. 43, no. 8, pp. 2240–2250, 2009.
- [20] M. Kunaschk, V. Schmalz, N. Dietrich, T. Dittmar, and E. Worch, “Novel regeneration method for phosphate loaded granular ferric (hydr) oxide—a contribution to phosphorus recycling,” *Water research*, vol. 71, pp. 219–226, 2015.
- [21] Axens Solutions, *Actiguard®- water treatment series - arsenic metals removal from water*, <https://www.axens.net/product/catalysts-a-adsorbents/228/actiguard-aafs50.html>, 2017 (accessed October, 2019).
- [22] ABS Wastewater, *Biomax™ stormwater & phosphorus removal solutions*, 2016 (accessed February 28, 2019). [Online]. Available: <http://abswastewater.com/markets-served/stormwater-treatment/>.
- [23] C. J. Penn and J. M. Bowen, *Design and construction of phosphorus removal structures for improving water quality*. Springer, 2017.
- [24] M. R. Awual, A. Jyo, T. Ihara, N. Seko, M. Tamada, and K. T. Lim, “Enhanced trace phosphate removal from water by zirconium (iv) loaded fibrous adsorbent,” *Water research*, vol. 45, no. 15, pp. 4592–4600, 2011.
- [25] J. Murphy and J. P. Riley, “A modified single solution method for the determination of phosphate in natural waters,” *Analytica chimica acta*, vol. 27, pp. 31–36, 1962.

- [26] USEPA, Environment and Climate Change Canada, *Annex 4 objects and targets task team, 2015: Recommended phosphorus loading targets for lake erie*, May 2015. [Online]. Available: <https://www.epa.gov/sites/production/files/2015-06/documents/report-recommended-phosphorus-loading-targets-lake-erie-201505.pdf>.
- [27] M. B. McBride, *Environmental Chemistry of Soils*. New York: "Oxford University Press, Inc.", 1994.
- [28] F. Cabrera, P. De Arambarri, L. Madrid, and C. Toga, "Desorption of phosphate from iron oxides in relation to equilibrium ph and porosity," *Geoderma*, vol. 26, no. 3, pp. 203–216, 1981.

Table 3.1. Chemical characterization of PSMs: Average elemental composition and pH.

Sample	Aluminum	Calcium	Iron	Magnesium ⁽¹⁾	pH ⁽²⁾
	mg kg ⁻¹				
Alcan	350,975	348	20,286	0	6.49
Biomax	297,508	356	56,502	0	6.85
PhosRedeem	7567	86,726	335,646	2917	11.49

⁽¹⁾ Elemental composition derived from acid digestions;

⁽²⁾ pH in water.

Table 3.2. Preliminary performance and subsequent maximum phosphorus (P) removed (P_{Max}) by three P sorption materials (PSMs) under flow-through conditions of 0.5 and 50 mg P L⁻¹ inflow and 0.284 min residence time. The P_{Max} values were used as the target for initial P saturation in regeneration experiments.

PSM	Sample	Flow-Through Model ⁽¹⁾	P_{Max} ⁽²⁾
Alcan 0.5 mg L ⁻¹	A05A	$64.98e^{-4.03*10^{-5}x}$	12,043
	A05B	$58.90e^{-2.30*10^{-5}x}$	16,817
	AVERAGE		14,430
	STD DEV ⁽³⁾		3376
Biomax 0.5 mg L ⁻¹	B05A	$63.46e^{-4.87*10^{-5}x}$	9469
	B05B	$64.06e^{-7.604*10^{-5}x}$	6193
	AVERAGE		7831
	STD DEV		2322
PhosRedeem 0.5 mg L ⁻¹	P05A	$79.41e^{-6.10*10^{-4}x}$	1123
	P05B	$76.42e^{-5.56*10^{-4}x}$	1164
	AVERAGE		1144
	STD DEV		16
Alcan 50 mg L ⁻¹	A50A	$68.38e^{-2.84*10^{-5}x}$	18,874
	A50B	$64.34e^{-2.82*10^{-5}x}$	16,849
	AVERAGE		17,861
	STD DEV		1432
Biomax 50 mg L ⁻¹	B50A	$65.62e^{-2.48*10^{-5}x}$	19,992
	B50B	$68.01e^{-2.5*10^{-5}x}$	21,231
	AVERAGE		20,612
	STD DEV		876
PhosRedeem 50 mg L ⁻¹	P50A	$110.99e^{-4.51*10^{-5}x}$	22616
	P50B	$102.48e^{-5.77*10^{-5}x}$	16,308
	AVERAGE		18,884 ⁽⁴⁾
	STD DEV		2829

¹ Exponential general model: $f(x) = a \times e^{b \times x}$, where x is the cumulative P added to PSM in mg kg⁻¹, and $f(x)$ is the cumulative P removal (%);

² Maximum P sorption in the flow-through experiments corresponds to the point in which the PSM sample is P saturated;

³ Standard deviation of replicates;

⁴ Average was calculated based on four replicates and two of them are shown in the table.

Table 3.3. Experimental sequence for sorption and desorption cycles for the regeneration of Al/Fe-rich P sorption materials (PSMs). The same cycles were tested at both low level (0.5 mg P L^{-1}) and high level (50 mg P L^{-1}) P treatments. All experiments were conducted in duplicate.

	SORPTION PHASE	⇒	DESORPTION PHASE/REGENERATION
Cycle 0	Phase S0		Phase D0
	<i>Batch sorption isotherm</i>		<i>Flow-through system</i>
	SORPTION PHASE	⇒	DESORPTION PHASE/REGENERATION
Cycle 1	Phase S1		Phase D1
	<i>Flow-through system</i>		
	SORPTION PHASE		
Cycle 2	Phase S2		
	<i>Flow-through system</i>		

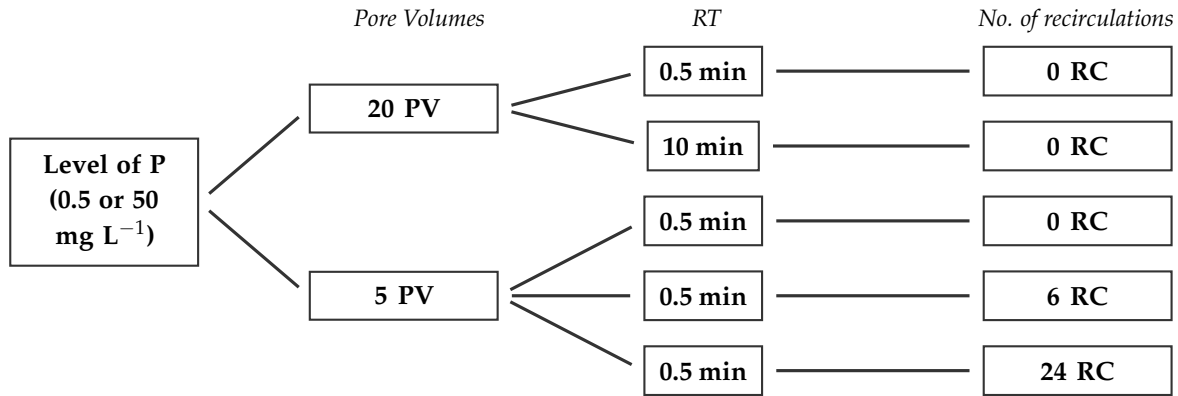


Figure 3.1. Experimental conditions and phosphorus (P) regeneration treatments tested. PV = pore volume; RT = residence time; RC = recirculation.

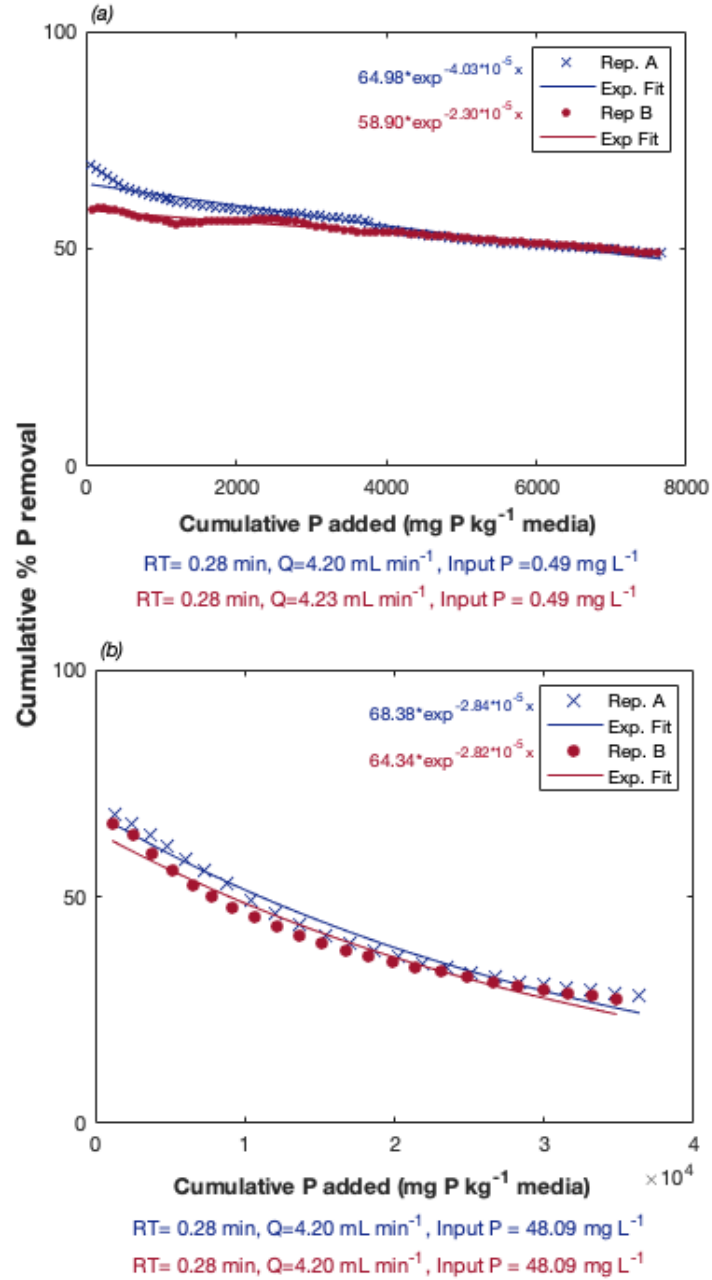


Figure 3.2. Preliminary evaluation of phosphorus (P) removal ability of Alcan in flow-through experiments conducted at a residence time (RT) of 0.28 min and inflow P concentrations of (a) 0.5 mg L⁻¹ and (b) 50 mg L⁻¹. Cumulative P removal is plotted as a function of cumulative P added.

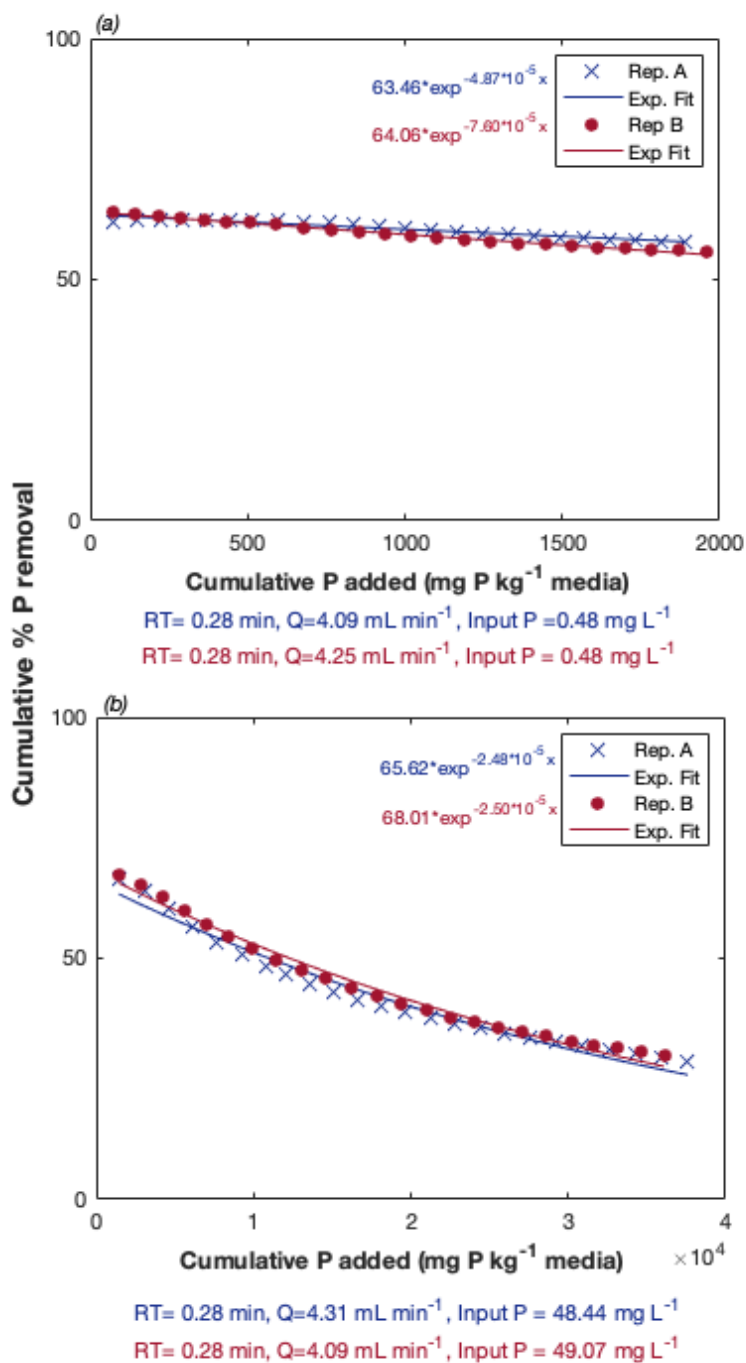


Figure 3.3. Preliminary evaluation of phosphorus (P) removal ability of Biomax in flow-through experiments conducted at a residence time (RT) of 0.28 min and inflow P concentrations of (a) 0.5 mg L⁻¹ and (b) 50 mg L⁻¹. Cumulative P removal is plotted as a function of cumulative P added.

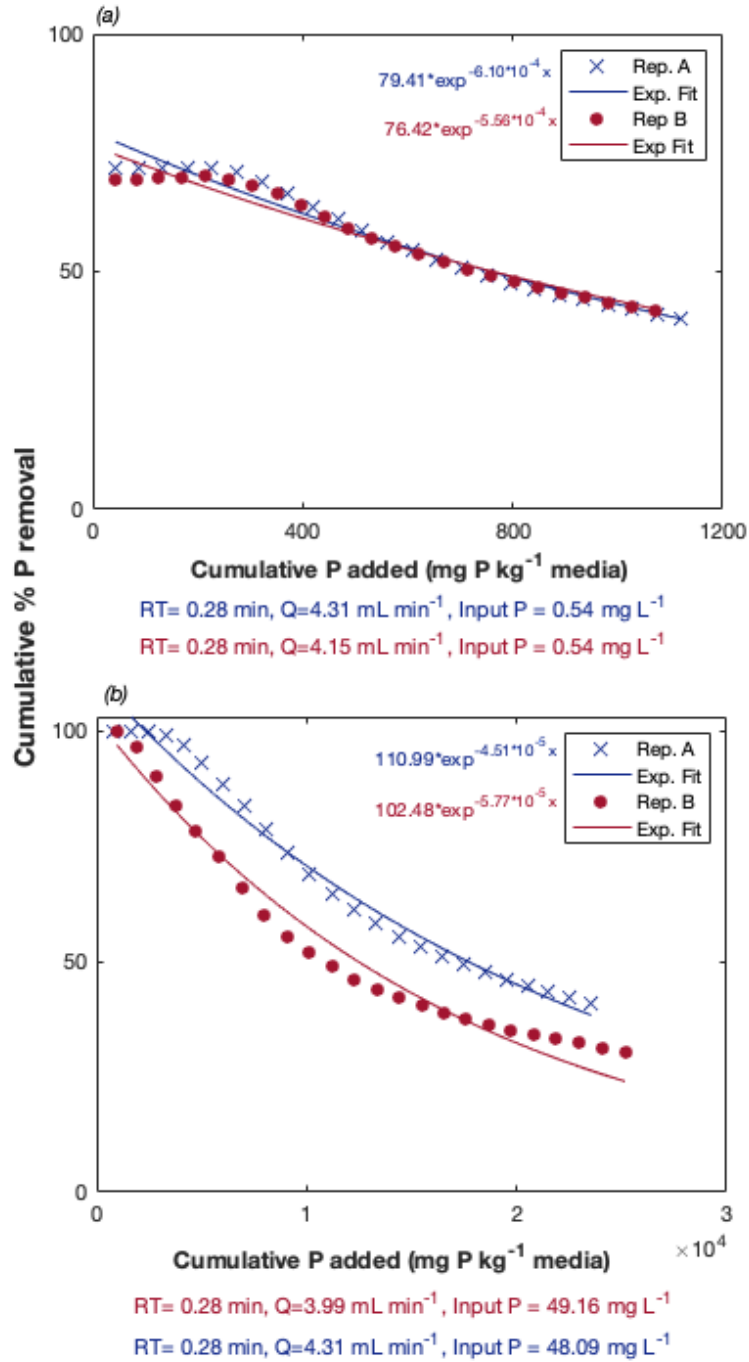


Figure 3.4. Preliminary evaluation of phosphorus (P) removal ability of PhosRedeem in flow-through experiments conducted at a residence time (RT) of 0.28 min and inflow P concentrations of (a) 0.5 mg L^{-1} and (b) 50 mg L^{-1} . Cumulative P removal is plotted as a function of cumulative P added.

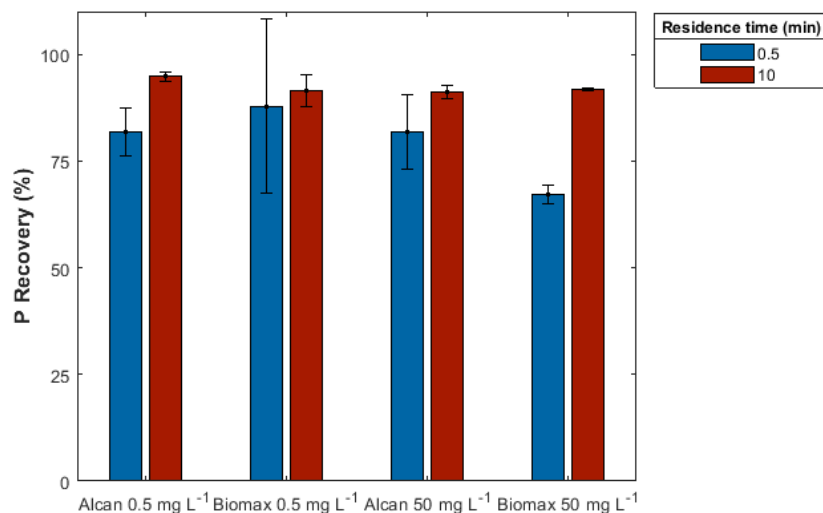


Figure 3.5. Effects of regeneration residence time on phosphorus (P) recovery from P sorption materials (PSM). Phosphorus recovery is shown after the first sorption cycle (S0-D0) only, treated with 20 pore volumes of 1 M KOH and no recirculation. Treatments separated based on PSM type and P concentration used during the sorption phase.

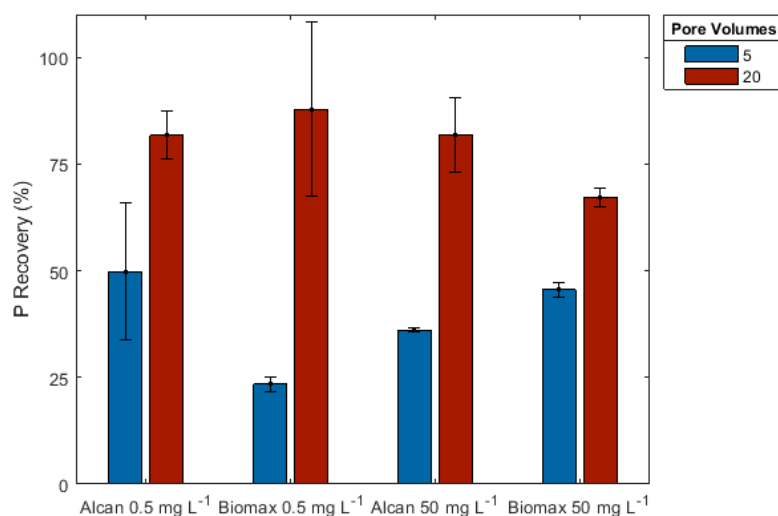


Figure 3.6. Effects of regenerative solution pore volume (PV) on phosphorus (P) recovery from P sorption materials (PSMs). Phosphorus recovery is shown after the first sorption cycle (S0-D0) only, treated with 1 M KOH at a residence time of 0.5 min with no recirculation. Treatments separated based on PSM type and P concentration used during the sorption phase.

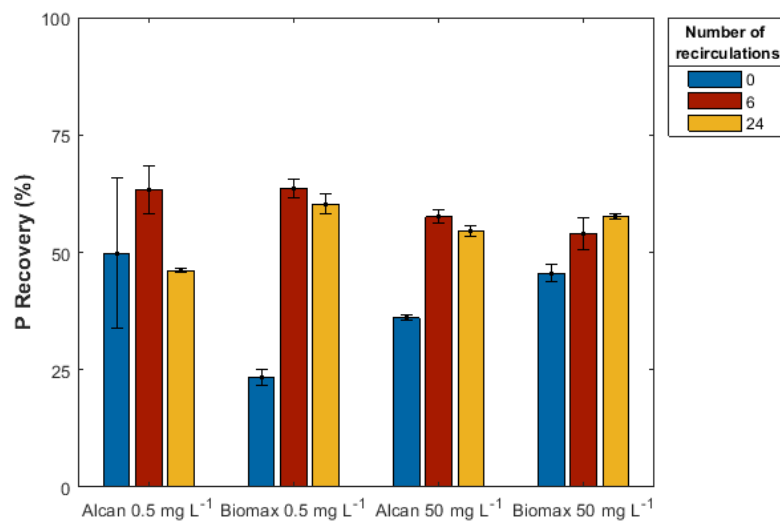


Figure 3.7. Effects of the number of recirculation of regenerative solution on phosphorus (P) recovery from P sorption materials (PSMs). Phosphorus recovery is shown after the first sorption-desorption cycle (S0-D0) only, treated with five pore volumes of 1 M KOH at a residence time of 0.5 min. Treatments separated based on PSM type and P concentration used during the sorption phase.

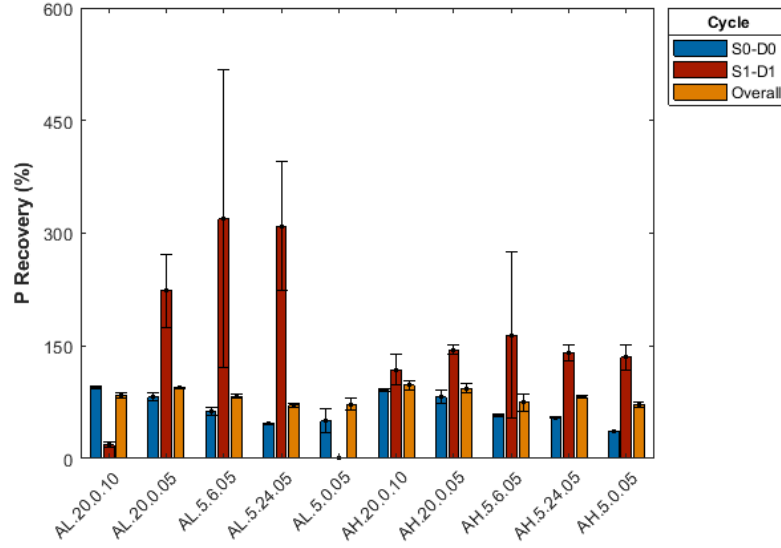


Figure 3.8. Phosphorus (P) recovery across all evaluated cycles and treatments for Alcan. The treatments identified on the x-axis follow the notation: AX.PV.RC.RT, with X being the level of P concentration (L for low or 0.5 mg L⁻¹ and H for high or 50 mg L⁻¹), PV: pore volume (5 or 20), RC: number of recirculations (0,6 or 24) and RT: residence time used in the desorption phase. Phosphorus recovery in the S1-D1 cycle was omitted for the treatment AL.5.0.05, which showed an average of 3233% with standard deviation (S_x) of 2997.

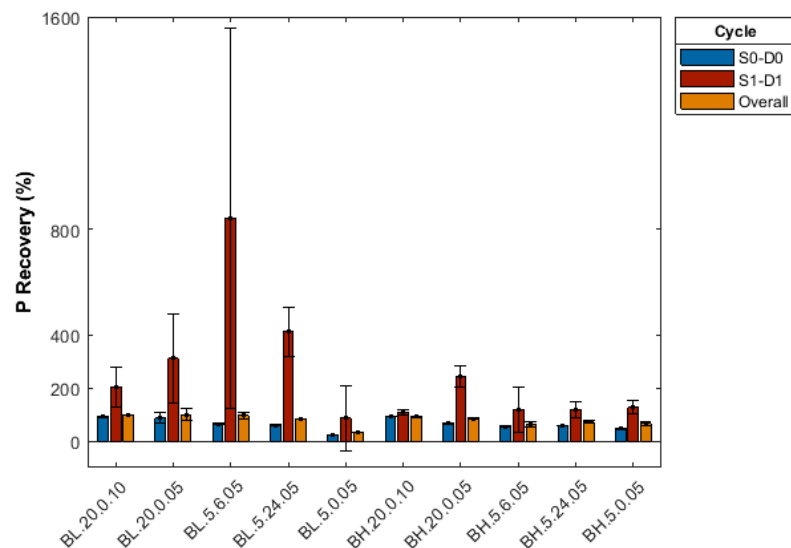


Figure 3.9. Phosphorus (P) recovery across all evaluated cycles and treatments for Biomax. The treatments identified on the x-axis follow the notation: PX.PV.RC.RT, with X being the level of P concentration (L for low or 0.5 mg L⁻¹ and H for high or 50 mg L⁻¹), PV: pore volume (5 or 20), RC: number of recirculations (0, 6, or 24) and RT: residence time used in the desorption phase.

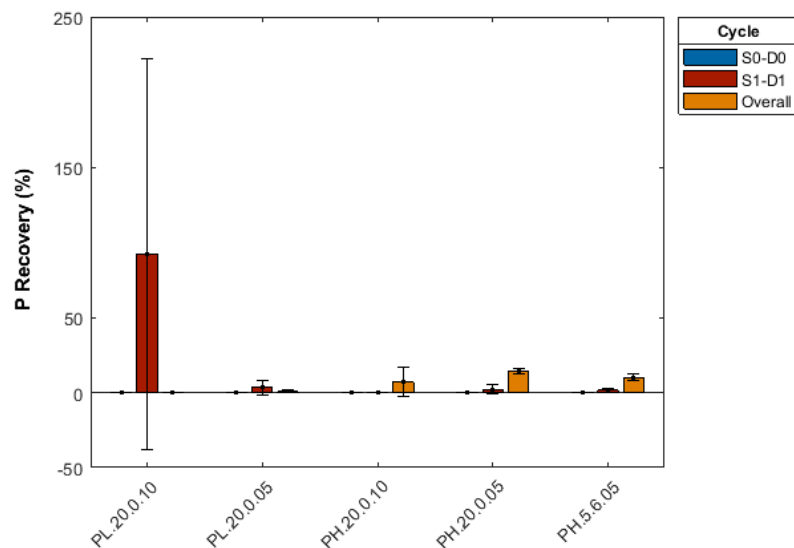


Figure 3.10. Phosphorus (P) recovery across all evaluated cycles and treatments for PhosRedeem. The treatments identified on the x-axis follow the notation: PX.PV.RC.RT, with X being the level of P concentration (L for low or 0.5 mg L^{-1} and H for high or 50 mg L^{-1}), PV: pore volume (5 or 20), RC: number of recirculations (0, 6, or 24) and RT: residence time used in the desorption phase.

4. THE USE AND BEHAVIOR OF PHOSPHORUS SORPTION MATERIALS IN ANOXIC ENVIRONMENTS

4.1 Abstract

Phosphorus (P) removal structures are a best management practice able to sequester dissolved P from surface runoff, subsurface drainage and wastewater. Utilization of P removal structures with bottom-upward flow is of great interest, but it creates an intrinsic complication: between flow events, the presence of stagnant water may cause structures to develop anoxic conditions. The behavior of P sorption materials (PSMs), i.e., the core components of P removal structures, may determine the feasibility of such a design, specifically, the potential impact of anoxic conditions on solubility of previously adsorbed P. The interference of redox-induced changes on P removal under intermittent anoxic conditions is yet to be understood. The objective of this research was to investigate the (I) development of anoxic conditions in the presence of PSM and tile drainage, (II) changes in P sorption capacity of iron(Fe)-rich PSMs after oxic conditions are restored and (III) Fe-bound P mobilization and solubility. Three Fe-rich PSMs were tested in batch incubation studies: acid mine drainage residual, Fe-coated alumina and steel metal shavings. Original and P-loaded PSM samples were incubated in biogeochemical reactors for as long as necessary to reach $E_h = -200$ mV, which is below the lower bound of the redox potential that corresponds to Fe reduction. A constant flow of CO_2/N_2 prevented oxygen within incubation cells. After incubation, dissolved P concentrations in P-treated samples and non-treated samples were similarly low, indicating stability of P retention of PSMs under anoxic conditions. The P removal ability of non-treated PSMs before and after undergoing incubation was not significantly altered; flow-through experiments showed similar P removal among pre-incubated and incubated samples. Potentially harmful trace metals were not detected in solutions during anoxic incubation. Our research shows that the Fe-bound P dissolution does not significantly impact the effectiveness of P removal structures, and that the P removal ability of PSMs persists after oxic conditions are reestablished.

4.2 Introduction

Phosphorus (P) removal structures are a best management practice able to mitigate the transport of dissolved P to water systems [1], [2]. They rely on P sorption materials (PSMs), media with chemical affinity for dissolved P that capture P in surface and subsurface flows. Phosphorus removal structures are usually constructed under free-draining conditions, with water flowing in at the top and flowing out at the bottom of the structure filled with PSM. This top-down flow direction creates an intrinsic limitation for the structure design: PSM depth is limited to the water level at the point of discharge (Figure 4.1). As a result, the structures are constructed with a large footprint to compensate for situations with shallow depths, which reduces feasibility and adoption of P removal structures. This limitation is particularly concerning in flat landscapes and shallow ditches, a common scenario found in agricultural areas in the U.S. Midwest. Because these areas are among the greatest contributors of P to Lake Erie and the Gulf of Mexico, effectively managing P export is crucial to attain water quality goals. For instance, the United States Environmental Protection Agency [3] recommends a 40% reduction of dissolved P inputs from the western and central Lake Erie basin for lessening the extent and frequency of algal blooms. A wider implementation of P removal structures can help reach this goal.

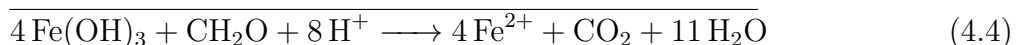
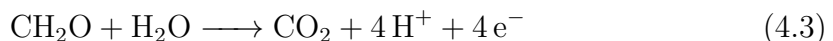
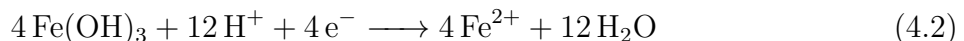
The design of P removal structures with bottom-upward flow is then of great interest, because it offers the possibility to build deeper structures, with a smaller footprint and a potentially better operational ability in flat landscapes. However, because of the direction of flow, stagnant water will remain in the structure in-between flow events, since it is not free-draining as in the top-down flow direction. Standing water can potentially create anoxic conditions in the structure, promoting redox-induced changes in solution and in redox-sensitive components of PSMs. The objective of this research was to analyze how Fe-bound P solubility and Fe-rich PSM chemistry are affected by the presence of stagnant water. More specifically, this paper addresses the question of whether bottom-up flow P removal structures can function as effectively as top-down flow structures based on the Fe-rich PSM redox behavior.

Under oxic conditions, P removal by Fe-rich PSMs in circumneutral pHs occurs primarily through adsorption[4]. The Fe beneath the surface hydroxyl acts as a Lewis acid, exchanging the OH^- groups for phosphate ($\text{H}_x\text{PO}_4^{(2-x)}$)[5]. A greater number of valence-unsatisfied hydroxyl groups on the surface of the mineral translates to more P adsorption (ligand exchange)[6]:



Equation 4.1 shows that pH plays an important role in the adsorption mechanism. Not only does it influence the surface charge of the PSM and stability of functional groups, but also the solution phosphate chemistry [4]. As pH increases, an increasing competitive effect between OH^- and H_2PO_4^- occurs, and with that, adsorption capacity decreases [4]. This is important because, comparatively, as reducing conditions develop in soils, pH generally increases.

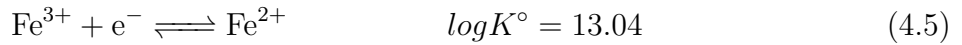
In the soils and sediment literature, authors have shown pH increase in acidic and neutral soils after long submerged periods, while others reported a pH tendency towards neutral values in alkaline soils due to buffering by silicates and carbonates [7], [8]. The consumption of H^+ under anoxic conditions, resulting in the increase of pH, is illustrated in the reduction-oxidation (redox) sequence below [9]:



The reduction process shown is a reductive dissolution of Fe(III) resulting from the oxidation of organic matter,¹ and this process occurs under considerably low redox potentials. Redox potential (Eh) characterizes the redox state of the solution, by measuring the electron availability within the system [9]. Knowing the degree of reduction in a system, one can

¹In soils, reduction-oxidation reactions can also occur as a result of abiotic reactions with inorganic or organic reductants [10].

predict the stability of compounds and the prominent oxidant, as electron acceptors become scarce with decrease of Eh. In soil environments, after oxygen is completely utilized and eliminated ($Eh \approx +350$ mV), nitrate (NO_3^-) is consumed ($Eh \approx +250$ to $+350$ mV), after which a sufficient supply of electrons is available to support the reduction of manganese (Mn^{4+} ; $Eh \approx +200$ to $+250$ mV), and finally, ferric iron (Fe^{3+} ; $Eh \approx -100$ to $+100$ mV) [11], through the mechanism shown in Equation 4. The ratio of Fe^{2+}/Fe^{3+} is defined by Equation 4.5:



for which:

$$\log \frac{Fe^{2+}}{Fe^{3+}} = 13.04 - pe \quad (4.6)$$

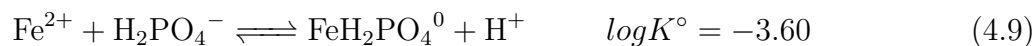
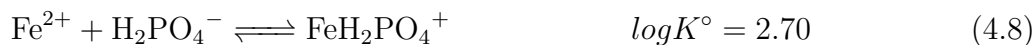
where pe is the negative logarithm of the activity of electrons.² Iron(II) and Fe(III) are thermodynamically stable under anoxic and oxic conditions, respectively [10]. Under anoxic conditions, because of the higher Fe^{2+}/Fe^{3+} ratios, the solubility of Fe-minerals and associated chemical species is impacted. Phosphorus compounds in reduced oxidation state have also been studied in the literature, but their occurrence is rare and usually associated with Carbon(C)-P bonds; therefore, they were not considered in this study. Phosphates alone are generally regarded as redox-insensitive [12].

While a decline in P adsorption and an increase in pH are expected under anoxic conditions due to the decrease of PSM Fe(III) concentrations, Fe(II) can also react with phosphate [13]. Such Fe(II) reactions may offset the expected impact of the reductive dissolution of Fe(III) on P removal. Equations 4.8 and 4.9 describe the process of P removal by Fe(II):

² pe is nondimensional and it relates to Eh (measured in volts) through the following equation:

$$Eh = \frac{2.3RTpe}{F} \quad (4.7)$$

where R is the gas constant, T is the temperature and F is the Faraday constant. At 25°C, Eh is $0.059 \times pe$.



For instance, Zhang *et al.* [14] reported that ferrous iron (Fe^{2+}) addition resulted in a superior P removal from municipal wastewater compared to the addition of ferric salts. The exact mechanisms for forming iron-phosphate minerals as a result of the interaction between dissolved Fe^{2+} and P can be complex [5]. The formation process, pH and redox potential will define the stability of these minerals. For example, Wang *et al.* [15] reported the formation of vivianite ($\text{Fe}_3^{(2+)}(\text{PO}_4)_2 \cdot 8 \text{H}_2\text{O}$) during anaerobic digestion of sewage sludge. The authors suggested that prior to Fe(III) reduction, P is adsorbed by ferric iron oxides. Then, phosphate is released during the reduction of Fe(III) and re-precipitates with dissolved Fe(II) as vivianite, showing a potential recovery route for P under anoxic conditions.

Still, in soils, reducing conditions have been associated with P release due to organic matter mineralization, reduction of Fe and manganese (Mn) oxides, and changes in pH [7]. For instance, in studying the dynamics of Fe in flooded soils, Shahandeh *et al.* [16] reported an increase in extractable Fe and P in solution under anaerobic conditions in comparison to the same soils under aerobic conditions. The authors attributed the increase to the dissolution of Fe and P poorly-crystalline minerals. By testing sediment suspensions under controlled pH and redox potentials, De Laune *et al.* [17] observed that dissolved P increased with decreasing redox potential and decreasing pH: soluble P was highest at $\text{Eh} = -200 \text{ mV}$. Similarly, the authors attributed the increase in P concentrations to the dissolution of ferric compounds.

The redox-induced release of P was also the object of studies concerning P dynamics in constructed wetlands [18], [19], which showed that a low redox potential may induce high concentrations of P following sediment-P release. Particularly, Vohla *et al.* [19] reported that a low redox potential (-21.8 mV) was associated with high Fe and P concentrations in the outflow after wastewater flowed through a filter material in a constructed wetland. The authors recommended adequate aeration in order to improve P removal capacity and accu-

mulation in the filter bed. Also in the context of wetland substrates, Drizo *et al.* [20] studied the suitability of steel slag for constructed wetland systems. After saturating the media with P and allowing a resting period (drained media column), the column experiments were restarted with incoming P-rich solution. The authors observed an increase in P adsorption capacity of the media, and attributed it to the decrease in Eh (180-240 mV to 160-210 mV), as observed in the effluent solution. They suggested that the lower Eh provoked a transformation of crystalline Fe and Al minerals to amorphous forms, which caused the increase in P adsorption. Pratt *et al.* [21] also studied the effect of redox conditions on P retention by slag, in the context of wastewater treatment. Contrary to Drizo *et al.* [20], the authors observed P release under low Eh: 95% of total P and 25% of total Fe were released from the melter slag under low values of Eh (-400 mV) and pH (4.9), due to the dissolution of Fe minerals.

Based on current literature on soils, wastewater, and P-filter media, there seems to be no consensus as to whether the Fe-bound P release caused by anoxic conditions can significantly compromise P removal. Our work aims to address this gap, investigating the behavior of Fe-rich PSMs when undergoing anoxic periods. Reducing conditions may cause changes in PSM mineralogy, pH, and chemical equilibrium, which would directly affect the P sorption capacity of Fe-rich PSMs and the Fe-bound P solubility of P-loaded (henceforth referred to as “P-treated”) PSMs. The hypothesis of this work is that under reducing conditions, the ability of PSMs to remove and retain P is impaired, because of biochemical changes on the solubility of redox-sensitive components, such as Fe.

4.3 Material & Methods

The PSMs used in this study were Actiguard AAFS50 (henceforth referred to as Alcan), metal shavings and acid mine drainage residual (AMDR). Alcan (Axens Solutions, Rueil-Malmaison, France) is an iron-enhanced activated alumina, commercialized for contaminant (phosphorus, nitrate and arsenic) removal. The AMDR originated from treating acid mine drainage at the Blue Valley Mine drainage treatment and fish culture station (Brandy Camp, PA, USA). The metal shavings are carbon steel shavings (no aluminum or stainless steel) from a metal recycling facility (OmniSource, Fort Wayne, IN, USA).

Prior to the analysis, Alcan was washed through a geotextile fabric to remove fine particles (equivalent to the textile used in the construction of P removal structures and blind inlets). The AMDR was sieved to select particles with diameter between 0.5 mm and 4 mm. Metal shavings were washed with soap to remove oil remnants derived from its generation process. To induce oxidation, the metal was soaked in a 0.1 M HCl solution for 12 hours, then rinsed and dried. Following these initial preparations, the methodology used in this paper can be divided in three parts: (1) pre-incubation analysis, (2) incubation analysis, and (3) post-incubation analysis. Below, each of the experimental phases are described in detail.

4.3.1 Pre-incubation

Characterization of media

For evaluating the chemical and physical properties of the media, acid digestions, ammonium oxalate extractions, and measurements of pH, EC, bulk density and particle density were conducted.

For the acid digestions, the Environmental Protection Agency (EPA) method 3050B [22] was used to obtain the total chemical constitution of the media. The samples were analyzed for major elements, including calcium (Ca), Fe, Al, magnesium (Mg), as well as for minor elements, such as chromium (Cr), cobalt (Co), zinc (Zn) and lead (Pb). The ammonium oxalate extractions were conducted according to the methodology described in Penn & Bowen [1]. The objective of this analysis was to assess the amorphous or poorly-crystallized Al and Fe content, i.e., the fractions readily available for P removal reactions, as poorly crystalline Fe compounds have a highly reactive surface area for P sorption [16]. All extraction and digestion samples were conducted in duplicates and analyzed by inductively coupled plasma atomic emission spectrometry (ICP-AES), using the respective solution matrices.

pH and EC samples (triplicate) were prepared in DI water, in a 1:5 solid-solution ratio, after repeating the process of shaking for 1 minute and equilibrating for 20 minutes twice, followed by measurement with calibrated benchtop pH (Thermo Orion STARA2115 Star A211 pH meter) and electrical conductivity (Mettler Toledo S230-USP conductivity meter) calibrated meters. Finally, bulk density and particle density were measured in duplicates,

following the methodology described by Penn & Bowen [1]. The PSM characterization analysis was conducted on both non-treated and P-treated samples.

Flow-through experiments and batch isotherms

Flow-through experiments were conducted to assess the original P removal capacity of the PSMs. These are dynamic sorption tests, that aim to reproduce at the laboratory scale the processes and mechanisms occurring in a field-scale P removal structure.³ In these experiments, a continuous inflow of 0.5 mg L^{-1} of P passed through a cell containing the PSM of interest. The flow is calibrated according to the desired residence time (RT), as indicated in the equation:

$$\text{Residence time (min)} = \frac{\text{Pore volume (mL)}}{\text{Flow rate (mL} \cdot \text{min}^{-1})} \quad (4.10)$$

In previous tests, the sufficient RT for each of the PSMs was established. Although they are all Al/Fe-rich PSMs (and because of that, in theory, less dependent on RT), only Alcan performed well under rapid flow rates (lower RT; data not shown). The P removal capacity of both AMDR and metal shavings is influenced by RT, and the longer contact between dissolved P and the PSMs resulted in a greater P removal. Figure 4.2 shows the P removal estimated in the preliminary flow-through experiments for all PSMs, using their respective optimal RT.

Figure 4.2 illustrates the different P removal capacity of the PSMs, normalized as a function of the cumulative P loaded to each PSM, per unit mass. One can observe the superior P removal capacity of metal shavings in comparison to the other two media, as it continued to remove more than 50% of the incoming P after $12,000 \text{ mg P} \cdot \text{kg}^{-1}$ media had been loaded. Experiments were conducted in duplicates; however, for AMDR, five replicates were conducted, because of the large degree of variability. The behavior of this media (even from the same batch) can vary and we therefore considered this variability an intrinsic property of its generation process.

³The flow-through procedure is further detailed in Penn & Bowen [1].

After quantifying the P removal character of the PSMs under flow conditions, the amount of P sorbed correspondent to 40% of cumulative removal was calculated. This value is a typical P-saturation target for PSMs used in field-scale units[23]–[25], at which time the PSMs would be replaced. For the PSMs that did not reach the 40% cumulative removal target during the flow-through experiments (i.e., Alcan and metal shavings), the exponential models (shown in Figure 4.2) were used to estimate the amount of sorbed P when 40% of the cumulative added P was removed, i.e, $P_{40\%}$.

Knowing the concentration of P sorbed onto each PSM that corresponded with the target of 40% cumulative removal ($P_{40\%}$), it was possible to create a larger batch of P-treated samples for use in the redox experiments. This was achieved through use of a batch isotherm, as described in Scott *et al.* [26]. Phosphorus adsorption isotherms were then conducted on all three PSMs, using P concentrations from 0-1000 mg L⁻¹. The isotherms revealed a linear relationship between input P concentrations and P in samples after equilibrium (mg P·kg⁻¹ media) for all PSMs. This linear relationship and the $P_{40\%}$ established in the flow-through experiments (Table 4.1) were used to determine the P concentration to treat the PSM samples in batch isotherms. Later, both P-treated and non-treated samples were used in the redox incubation phase.

4.3.2 Incubation studies

A biogeochemical reactor constructed at the National Soil Erosion Research Laboratory (NSERL, ARS/USDA) was used for the incubation studies. The reactor allows for control of the micro-atmosphere in the incubator vessel through the inflow of other gases. Anoxic conditions were maintained by continuously flowing CO₂/N₂ into the vessels. Open gas exchange between the vessels and the atmosphere prevented CO₂ build-up. A constant air pressure of 30 psi was supplied from the CO₂/N₂ tank to a manifold that delivered the gas to the vessels. The flow rate was adjusted individually via flow regulators connected to the manifold. In a test run, 15 cm³ min⁻¹ was found appropriate for the incubations, as it allowed continuous purging of the air in the vessels every 10 minutes, approximately.

The vessels were 250-mL centrifuge bottles possessing fittings on their lid for a gas inflow needle, gas outflow needle, and Eh and pH sensors. Redox potential and pH were automat-

ically recorded every 5 minutes, as the meters were connected to a computer that received voltage signals from an electrode amplifier. Prior to the incubations, the Eh meters were calibrated in pH-buffered quinhydrone solution at pH 4 and 7, and the pH meters in pH buffers only (4, 7 and 10), and a linear relationship between the measurement on the meters and the voltage signals was established. The apparatus is illustrated in Figure 4.3 and is further described in De Campos [27].

The reactor allowed for the incubation of 12 samples at a time. Four incubation sets were conducted, with randomized non-treated and P-treated samples. Each treatment was defined by the combination of PSM (Alcan, AMDR and metal shavings) and P addition (non-treated or P-treated), and was repeated three times. Twenty-five grams of the PSM, 95 mL of tile drainage, and 5 mL of a 5% D-Glucose solution were added to each bottle. A control sample containing only tile drainage was also incubated in each set. The tile drainage was collected in a 20-L container at a corn/soybean rotation field, with corn as the last planted crop (2019). At the time of collection, the 2020 crop was not yet planted, so there was no Spring P application. The major elemental composition of the tile drainage is shown in Table 4.2, determined by ICP-AES in unfiltered samples. Total oxidized nitrogen and P were analyzed colorimetrically (Fisher Sci. Inc. Gallery™ Discrete Analyzer).

Although glucose was added to the samples in order to provide prime conditions for microorganisms to grow, samples without the carbon source were also incubated to evaluate whether reduced conditions would develop, and if so, if there were any differences regarding the time needed to reach the target Eh. These are referred to as “reference” samples throughout the paper, and were also conducted in triplicates.

The time of incubation varied between 96 and 600 hours, depending on the sample. The objective was to remove the samples from the reactor as they reached $Eh = -200$ mV, although some of them reached that target rapidly and were kept in the reactor for longer. Once removed, the solution samples were divided in two 20-mL portions for posterior analysis: a 0.45- μ m filtered and acidified (0.5 mL 50% HCl) sample, and a 0.45- μ m filtered sample. The solid samples were air-dried for posterior use.

4.3.3 Post-incubation: sample analysis and flow-through tests

Once removed from the incubation and filtered, the solution samples were immediately analyzed for Fe(II) through the ferrozine method, described in detail in Viollier *et al.* [10]. Essentially, the objective of this method is to sequentially determine Fe(II)/Fe(III) speciation in liquid samples. The Fe(II)-ferrozine complex was analyzed by measuring absorbance at 562 nm in a UV spectrophotometer (Fisher Sci. Inc. Thermo Genesis 10uv) before and after reduction with hydroxylamine. The filtered and acidified samples were analyzed in the ICP-OES for the same macro and micro elements as described earlier for the digestates. Phosphorus concentrations were determined colorimetrically.

After drying, non-treated PSM samples were tested for P removal in the flow-through system, using 0.5 mg L^{-1} P as the input concentration and the appropriate RT for each sample. With this analysis, the intention was to examine the effects of anoxic conditions on P removal ability by comparing post-incubation with pre-incubation flow-through results.

After collecting the filtered aliquots, samples from treatments that did not receive 5% D-glucose solution (reference samples) were left open in a temperature-controlled room. The objective was to examine possible changes on the chemical composition of the solution as the oxic conditions were reestablished. Sub-samples were collected at 72 and 144 hours after removal from the incubator.

4.4 Results and discussion

4.4.1 Characterization of PSMs

Chemical composition varied between PSM samples. Alcan is an Al- and Fe-rich PSM, while AMDR and metal shavings can be characterized as Fe-rich PSMs, as indicated by the total elemental concentrations. Alcan and AMDR also contain appreciable amounts of Ca. The presence of Al and Ca in addition to Fe can be significant for P removal, because these elements can also participate in P removal processes, which indicates the possibility of different P removal mechanisms. Because of this, there was a suspicion that anoxic conditions would impact the PSMs in different ways, with less P release expected for the PSMs containing Ca, Al in their composition.

Table 4.3 shows the results of the chemical characterization of the PSMs. Alcan and metal shavings showed an acidic to neutral pH, while AMDR is a slightly alkaline material. This is important because of the dependence of P removal processes on the pH of solution. For instance, the higher pH of AMDR indicates that Ca-PO_4 precipitation may be a viable P removal process, which would make the P removal capacity of this PSM less influenced by the changes on Fe redox chemistry. The difference in pH between the non-treated and P-treated PSM is minor, although a decrease in pH after P treatment is evident. The most remarkable differences between non-treated and P-treated PSMs are in regard to electrical conductivity (EC). Electrical conductivity was lower in the P-treated PSMs, which may be explained by soluble compounds being rinsed out through the shaking-equilibration-filtration process involved with P treatment, and/or a reduction in solubility of various cations due to the presence of P. As expected, P concentrations were higher in the P-treated PSMs, and according to the analysis of the incubation solutions before and after P-treatment, surface P concentrations were as high as the 40% correspondent target. The total elemental composition did not reflect the actual levels of P-loading, although for Alcan and Metal shavings, it did indicate higher P concentrations for the treated samples. That inconsistency was attributed to the digestion methodology, which was unable to capture the subtle differences on P content of AMDR loaded samples, as shown in Table 4.3.

Phosphorus content in the ammonium oxalate extractions was also analyzed. For all non-treated materials, the final concentration of P was 0 in all samples (not reported in Table 4.3). Metal shavings and AMDR contained higher total and oxalate-extractable Fe concentrations in comparison to Alcan, which, in turn, showed higher Al concentrations than the other PSMs. Oxalate-extractable P was identified in both P-treated Alcan ($\bar{X} = 571.4 \text{ mg P kg}^{-1} \text{ PSM}$; Standard deviation[S] = $54.7 \text{ mg P kg}^{-1} \text{ PSM}$) and metal shavings ($\bar{X} = 2,584 \text{ mg P kg}^{-1} \text{ PSM}$; $S = 273 \text{ mg P kg}^{-1} \text{ PSM}$) at lower concentrations when compared to the total digestates. In AMDR, no phosphorus was extracted with oxalate, providing further evidence that sorbed P was possibly associated with Ca, which was abundant in this PSM. The oxalate-Fe pool is important because, for example, in studying the P sorption characteristics of estuarine sediments, Pant *et al.* [28] observed high oxalate-extractable Fe associated with higher P concentrations in solution after anoxic incubation. Following the

same rationale, a higher P desorption was expected for P-treated metal shavings and AMDR, PSMs that showed high oxalate-extractable Fe.

Other elements of interest include sulfur (S) and manganese (Mn). Alcan and AMDR showed an appreciable S content, while AMDR and metal shavings contained high Mn concentrations. Both are redox-sensitive elements, but because S does not normally directly interact with P [13], its behavior under anoxic conditions is out of the scope of this paper. Manganese, on the other hand, can form complexes with P, which can make the regulation of P dynamics more complex.

The analysis of minor components revealed the presence of Cr, Co, nickel (Ni) and Zn in some of the PSMs, as detailed in Table 4.4. No boron (B) was identified in any of the PSM samples. The presence of these elements in digestates does not signify that PSMs will be sources of contaminants. Their presence in the incubated solutions will be discussed in the next section.

4.4.2 Incubation Analysis

Prior to the main incubation batches, a test incubation was conducted to assess whether the PSMs would develop reduced conditions. The PSMs did undergo anoxic conditions, and after 2 weeks in the biogeochemical reactor, they reached values of Eh as low as -600 mV.

The Eh-related results of the incubations are described in Table 4.5. All samples, with and without added carbon (glucose), developed anoxic conditions after incubation started, although the time to reach the target Eh of -200 mV varied between samples. For instance, the reference samples (no glucose) required an average of 163 hours to reach Eh₋₂₀₀ ($S = 190$ hours), in comparison to 71 ($S = 100$ hours) and 22 ($S = 12$ hours) hours for the non-treated and P-treated samples, respectively. Eh₋₂₀₀ corresponds to the discrete Eh value observed that was closest to -200 mV, which is below the lower bound of Fe³⁺ reduction. The control samples, containing tile drainage only, required an average of 35 hours to reach the target Eh ($S = 13$ hours). The null hypothesis that the time to reach -200 mV for the different groups (control, reference, non-treated and P-treated samples) came from the same distribution (Kruskal-Wallis test; degrees of freedom = 3, $\chi^2 = 6.38$; $p\text{-value}=0.09$) failed to be rejected. Kruskal-Wallis test was used because the data was non-normal and common

data transformations (Box-Cox transformations) were unsuccessful. The test indicated that no groups had mean ranks significantly different from the others, meaning that, on average, the samples required similar amount of time to reach -200 mV. These findings indicate that, on average, the conditions encountered in P removal structures (i.e., presence of PSM and stagnant water) have no effects on the time to reach anoxic conditions. It is notable, however, that the only samples that did not reach -200 mV during the incubations were in the groups control (1 replicate) and reference (2 Alcan replicates and 3 AMDR replicates), which suggest that the non-treated and P-treated samples provide better conditions than the other groups for the development of anoxic conditions.

The pH and pe data collected during the incubations are shown in Figures 4.4, 4.5 and 4.6. For all treatments, little variation in pH was observed as anoxic conditions were established, although different trends could be identified: (I) a decrease towards neutral values (Alcan Reference, non-treated AMDR and Alcan, and P-treated AMDR and Alcan), (II) little change in pH values (AMDR Reference, non-treated and P-treated metal shavings) or (III) a slight increase in pH (metal shavings reference). Overall, the low variability of pH agrees in part with De Campos [27]. The authors also reported minor pH fluctuation during incubation of uncultivated soils, increasing from 6.4 to 7.0 and remaining near neutrality after 5 days. Heiberg *et al.* [29] also showed an increase and stabilization of pH after 15-20 days of soil incubation.

Notice the marked short-term fluctuations in pe of reference samples in comparison to the non-treated and P-treated samples, particularly for the Alcan and AMDR samples. For Alcan, the predominant behavior of the non-treated samples shows a clear and steep decrease in pe. The steep decrease can also be observed in the P-treated Alcan samples, however, it appears to occur in 2 stages: (1) at $pe=0$ ($Eh = 0$ mV) and (2) at $-2 \leq pe \leq -4$ ($-120 \leq Eh \leq -230$ mV). The 2-stage decrease can be seen in both non-treated and P-treated AMDR samples, at $pe = 0$ and $pe=-2$. There seems to be a limit for that decrease around $pe = -10$ ($Eh=-600$ mV), where pe stabilizes asymptotically. The valley at pe of -10 was also observed for the P-treated Alcan and P-treated metal shavings. The behavior of pe in the metal shavings incubations was more variable. For both non-treated and P-treated samples, the pe decrease is rapid in the beginning, quickly reaching the target pe. However, between

replications, the fluctuations in pe are broader and pe decreases and increases with time. A possible explanation is the presence of Fe^0 and continuous exposing of Fe on the surface of the PSM, providing new sources of electron receptors for the redox reactions during incubation. For instance, P-treated metal shavings samples showed an increase in pe around pe=-6 (Eh = -350 mV) and then a steep decrease towards pe = -10, after which pe stabilized.

There were more similarities between the P-treated and non-treated AMDR samples in comparison to the other PSMs, which may be explained by the lower P loading, because, comparatively, the P concentration necessary to meet $\text{P}_{40\%}$ (Figure 4.2b) on AMDR was 50-100 times lower.

4.4.3 Post-incubation analysis: P release and P removal ability of PSMs

Analysis of incubated samples

The ferrozine analysis of the incubated samples indicated that not all Fe(III) had been reduced, although Fe(II) concentrations were higher than Fe(III) concentrations in all P-treated and non-treated solution samples, except for non-treated metal shavings. Phosphorus-treated metal shavings registered the highest Fe(II) concentrations (Table 4.6), which implied a potential loss of P and Fe. Still, for all samples, the amount of soluble Fe in post-incubation solutions were insignificant when compared to total Fe and ammonium oxalate extractable Fe. Therefore, Fe is still abundant in the PSMs, available for P removal and/or it is still associated with previously sorbed P. Nevertheless, Heiberg *et al.* [29] argued that most of the Fe(II) produced during incubation of soils was found in solid form and extracted with HCl, i.e., Fe(II) became part of the structure of phyllosilicates. The water-soluble Fe concentrations were 40-70 times lower than the HCl-extractable Fe(II). Other authors associated the low concentrations of Fe(II) in solution with Fe^{2+} scavenging by FeS and FeS_2 in sediment incubations [30], [31]. The appreciable concentrations of S in Alcan and AMDR suggests that Fe-S precipitation might have occurred, which would decrease Fe(II) concentrations in solution. Because of the low dissolved P concentrations post-incubation (Table 4.7), this mechanism (if present) did not contribute to P release by Fe-rich PSMs.

The solution Fe concentration of P-treated metal shavings was significantly higher in comparison to the non-treated sample, while, for the other PSMs, the contrary was true. Low concentrations of Fe were identified on the P-treated Alcan and AMDR samples, indicating that these PSMs potentially retained the P previously added to them. This finding suggests that anoxic conditions did not affect P retention in these PSMs. Analysis of P in the incubated samples corroborated this hypothesis, as P was below detection limit for P-treated Alcan and AMDR (Table 4.7).

Indeed, P was identified in the incubated solutions from P-treated metal shavings (Table 4.7), but the amount of P desorbed was close to 0.01% of the total concentration of the P-treated PSM ($1250 \text{ mg P} \cdot \text{L}^{-1}$). In addition, the solution P concentration for incubated P-treated metal shavings was less than the solution P concentration of the inflow P solution from the original flow-through experiment designed to simulate field conditions (0.5 mg L^{-1}) and 70% of its output concentration corresponding to $P_{40\%}$ (0.35 mg L^{-1}). Phosphorus was also identified in the non-treated AMDR samples, at even lower concentrations (virtually 0 mg P L^{-1}). Phosphorus loss is likely associated to Fe, since these samples also showed higher Fe concentrations in solution.

In summary, P release under anoxic conditions was not appreciable in the P-treated PSMs. Because P release was detected in the same solutions in which Fe release was identified, P was potentially Fe-bound. Although the results attest to the reductive dissolution of Fe(III), the low P release may be explained by P readsorption or precipitation, as observed by other authors throughout the literature [15], [29]. The fact that no P was found in incubated P-treated ALCAN solutions may be explained by the abundance of Al found in that PSM, that contributed to the readsorption of P, as described by Heiberg *et al.* [29]. The solution pH supports this hypothesis. For AMDR, the hypothesis is that P was precipitated as an Fe(II) mineral under anoxic conditions as well as Ca-PO_4 minerals, given the abundance of this element in the PSM's composition and pH. Although the circumneutral solution pH does not favor Ca mineral dissolution (and therefore, under lower Ca/P molar ratios, Ca-PO_4 precipitation is limited), Lindsay [13] shows that in circumneutral pHs, several Ca-PO_4 minerals can co-exist. An increase in Ca-P pool among anoxic environments

has been observed in coastal sediments, for instance [30]. The consumption of inorganic P by bacteria can also be considered a potential path for the dissolved P pool.

Similar results regarding P release were observed by Oliver *et al.* [32]. The authors reported rates of P retention of 98% or higher when using Fe-dominated water treatment residuals, regardless of aeration conditions. This study corroborates their results, demonstrating an insignificant impact of redox status on P retention by Fe-rich PSMs. At similar circum-neutral pH values, Pratt *et al.* [21] reported negligible release of P and Fe from exhausted melter slag (Ca- and Fe-rich media) after 12 hours and 10 days of incubation (Eh=-400 mV, pH=6.7). The authors hypothesized that P and Fe were captured by organic flocculants at this range of pH, although the origins of the flocculation layer were unknown. Their results suggested that low pH has a stronger impact on P release than low Eh, since P losses were as high as 90% after 10 days of incubation under similar Eh values (Eh=-400 mV), but lower pH (4.9).

As expected, no P was identified in the incubated solutions after oxic conditions were reestablished, as measured in the reference samples after 72 and 144 hours of removing from the reactor. The solution concentration of other elements also showed stability during post-incubation, except for Al, that at 72-h post-incubation had its concentrations decreased to virtually zero in Alcan and AMDR solutions.

None of the minor components (B, Cr, Co, Ni, Pb and Zn) were identified in the incubated solution samples. Manganese (Mn) was identified in non-P treated AMDR and P-treated metal shavings, but at considerably lower concentration in comparison to their total concentrations on the solid material. The presence of Mn in solution indicates that it may have had a role in anaerobic metabolism, potentially offsetting losses of Fe-bound P pool. In the literature, the ability of Mn reduction and re-oxidation to maintain low Fe(II) concentrations is reported as a mechanism to prevent P release [30]. However, because higher concentrations of Mn were found in incubated solutions that also showed a high content of P and Fe, the Mn-driven preservation of Fe(III) was considered not significant.

Post-incubation flow-through experiments

Based on the results from the ferrozine and post-incubation elemental analysis, the anoxic conditions did not appreciably influence P removal behavior of PSMs. The post-incubation flow-through experiments confirmed this hypothesis, as the P retention before and after undergoing anoxic conditions was similar among PSMs. For metal shavings, the similarity is visually lower, as seen in Figure 4.7, and the pre-incubation samples appear to perform better in terms of P removal in comparison to the post-incubation samples.

In order to quantitatively investigate the P removal ability of PSMs, the P sorption (%) after $700 \text{ mg P} \cdot \text{kg}^{-1}$ PSM were added to the PSMs was evaluated. This value was chosen because it was the maximum value for which there were observations for all replicates. Table 4.8 shows the average and standard deviation P removal for each PSM P removal, pre and post anoxic incubation. The fact that P removal by AMDR and metal shavings was dependent on residence time (shorter residence times were tested during the pre-incubation experiments) reveals important characteristics about these PSMs with regards to P removal mechanisms. Given the alkaline pHs and higher content of Ca of the AMDR samples, Ca-PO_4 was a potentially significant P removal path. This hypothesis agrees with Penn *et al.* [33], who observed that 58% of the total P removed by AMDR was Ca-associated P. For metal shavings, the longer residence time allowed for constant oxidation of the media, exposing more P sorption sites with time.

Based on a two-sided Wilcoxon rank sum test (non-parametric test; H_0 : data are samples from continuous distributions with equal medians), pre- and post-incubation P removal performances for Alcan were not significantly different from each other (ranksum statistic = 13; $p\text{-value} = 0.18$). The same conclusion was reached for AMDR (ranksum statistic = 29; $p\text{-value} = 0.93$) and metal shavings (ranksum statistic = 21; $p\text{-value} = 0.07$). This indicates that the P removal ability of PSMs was not significantly impacted by the anoxic conditions according to the evaluated metric. Heiberg *et al.* [29] also observed similar P sorption capacity in sandy soils under oxic and anoxic conditions, explained by the increase in available Al in the reduced soil. However, their increase was both a result of reduction and pH increase,

which was not observed in the PSMs. Still, given the higher concentrations of Al in Alcan, for instance, and the neutral range of pH, Al fixation may have occurred.

The overall behavior of the P removal curve indicates that PSMs did not undergo significant chemical and mineral alteration under anoxic conditions. Additionally, the reductive dissolution of Fe(III) did not significantly impact the amount of available sorption sites for P removal. In practical terms, after a P removal structure undergoes anoxic condition, its lifetime and ability to retain P will not be significantly impaired by the changes on redox chemistry.

4.5 Conclusions and implications

The incubation of Fe-rich PSMs under no oxygen conditions resulted in a decreased redox potential for PSMs with and without the glucose carbon source alike, meaning that Fe-rich PSMs did undergo anoxic conditions in the presence of a tile drainage matrix. In the absence of glucose (reference samples), which is a scenario representative of a P removal structure, the PSM samples required, on average, the same amount of time to reach the target Eh in comparison to the samples with glucose. However, some of the reference and control replicates did not reach as low Eh values as the glucose-amended samples. No unique tendency was observed for pH during the incubations, although, overall, pH values did not alter significantly under anoxic conditions.

This study confirmed the reductive dissolution of Fe(III) in Fe-rich PSMs, however the effect on P removal was minor, both in terms of Fe-bound P release and P sorption capacity. Phosphorus released from the P-treated PSMs was possibly readsorbed or precipitated. The P sorption capacities of PSMs pre- and post-incubation were not significantly different. Potentially harmful trace metals were not detected in the incubated solutions, indicating that there is no environmental risk of the PSMs undergoing anoxic conditions.

The implications of our study are the confirmation that P removal structures with bottom-upward flow are feasible for these Fe-rich PSMs, as the presence of stagnant water will not significantly impair the PSM ability to remove and retain P. Future works should include the changes in P pools on the P-treated PSMs before and after incubation in order to investigate the solid forms of Fe-P. Such information may shed a light on the specific P

removal processes under anoxic conditions, based on which adaptations for an improved P removal can be developed.

References

- [1] C. J. Penn and J. M. Bowen, *Design and construction of phosphorus removal structures for improving water quality*. Springer, 2017.
- [2] C. Penn, I. Chagas, A. Klimeski, and G. Lyngsie, “A review of phosphorus removal structures: How to assess and compare their performance,” *Water*, vol. 9, no. 8, p. 583, 2017.
- [3] United States Environmental Protection Agency, “Recommended phosphorus loading targets for lake erie,” Washington, DC, Tech. Rep., 2015.
- [4] M. Li, J. Liu, Y. Xu, and G. Qian, “Phosphate adsorption on metal oxides and metal hydroxides: A comparative review,” *Environmental Reviews*, vol. 24, no. 3, pp. 319–332, 2016.
- [5] P. Wilfert, P. S. Kumar, L. Korving, G.-J. Witkamp, and M. C. van Loosdrecht, “The relevance of phosphorus and iron chemistry to the recovery of phosphorus from wastewater: A review,” *Environmental science & technology*, vol. 49, no. 16, pp. 9400–9414, 2015.
- [6] M. B. McBride, *Environmental Chemistry of Soils*. New York: ”Oxford University Press, Inc.”, 1994.
- [7] A. B. De-Campos, C.-h. Huang, and C. T. Johnston, “Biogeochemistry of terrestrial soils as influenced by short-term flooding,” *Biogeochemistry*, vol. 111, no. 1-3, pp. 239–252, 2012.
- [8] Y. Pan, G. F. Koopmans, L. T. Bonten, J. Song, Y. Luo, E. J. Temminghoff, and R. N. Comans, “Influence of ph on the redox chemistry of metal (hydr) oxides and organic matter in paddy soils,” *Journal of soils and sediments*, vol. 14, no. 10, pp. 1713–1726, 2014.
- [9] R. DeLaune and K. Reddy, “Redox potential,” in *Encyclopedia of Soils in the Environment*, D. Hillel, Ed., Oxford: Elsevier, 2005, pp. 366–371, ISBN: 978-0-12-348530-4. DOI: <https://doi.org/10.1016/B0-12-348530-4/00212-5>. [Online]. Available: <http://www.sciencedirect.com/science/article/pii/B0123485304002125>.

- [10] E. Viollier, P. Inglett, K. Hunter, A. Roychoudhury, and P. Van Cappellen, "The ferrozine method revisited: Fe (ii)/fe (iii) determination in natural waters," *Applied geochemistry*, vol. 15, no. 6, pp. 785–790, 2000.
- [11] M. E. Essington, *Soil and water chemistry: an integrative approach*. Boca Raton, FL: CRC press, 2015.
- [12] M. A. Pasek, J. M. Sampson, and Z. Atlas, "Redox chemistry in the phosphorus biogeochemical cycle," *Proceedings of the National Academy of Sciences*, vol. 111, no. 43, pp. 15 468–15 473, 2014.
- [13] W. L. Lindsay, *Chemical equilibria in soils*. Chichester, UK: John Wiley & Sons, 1979.
- [14] Z. Zhang, Y. Wang, G. L. Leslie, and T. D. Waite, "Effect of ferric and ferrous iron addition on phosphorus removal and fouling in submerged membrane bioreactors," *Water Research*, vol. 69, pp. 210–222, 2015.
- [15] R. Wang, P. Wilfert, I. Dugulan, K. Goubitz, L. Korving, G.-J. Witkamp, and M. C. van Loosdrecht, "Fe (iii) reduction and vivianite formation in activated sludge," *Separation and Purification Technology*, vol. 220, pp. 126–135, 2019.
- [16] H. Shahandeh, L. Hossner, and F. Turner, "A comparison of extraction methods for evaluating fe and p in flooded rice soils," *Plant and soil*, vol. 165, no. 2, pp. 219–225, 1994.
- [17] R. D. De Laune, C. N. Reddy, and W. H. Patrick Jr, "Effect of ph and redox potential on concentration of dissolved nutrients in an estuarine sediment," *Journal of Environmental Quality*, vol. 10, no. 3, pp. 276–279, 1981.
- [18] K. M. Johannesson, J. L. Andersson, and K. S. Tonderski, "Efficiency of a constructed wetland for retention of sediment-associated phosphorus," *Hydrobiologia*, vol. 674, no. 1, pp. 179–190, 2011.
- [19] C. Vohla, R. Alas, K. Nurk, S. Baatz, and Ü. Mander, "Dynamics of phosphorus, nitrogen and carbon removal in a horizontal subsurface flow constructed wetland," *Science of the Total Environment*, vol. 380, no. 1, pp. 66–74, 2007.
- [20] A. Drizo, Y. Comeau, C. Forget, and R. P. Chapuis, "Phosphorus saturation potential: A parameter for estimating the longevity of constructed wetland systems," *Environmental science & technology*, vol. 36, no. 21, pp. 4642–4648, 2002.
- [21] C. Pratt, A. Shilton, S. Pratt, R. G. Haverkamp, and I. Elmetri, "Effects of redox potential and ph changes on phosphorus retention by melter slag filters treating wastewater," *Environmental science & technology*, vol. 41, no. 18, pp. 6585–6590, 2007.

- [22] EPA, “Method 3050b. acid digestion of sediments, sludges, and soils. revision 2,” *Test Methods for Evaluating Solid Wastes: Physical/Chemical Methods*, EPA SW-846Section a, 3050B–1e3050B, 1996.
- [23] J. M. Gonzalez, C. J. Penn, and S. J. Livingston, “Utilization of steel slag in blind inlets for dissolved phosphorus removal,” *Water*, vol. 12, no. 6, p. 1593, 2020.
- [24] C. Penn, S. Livingston, V. Shedekar, K. King, and M. Williams, “Performance of field-scale phosphorus removal structures utilizing steel slag for treatment of surface and subsurface drainage,” *Water*, vol. 12, no. 2, p. 443, 2020.
- [25] V. S. Shedekar, C. J. Penn, L. Pease, K. W. King, M. M. Kalcic, and S. J. Livingston, “Performance of a ditch-style phosphorus removal structure for treating agricultural drainage water with aluminum-treated steel slag,” *Water*, vol. 12, no. 8, p. 2149, 2020.
- [26] I. S. P. C. Scott, C. J. Penn, and C.-h. Huang, “Development of a regeneration technique for aluminum-rich and iron-rich phosphorus sorption materials,” *Water*, vol. 12, no. 6, p. 1784, 2020.
- [27] A. B. De Campos, “Effects of redox on the solution chemistry and aggregate stability of midwest upland soils,” Ph.D. dissertation, Purdue University, 2006.
- [28] H. Pant and K. Reddy, “Phosphorus sorption characteristics of estuarine sediments under different redox conditions,” *Journal of environmental quality*, vol. 30, no. 4, pp. 1474–1480, 2001.
- [29] L. Heiberg, C. B. Koch, C. Kjaergaard, H. S. Jensen, and H. C. B. Hansen, “Vivianite precipitation and phosphate sorption following iron reduction in anoxic soils,” *Journal of Environmental Quality*, vol. 41, no. 3, pp. 938–949, 2012.
- [30] M. Zilius, G. Giordani, J. Petkuvienė, I. Lubienė, T. Ruginis, and M. Bartoli, “Phosphorus mobility under short-term anoxic conditions in two shallow eutrophic coastal systems (curonian and sacca di goro lagoons),” *Estuarine, Coastal and Shelf Science*, vol. 164, pp. 134–146, 2015.
- [31] J. Lehtoranta and A.-S. Heiskanen, “Dissolved iron: Phosphate ratio as an indicator of phosphate release to oxic water of the inner and outer coastal baltic sea,” *Hydrobiologia*, vol. 492, no. 1-3, pp. 69–84, 2003.
- [32] I. W. Oliver, C. D. Grant, and R. S. Murray, “Assessing effects of aerobic and anaerobic conditions on phosphorus sorption and retention capacity of water treatment residuals,” *Journal of environmental management*, vol. 92, no. 3, pp. 960–966, 2011.

- [33] C. Penn, R. B. Bryant, M. Callahan, and J. McGrath, “Use of industrial by-products to sorb and retain phosphorus,” *Communications in Soil Science and Plant Analysis*, vol. 42, no. 6, pp. 633–644, 2011.

Table 4.1. Calculated P sorbed to P sorption materials (PSMs) in flow-through experiments at 40% cumulative removal of P input (figure 4.2 at 40% $[P_{40\%}]$) and corresponding P concentrations added in batch isotherms to reach $P_{40\%}$ using a solid:solution ratio of 1:15.

Sample	$P_{40\%}$ (mg P·kg ⁻¹ PSM)	Concentration in isotherm (mg L ⁻¹)
Alcan A	6006	540
Alcan B	8471	
AMDR A	288	12
AMDR B	72	
AMDR C	910	
AMDR D	932	
AMDR E	171	
Metal Shavings A	14900	1250
Metal Shavings B	23646	

Table 4.2. Chemical composition of tile drainage used in incubations. The reported concentrations are the average among three replicates, except for nitrogen (duplicates). Standard deviation is listed in parenthesis.

	Al	Fe	Mg	P	Ca	K	S	TON ¹
	<i>mg L⁻¹</i>							
Tile Drainage	0.1	0	22.9	0	63.1	0.8	1.3	9.3
	(0.08)	(0)	(2.7)	(0)	(4.62)	(0.6)	(0.5)	(0.3)

¹ Total oxidized nitrogen (NO₂ and NO₃)

Table 4.3. Chemical characterization of the non-treated and P-treated P sorption materials. Average and standard deviation are reported.

Sample	pH ¹	EC ¹		Amorphous ²		Total ³						
		($\mu\text{S cm}^{-1}$)	($\mu\text{S cm}^{-1}$)	Al	Fe	Al	Fe	S	Mg	Ca	P	P ⁽⁴⁾
		(g kg ⁻¹)	(g kg ⁻¹)	(g kg ⁻¹)	(g kg ⁻¹)	(g kg ⁻¹)	(g kg ⁻¹)	(g kg ⁻¹)	(mg kg ⁻¹)	(mg kg ⁻¹)	(mg kg ⁻¹)	(mg kg ⁻¹)
Alcan	6.74 (0.02)	1550.0 (77)	2.3 (0.2)	20.6 (1.6)	221.1 (8.2)	22.9 (0.5)	10.3 (0.9)	35.7 (2.1)	710.0 (14.1)	50.0 (70.7)		
P-Alcan	6.00 (0.14)	401.0 (13)	2.2 (0.9)	17.7 (1.4)	192.2 (3.5)	9.7 (1.5)	7.8 (0.3)	31.6 (7.4)	10.3 (2.3)	2238.0 (21.9)	8183.0	0
AMDR	8.02 (0.02)	1004.0 (19)	0.22 (0.04)	79.0 (3.5)	3.9 (0.4)	380.7 (14.4)	2.8 (0.2)	534.0 (74.9)	21655.0 (6130)	790.0 (14.1)		7628.5 (458.9)
P-AMDR	7.96 (0.03)	493.0 (26)	0.03 (0.002)	55.4 (12.5)	3.2 (0.6)	362.1 (7.8)	2.1 (0.005)	527.9 (31.7)	19985.0 (5254)	780.0 (14.1)	138.0	7663.5 (251.0)
Metal	6.04 (0.06)	77.7 (9.6)	0.15 (0.01)	69.0 (11)	1.96 (0.16)	754.7 (8.6)	0.8 (0.08)	0	0	33.5 (47.4)		4717.0 (110.3)
Shavings	5.97 (0.14)	(8)	0.01 (0.002)	44.6 (3.3)	2.1 (0.6)	749.7 (20.0)	0.7 (0.005)	0	0	4901 (111.7)	16241.0	4753.5 (119.5)

¹ Measurements in DI water conducted in triplicate.

² Amorphous Fe/Al content determined by ammonium oxalate extractions.

³ Total content determined by EPA 3050b digestion method. Method was conducted solely with non-treated samples

⁴ Real P content as determined by the analysis of the P-treatment solution before and after treatment.

Table 4.4. Pre-incubation analysis: total concentrations of trace metals in phosphorus sorption materials (PSMs). \bar{X} is the average among the two replicates of each non-treated PSM and S the standard deviation.

Sample		Cr	Co	Ni	Pb	Zn
		<i>(mg/kg PSM)</i>				
Alcan	\bar{X}	0.0	0.0	0.0	0.0	20.9
	S	0.0	0.0	0.0	0.0	14.1
AMDR	\bar{X}	0.0	8.5	15.3	46.2	231.5
	S	0.0	0.3	20.4	3.4	13.6
Metal Shavings	\bar{X}	1104.0	44.5	1807.0	152.0	145.0
	S	803.0	2.9	1665.3	52.2	7.7

Table 4.5. Redox potentials and experimental time required for reaching the target (Eh_{-200}) and final Eh values among P-treated and non-treated PSMs during incubation with no oxygen. “Reference” treatments refer to those that did not receive glucose addition.

Sample		Eh_{-200}	Time to Eh_{-200} (hours)	Final Eh	Total Exp. Time (hours)
Control Tile Drainage	Rep. 1	-200.26	31.40	-182.47	282.36
	Rep. 2	-199.93	20.86	-565.68	93.06
	Rep. 3	-53.34	44.98	-9.93	620.94
Alcan Reference	Rep. 1	-181.59	109.67	-159.30	455.12
	Rep. 2	-87.23	240.92	-68.91	333.38
	Rep. 3	-201.72	57.57	-151.25	333.54
Non-treated Alcan	Rep. 1	-199.56	38.98	-521.59	89.89
	Rep. 2	-200.48	306.15	-205.09	319.36
	Rep. 3	-199.37	16.28	-455.3	89.39
P-treated Alcan	Rep. 1	-198.61	22.03	-541.64	93.31
	Rep. 2	-197.93	22.12	-538.77	93.89
	Rep. 3	-201.62	39.14	-554.47	93.98
AMDR Reference	Rep. 1	-92.39	592.91	-92.39	620.78
	Rep. 2	-128.05	306.67	-123.59	333.88
	Rep. 3	-43.197	92.95	-25.46	333.71
Non-treated AMDR	Rep. 1	-203.82	37.31	-582.46	89.97
	Rep. 2	-200.38	29.96	554.84	93.06
	Rep. 3	-201.52	46.154	-558.33	114.84
P-treated AMDR	Rep. 1	-201.98	31.63	-550.22	89.22
	Rep. 2	-198.74	29.88	-608.77	92.73
	Rep. 3	-200.26	30. 55	-568.99	94.061
Metal Shavings Reference	Rep. 1	-198.93	61.76	-445.71	115.09
	Rep. 2	-202.04	2.67	-517.35	167.38
	Rep. 3	-198.46	4.50	-618.92	167.21
Non-treated Metal Shavings	Rep. 1	-197.38	1.00	-406.67	93.14
	Rep. 2	-201.49	4.84	-397.81	89.64
	Rep. 3	-200.36	167.27	-209.22	281.86
P-treated Metal Shavings	Rep. 1	-202.35	18.11	-616-7	94.90
	Rep. 2	-195.55	1.59	.576.5	89.72
	Rep. 3	-202.68	3.09	-562.33	94.65

Table 4.6. Ferrozine analysis of post-incubation solution samples for Fe(II) and (III), conducted under conditions of no oxygen for P-treated and non-treated P sorption materials. “Reference” treatment refer to those that did not receive glucose addition.

Sample			Fe(II) (mg/L)	Fe(III) (mg/L)
Tile Drainage	Control	\bar{X}	0	1.41
		S	0	1.12
Alcan	Reference	\bar{X}	0	1.43
		S	0	0.38
	Non-treated	\bar{X}	3.18	0.27
		S	5.15	0.24
	P-treated	\bar{X}	1.04	0.2
		S	0.73	0.12
AMDR	Reference	\bar{X}	0	1.46
		S	0	0.68
	Non-treated	\bar{X}	63.61	0.09
		S	53.53	0.15
	P-treated	\bar{X}	1.01	0.34
		S	0.54	0.15
Metal Shavings	Reference	\bar{X}	0.76	3.14
		S	0.66	2.98
	Non-treated	\bar{X}	4.22	7.67
		S	7.3	11.74
	Treated	\bar{X}	426.92	0
		S	238.09	0

Table 4.7. Post-incubation analysis: chemical composition of filtered and acidified solution samples collected after the respective incubation period. \bar{X} is the average among the three replicates in each treatment and S the standard deviation. No replicates exist for “tile drainage reference”, which contains no P sorption material. “Reference” treatments refer to those that did not receive glucose addition.

Sample			Al	Fe	Mg	P	Ca	K	Mn	S
			<i>(mg L⁻¹)</i>							
Tile Drainage	Control	\bar{X}	3.4	0.0	21.0	0.0	45.7	29.5	0.0	1.5
		S	0.2	0.0	1.6	0.0	18.6	20.3	0.0	0.8
	Reference		3.05	0.0	21.11	0.0	63.3	2.4	0.0	9.3
Alcan	Reference	\bar{X}	3.8	0.0	9.6	0.0	3.7	38.0	0.0	206.2
		S	0.3	0.0	0.6	0.0	2.4	9.8	0.0	15.1
	Non-treated	\bar{X}	3.8	0.0	11.9	0.0	9.3	22.2	0.0	239.6
		S	0.7	0.0	0.2	0.0	6.1	20.9	0.0	32.4
	P-treated	\bar{X}	3.7	0.0	18.4	0.0	26.9	9.43	0.0	41.8
		S	0.3	0.0	0.5	0.0	1.4	1.4	0.0	4.8
AMDR	Reference	\bar{X}	4.0	0.0	5.0	0.0	186.9	52.1	0.0	122.9
		S	1.1	0.0	7.2	0.0	15.9	64.7	0.0	3.8
	Non-treated	\bar{X}	3.57	14.0	19.4	0.12	901.5	35.5	9.78	190.4
		S	0.3	24.3	2.5	0.2	182.5	2.3	7.3	19.0
	P-treated	\bar{X}	3.2	0.0	12.77	0.0	650.2	14.4	0.0	113.1
		S	0.2	0.0	1.02	0.0	29.3	1.6	0.0	8.7
Metal Shavings	Reference	\bar{X}	3.6	0.0	3.4	0.0	13.7	14.3	0.0	1.9
		S	0.2	0.0	0.1	0.0	0.7	1.72	0.0	0.9
	Non-treated	\bar{X}	3.5	0.0	5.5	0.0	15.6	13.1	0.0	3.0
		S	0.4	0.0	0.6	0.0	4.7	7.0	0.0	2.6
	P-treated	\bar{X}	3.3	192.1	10.2	0.2	20.5	7.9	2.0	1.1
		S	0.2	107.9	1.6	0.3	4.8	1.0	1.6	0.7

Table 4.8. Cumulative P removal under flow-through conditions for pre- and post-incubation samples for each PSM after cumulative addition of 700 mg kg⁻¹. Values are average of all replicates.

Sample	Pre-incubation P removal		Post-incubation P removal	
	Average ¹	Std. Dev.	Average ²	Std. Dev.
Alcan	57.44	3.34	50.72	7.93
AMDR	46.19	14.06	41.70	2.91
Metal Shavings	74.85	2.67	62.74	3.30

¹Average P removal calculated across 2 replicates and 5 replicates for AMDR.

²Average P removal calculated across 6 replicates, 2 from each of the incubated samples.

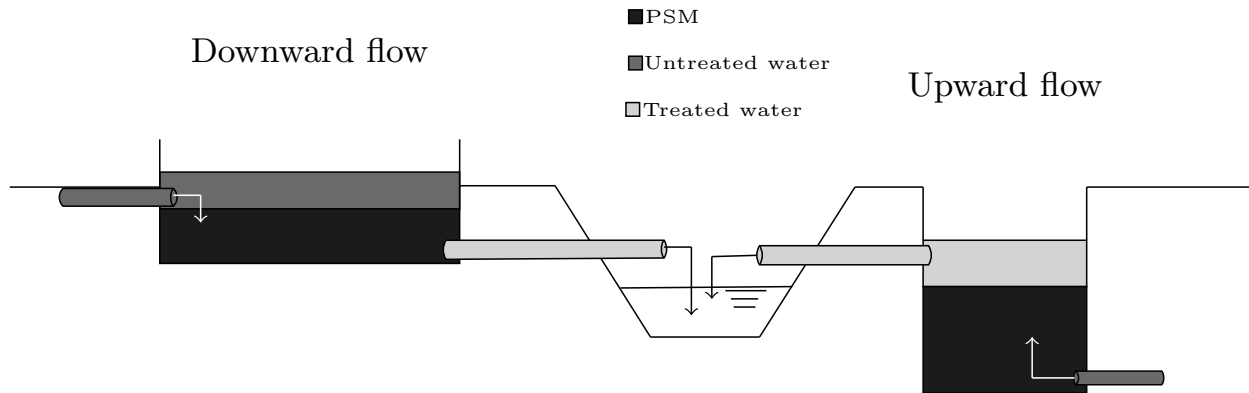


Figure 4.1. Examples of different flow direction in phosphorus (P) removal structures: the top-down or downward flow requires larger structures, because they are limited to the depth at the point of discharge (exemplified as a ditch in the figure). Phosphorus removal structures built with upward flow can be deeper and contain the same amount of PSM, having a smaller footprint.

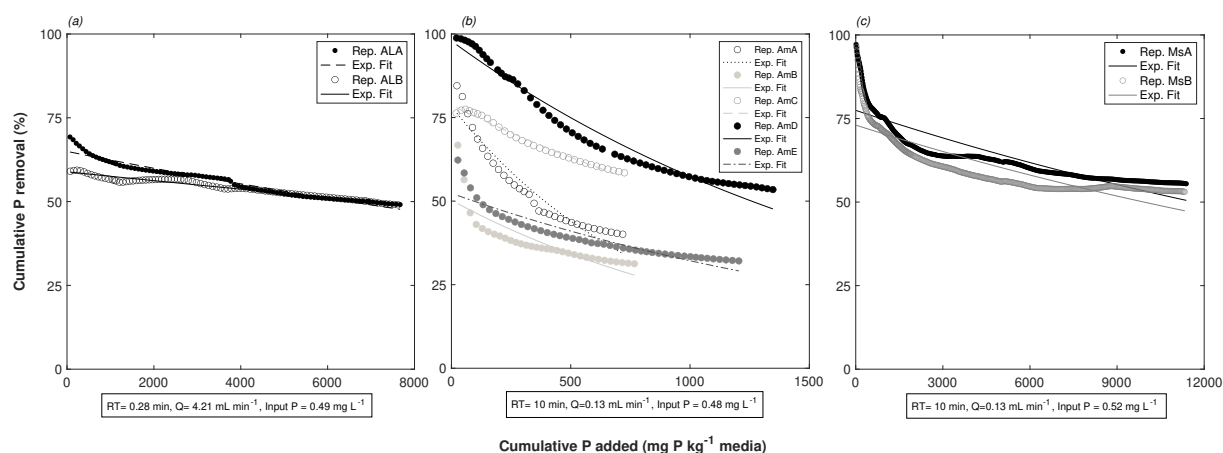


Figure 4.2. Phosphorus (P) removal curve for P sorption materials (PSMs) under flow-through conditions: (a) Alcan, two replicates, (b) AMDR, five replicates and (c) Metal shavings, two replicates. X-axis scale is different for each PSM illustrating the long-term P removal ability of metal shavings and Alcan.

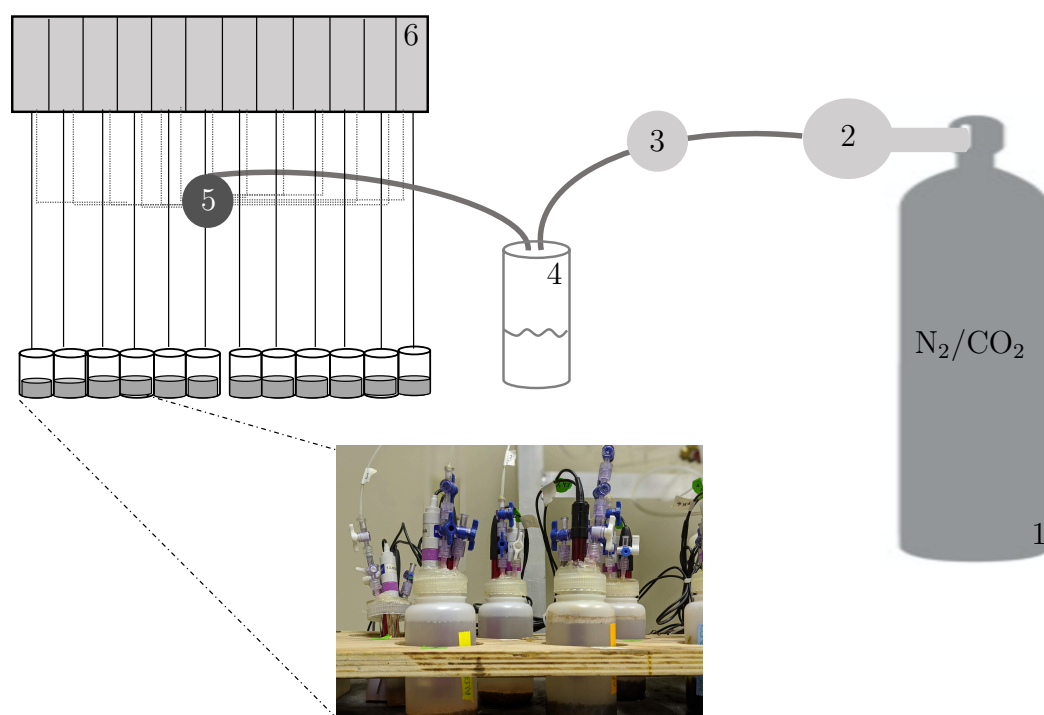


Figure 4.3. The biogeochemical reactor is composed of a (1) gas tank containing CO_2 and N_2 , followed by a 2-stage gas regulator (2) and a pressure regulator (3). The gas is delivered to a water container (4) and is then distributed to the incubator cells through a manifold (5). The gas flow is controlled by flow regulators (6). The inset shows the incubator vessels in detail.

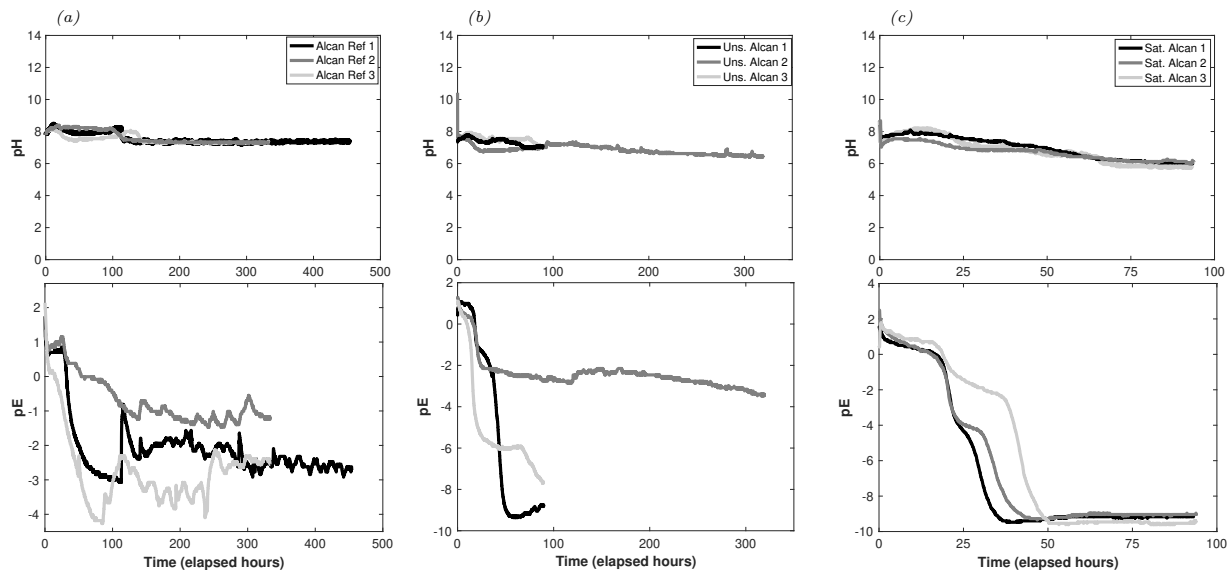


Figure 4.4. pH and pe data of Alcan incubated with no oxygen: (a) reference samples receiving no glucose, (b) non-treated samples and (c) P-treated samples. The range of pe and the duration of experiment differ for the different incubations.

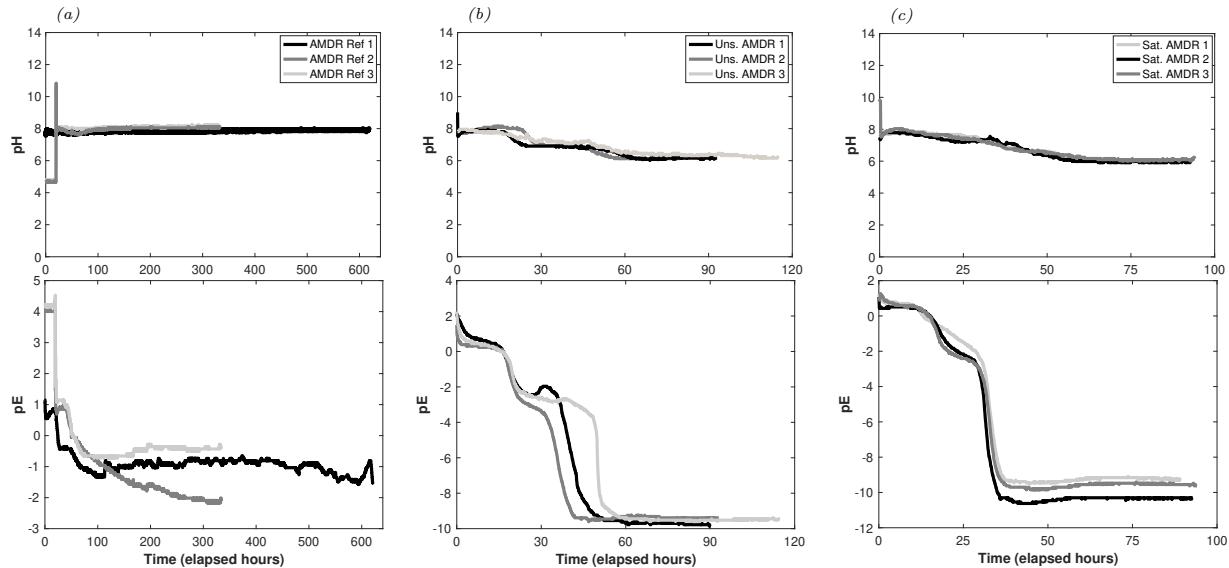


Figure 4.5. pH and pe data of AMDR incubated with no oxygen: (a) reference samples receiving no glucose, (b) non-treated samples and (c) P-treated samples. The range of pe and the duration of experiment differ for the different incubations.

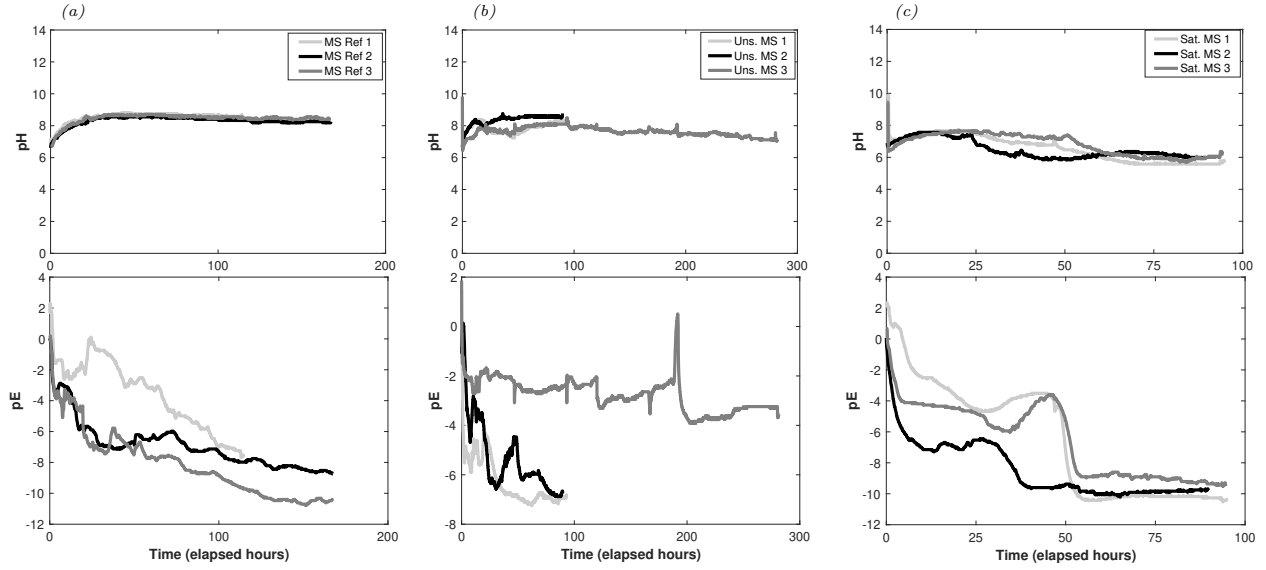


Figure 4.6. pH and pe data of metal shavings incubated with no oxygen: (a) reference samples receiving no glucose, (b) non-treated samples and (c) P-treated samples. The range of pe and the duration of experiment differ for the different incubations.

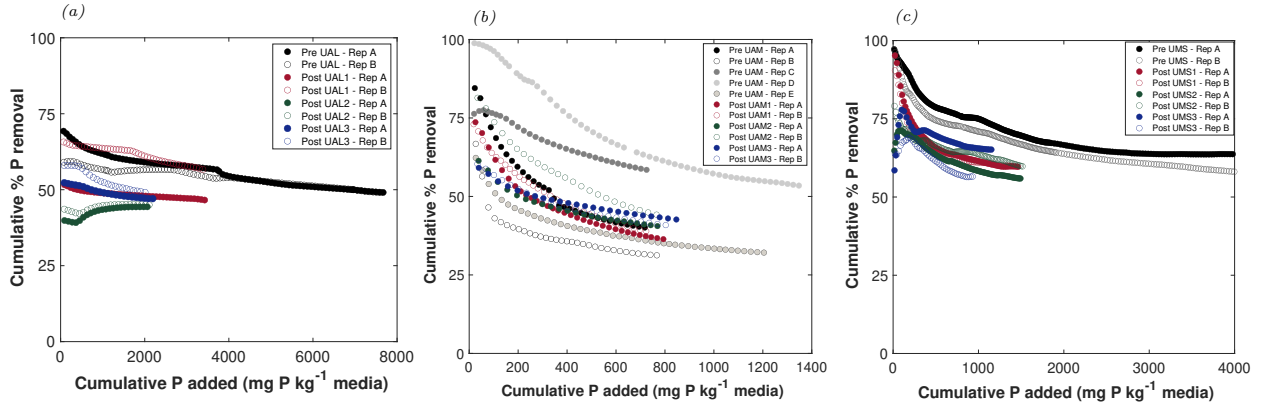


Figure 4.7. Phosphorus (P) removal expressed as a function of cumulative P added under flow-through conditions conducted on pre and post anoxic-incubated P sorption materials (PSMs): (a) non-treated Alcan (UAL), (b) non-treated AMDR (UAM) and (c) non-treated metal shavings (UMS). The graphs contain all pre- and post-incubation replicates and they are identified. For each incubated non-treated replicate (replicates 1,2,3), two flow-through experiments were conducted (replicates A and B). In all graphs, the pre-incubation results are shown in shades of black and gray. For the complete P removal curve for metal shavings, see Figure 4.2.

5. CONCLUSIONS

5.1 Summary

The main objective of this research was to investigate the behavior and management of PSMs for improving P removal performance. Phosphorus sorption materials are the core components of P removal structures, and their P sorption capacity is a function of intrinsic factors that depends on the inherent characteristics of the PSM, and extrinsic factors defined by the design attributes of the P removal structure. In this research, both intrinsic and extrinsic factors were explored, aiming to design better P removal structures, based on an improved understanding of PSMs.

First, the P removal capacity of steel slags was determined. Flow-through tests on 18 different samples of steel slags revealed a significant heterogeneity of P removal capacity, agreeing with the wide range of P removal by steel slag reported in the literature. Residence time (RT), an extrinsic property, was proven to have a significant effect on P removal. In comparing RTs representative of P removal structures, 9.85 minutes offered better conditions for steel slag to remove P than the lower RT of 0.28 minutes. Since Al-based PSMs are known to be less dependent on RT, an Al-coating technique was proposed to improve steel slag's performance under lower RTs. The technique was proven to be useful, since a higher level of coating resulted in a superior P removal performance under the lower RT. Additionally, Al-coating has the advantage of creating a more uniform media in regard to P removal capacity compared to their uncoated counterparts. This means that across different samples of coated steel slags, researchers and users can predict P removal behavior with more certainty than with the same uncoated samples, particularly when a thorough chemical and physical characterization is not feasible.

We identified the primary sources of variability in P removal by steel slags. The investigation revealed that overband magnetic separation produced less effective steel slags in regard to P removal, possibly due to the low porosity and low pH buffer index. However, generation process alone was unable to explain the variability of P removal by steel slag. We found that electrical conductivity (EC), Mg content, particle density and bulk density were the most influential characteristics for uncoated steel slags. The effect of these char-

acteristics on P removal was modeled, and the developed model can be used for predicting the P removal ability of unknown steel slag samples. For Al-coated steel slags, the intrinsic variables that could better explain P removal were EC, Ca content, Fe content and coating level. Characterization of steel slag for these properties will allow for more efficient steel slags to be selected, leading to the design and construction of better and more precise P removal structures.

Additionally, the environmental safety of the use of steel slags in P removal structures was evaluated. No environmental threats were identified, as none of the analyzed elements (including heavy metals) surpassed drinking-water and environmental criteria in the outflow samples.

Another major contribution of this research was the technique developed to regenerate spent Fe/Al-based PSMs. To allow the procedure to be conducted as a field-scale operation, low volumes of regenerative solution were proposed. After P-treatment of 3 different Fe/Al-rich PSMs using 2 levels of P concentrations, 5 or 20 pore volumes of KOH was recirculated 0, 6 or 24 times to recover the sorbed P. Phosphorus recovery was effective under all tested scenarios for PSMs in which the dominant P removal mechanism was adsorption by Al/Fe (hydr)oxides. The most effective regeneration treatment used 20 pore volumes of 1M KOH with no recirculation. The treatment can be repeated for at least 2 sorption cycles, with decreasing efficacy. Recirculation improved the effectiveness of the treatment when 5 pore volumes were used. This is important because, for field-scale applications, the success of the technique depends on the maintenance of the solid:solution ratio. When 20 pore volumes is not logistically feasible, 5 pore volumes of KOH recirculated 6 times can also effectively recover P. The proposed regeneration treatment is a one-step process that can increase the lifetime of PSMs in P removal structures and reduce maintenance operations, because it substitutes the frequent replacement of the P-saturated PSM.

Another key contribution of this research was the study of the behavior of Fe-rich PSMs under anoxic conditions. The effect of anoxic conditions on P mobilization has significant implications in soils, where P is primarily retained by Al/Fe minerals (except in alkaline soils). Because of similar P retention mechanisms, the expectation was that the same scenario would be observed with Fe/Al-rich PSMs in anoxic environments. In context, the presence

of stagnant water in P removal structures for extended periods of time could result in P release, hindering the construction of P removal structures with upward flow, where anoxic conditions may develop in-between flow events. To investigate how Fe-rich PSMs behave when undergoing anoxic conditions, P-treated and non-treated PSMs were incubated with tile drainage in a biogeochemical reactor. The continuous decrease of Eh in the presence and absence of glucose indicated that Fe-rich PSMs undergo anoxic conditions. This procedure confirmed the reductive dissolution of Fe(III) in PSMs; however, its effects on Fe-bound P release and P sorption capacity of the PSM were minor. These results suggest that the development of anoxic conditions is not a limitation for the construction of upward-flow P removal structures. The primary advantage of upward-flow structures is the smaller footprint due to the possibility of building deeper structures, which may facilitate a wider adoption of this BMP. A wider implementation of P removal structures, together with conventional best management practices and long-term P reduction strategies, can be the definitive answer to reducing the frequency and intensity of excessive-P related issues in watersheds.

These studies explored the variability of P removal capacity of PSMs according to (I) chemical and physical properties, (II) dominant P removal mechanisms, and (III) the operational properties of P removal structures. Variation in the expected performance of PSMs is a result of their intrinsic characteristics (e.g., EC and elemental content, capability of regeneration), as well as extrinsic characteristics of the structures (e.g., flow rates, direction of flow). The use of the proposed adaptations and the new techniques developed in these studies will be beneficial for the implementation of P removal structures. Our results offer a great opportunity for building more effective and cost-efficient P removal structures due to the better understanding of their operation in regard to the PSM performance.

5.2 Recommendations

The performance of P removal structures depends on its adequate design. As PSMs in part determine the potential of a structure to remove P from flowing waters, a thorough understanding of the media is critical for designing more efficient structures. We recommend an individual characterization of unknown PSMs, as intrinsic sources of variability, such as chemical composition and physical properties (i.e., intrinsic factors), which have been proved

to significantly impact the P removal efficacy. Using a linear modeling approach, P removal by steel slag was found to be especially impacted by the EC of the media, Mg content, bulk density and particle density. Therefore, by measuring these properties and inputting them in the model, a more effective PSM can be selected. Steel slags with a higher Mg content, EC and porosity showed greater P removal capacity and should be preferred. In regards to industrial generation processes of steel slags, this work indicate that overband magnetic separation slags should be avoided. For future work, the addition of more slag samples to the database and the validation of the model on test samples are recommended in order to assess and improve its prediction accuracy.

Extrinsic factors were also proven to affect the P removal ability of steel slag: longer residence times (RT) favored a superior P removal performance. Consequently, P removal structures built with steel slag must be designed to provide a long contact time between the media and the P-rich flow. A RT of 9.85 minutes is sufficient for satisfactory P removal. For locations where shorter residence times are expected, the use of Al-coating is recommended. By submerging the steel slag for 48 hours in a $95 \text{ g L}^{-1} \text{ Al}_2(\text{SO}_4)_3$ (100% coating level), a new path for P removal is created, due to the added layer of Al. With Al-coating, P removal structures designed for shorter RTs can still utilize steel slag, a widely available and inexpensive PSM. As discussed throughout this work, this adaptation is especially important considering the changes in precipitation patterns in the future. Additionally, when a thorough characterization of a new steel slag is not possible, the Al-coated PSM should be preferred, as Al-coating will generate a more homogeneous material in regard to P removal ability.

Evaluation of Fe-rich PSMs under anoxic conditions revealed that these PSMs undergo redox-induced changes, e.g., reductive dissolution of Fe(III). However, the impacts on Fe-bound P and P removal capacity of PSMs are minimal. Based on these research findings, upward-flow P removal structures with Fe-rich PSMs can be constructed when top-down flow is not feasible, since stagnant water in-between flow events will not be detrimental to the P removal ability of the Fe-rich PSM. We recommend that further research include the study of P pools before and after anoxic incubation, in order to better understand the mechanisms of readsorption and/or precipitation under anoxic conditions.

Regeneration of Fe-rich media was proposed as an opportunity to improve the efficiency of P removal structures. For regenerating P-saturated media, the circulation of 20 pore volumes of 1 M KOH is recommended, using a RT of 10 minutes, preferentially (RT of 0.5 minutes was also proven to offer satisfactory results when PSM samples were not heavily loaded). When the treatment with 20 pore volumes is deemed unfeasible, a 6-times recirculation of 5 pore volumes of 1 M KOH is suggested, which can provide similar desorption capacity. The desorbed P can then be recovered by treating the outflow of the regenerative solution with CaCl_2 , but further research is needed in order to establish the economic feasibility of this practice. The regeneration methodology can be used for recovering the P sorption ability of Fe/Al-dominated PSMs saturated by low- (e.g., agricultural surface and subsurface P-rich flows), as well as high-P flows (e.g., wastewater). The regeneration treatment can be repeated at least twice, with decreasing efficacy after each sorption cycle. Future research may include the repetition of sorption-desorption cycles until exhaustion.

These studies support the use of PSMs in P removal structures to mitigate excessive dissolved P in watersheds. The efficacy of PSMs can be improved through a better understanding of the media, and also, through coating and regeneration field-scale-feasible techniques. Additionally, the proposed change on the flow regime of P removal structures can broaden their adoption in different landscapes. Improving the P removal ability of PSMs in P removal structures will ultimately contribute to the remediation of many P-rich watersheds.

A. FLOW-THROUGH SYSTEM

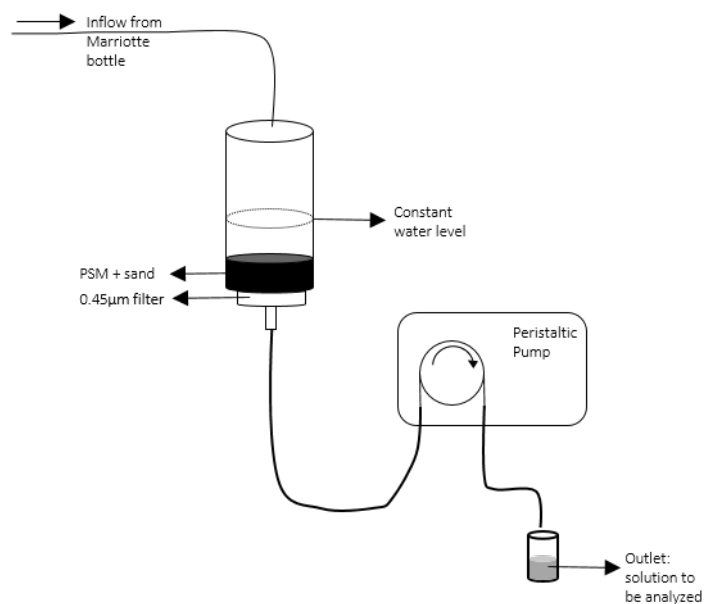


Figure A.1. Schematic describing the elements in the flow-through experiments, a tool that was utilized in all studies in this research for measuring the P removal capacity of diverse PSMs.

B. STATISTICAL ANALYSIS OF THE STEEL SLAGS PERFORMANCES

Table B.1. Pairwise comparison of cumulative P removal between slag samples: estimates of difference between groups, confidence intervals and level of significance of comparison.

Group A	Group B	Difference	Lower Limit	Upper Limit	p-value
1	2	43.96	-185.72	273.65	0.9999
1	3	153.53	-76.15	383.22	0.4733
1	4	205.96	-23.72	435.65	0.1142
1	5	59.78	-169.90	289.47	0.9985
1	6	69.97	-159.71	299.66	0.9945
1	7	-83.78	-313.47	145.90	0.9775
1	8	-59.55	-289.24	170.13	0.9986
1	9	-254.25	-483.94	-24.56	0.01953
1	10	-112.44	-342.13	117.24	0.85265
1	11	-40.86	-270.55	188.82	0.9999
1	12	-50.84	-280.53	178.84	0.9996
2	3	109.56	-120.12	339.25	0.8719
2	4	161.99	-67.69	391.68	0.3940
2	5	15.81	-213.87	245.50	1
2	6	26.00	-203.68	255.69	0.9999
2	7	-127.75	-357.44	101.93	0.7268
2	8	-103.52	-333.21	126.16	0.9076
2	9	-298.22	-527.91	-68.53	0.0031
2	10	-156.40	-386.09	73.28	0.4458
2	11	-84.83	-314.52	144.85	0.9753

continued on next page

Table B.1. *continued*

Group A	Group B	Difference	Lower Limit	Upper Limit	p-value
2	12	-94.81	-324.50	134.87	0.9467
3	4	52.43	-177.25	282.12	0.9995
3	5	-93.76	-323.44	135.93	0.9505
3	6	-83.56	-313.25	146.12	0.9779
3	7	-237.32	-467.01	-7.63	0.0376
3	8	-213.09	-442.78	16.59	0.0900
3	9	-407.78	-637.47	-178.09	2.25E-05
3	10	-265.97	-495.66	-36.28	0.0121
3	11	-194.40	-424.09	35.28	0.1648
3	12	-204.38	-434.07	25.30	0.1203
4	5	-146.18	-375.87	83.50	0.5458
4	6	-135.99	-365.68	93.69	0.6477
4	7	-289.75	-519.44	-60.06	0.0045
4	8	-265.52	-495.21	-35.83	0.0124
4	9	-460.22	-689.91	-230.53	2.24E-06
4	10	-318.40	-548.09	-88.71	0.0012
4	11	-246.83	-476.52	-17.14	0.0261
4	12	-256.81	-486.50	-27.12	0.0176
5	6	10.19	-219.49	239.88	1
5	7	-143.56	-373.25	86.12	0.5721
5	8	-119.33	-349.02	110.35	0.8003
5	9	-314.032	-543.72	-84.34	0.0015
5	10	-172.22	-401.91	57.46	0.3077
5	11	-100.64	-330.33	129.04	0.9221
5	12	-110.62	-340.31	119.06	0.8650
6	7	-153.76	-383.45	75.92	0.4711

continued on next page

Table B.1. *continued*

Group A	Group B	Difference	Lower Limit	Upper Limit	p-value
6	8	-129.53	-359.22	100.15	0.7102
6	9	-324.22	-553.91	-94.53	0.0009
6	10	-182.41	-412.10	47.27	0.2342
6	11	-110.84	-340.53	118.84	0.8635
6	12	-120.82	-350.51	108.86	0.7880
7	8	24.22	-205.46	253.91	0.9999
7	9	-170.46	-400.15	59.22	0.3217
7	10	-28.65	-258.34	201.03	0.9999
7	11	42.91	-186.77	272.60	0.9999
7	12	32.93	-196.75	262.62	0.9999
8	9	-194.69	-424.38	34.99	0.1634
8	10	-52.88	-282.57	176.80	0.9995
8	11	18.68	-211.00	248.37	0.999
8	12	8.71	-220.97	238.40	1
9	10	141.81	-87.87	371.50	0.5897
9	11	213.38	-16.30	443.07	0.0891
9	12	203.40	-26.28	433.09	0.1241
10	11	71.57	-158.11	301.26	0.9934
10	12	61.59	-168.09	291.28	0.9981
11	12	-9.97	-239.66	219.71	1

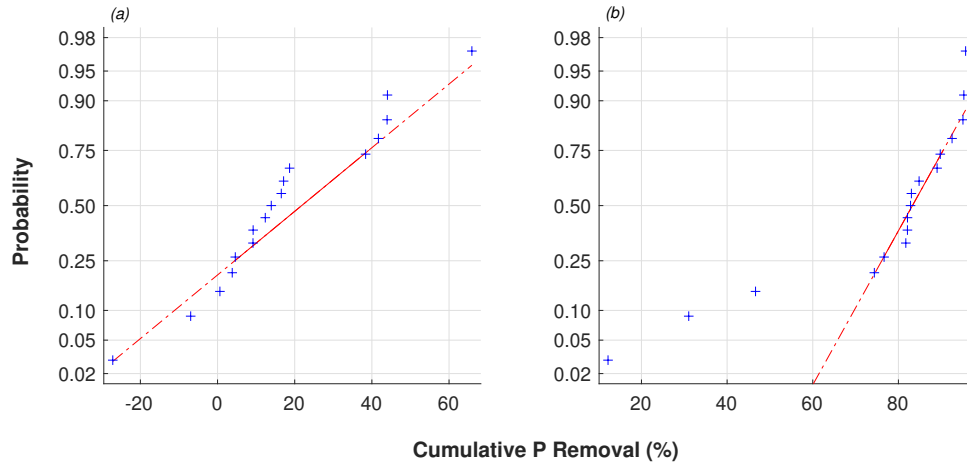


Figure B.1. Normal probability plots showing the lack of normality of the (a) low residence time and (b) high residence time datasets.

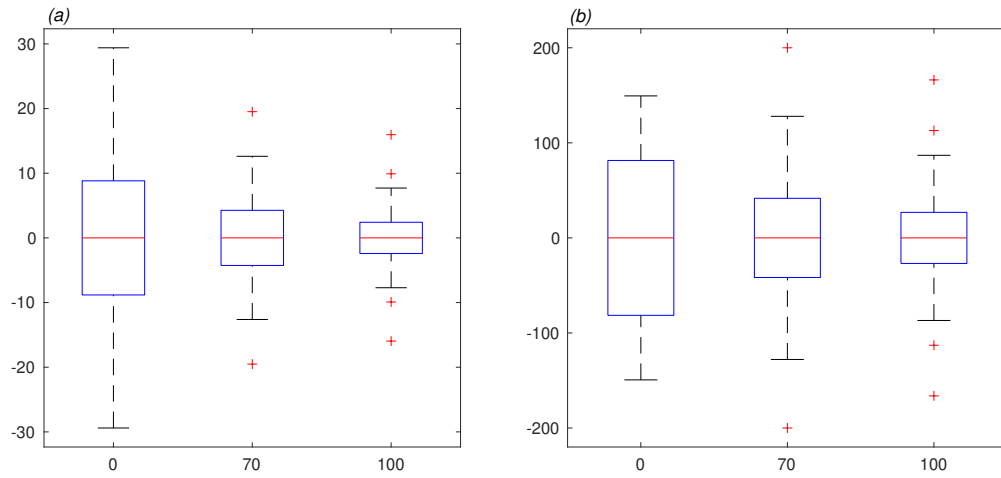


Figure B.2. Residuals distribution according to the different classes of coating: (a) shows the non-constant variance of the original residuals and (b) shows the residuals after transforming the data.

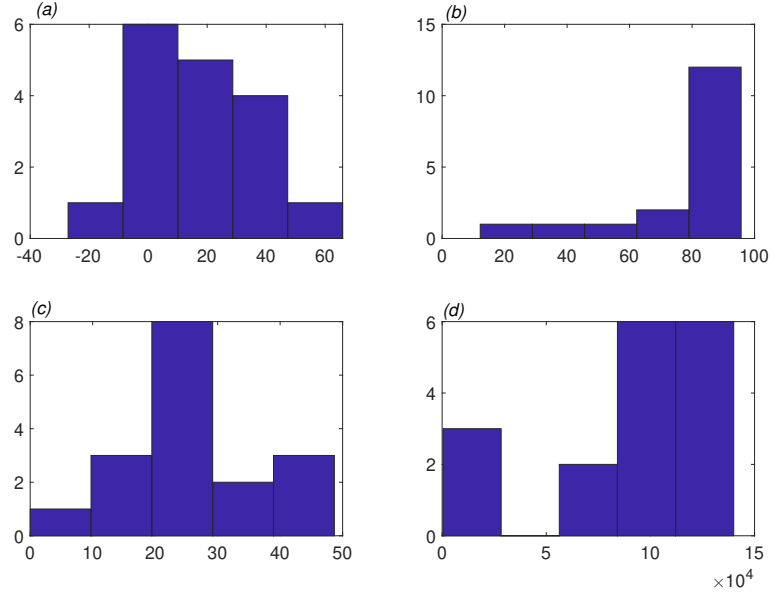


Figure B.3. Histograms for checking normality of data. (a) and (c) are respectively the original and the transformed low RT data ($\lambda = 0.8156$) and (b) and (d) show the distribution of the original and transformed high RT data ($\lambda = 2.8256$).

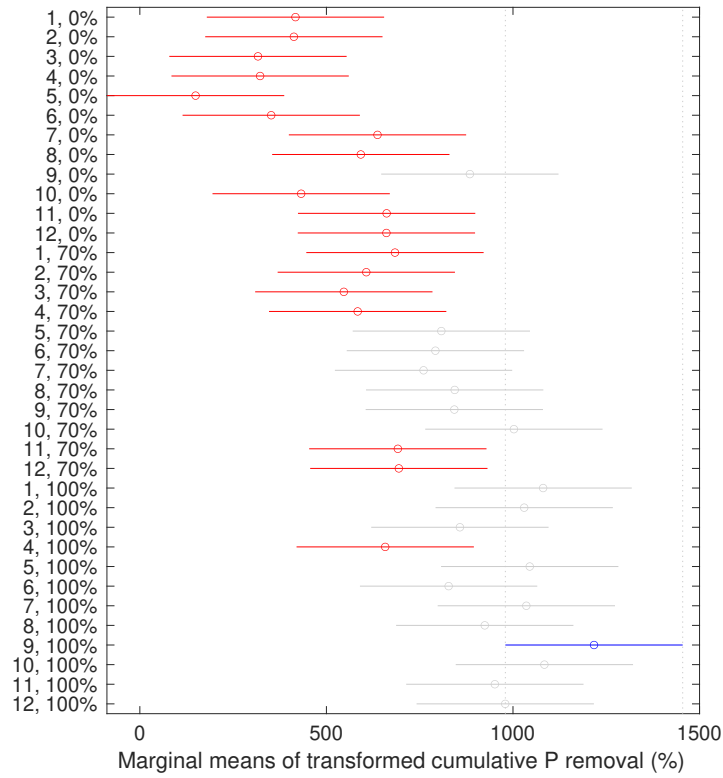


Figure B.4. Means and confidence intervals of transformed cumulative P removal of each combined treatment. Y-axis describe each combination of factors, with slag number first and level of Al-coating second. 100% coated slag 9 (in blue) had a superior performance and 18 groups (in red) showed population marginal means significantly different from Slag=9, Coating=100. The groups in gray had similar performance to 100% coated slag 9.

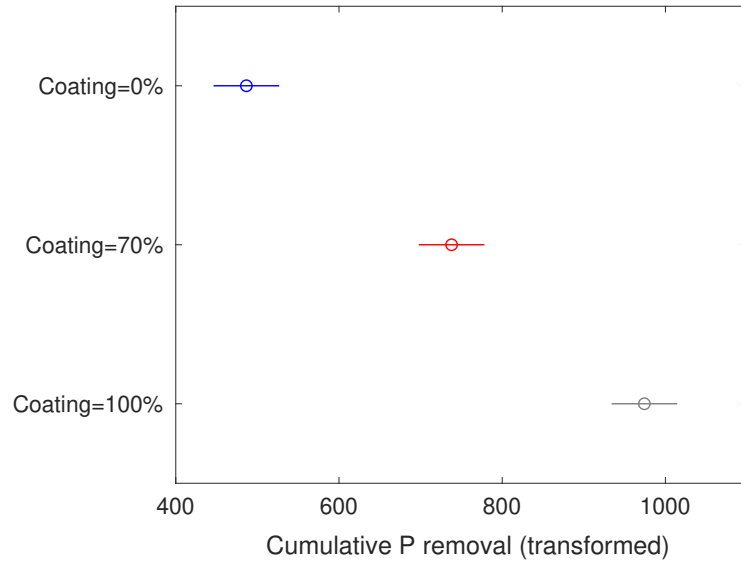


Figure B.5. Coating Levels: group means represented by circle and the confidence interval represented by the line. All groups were statistically different from each other ($\alpha = 0.05$).

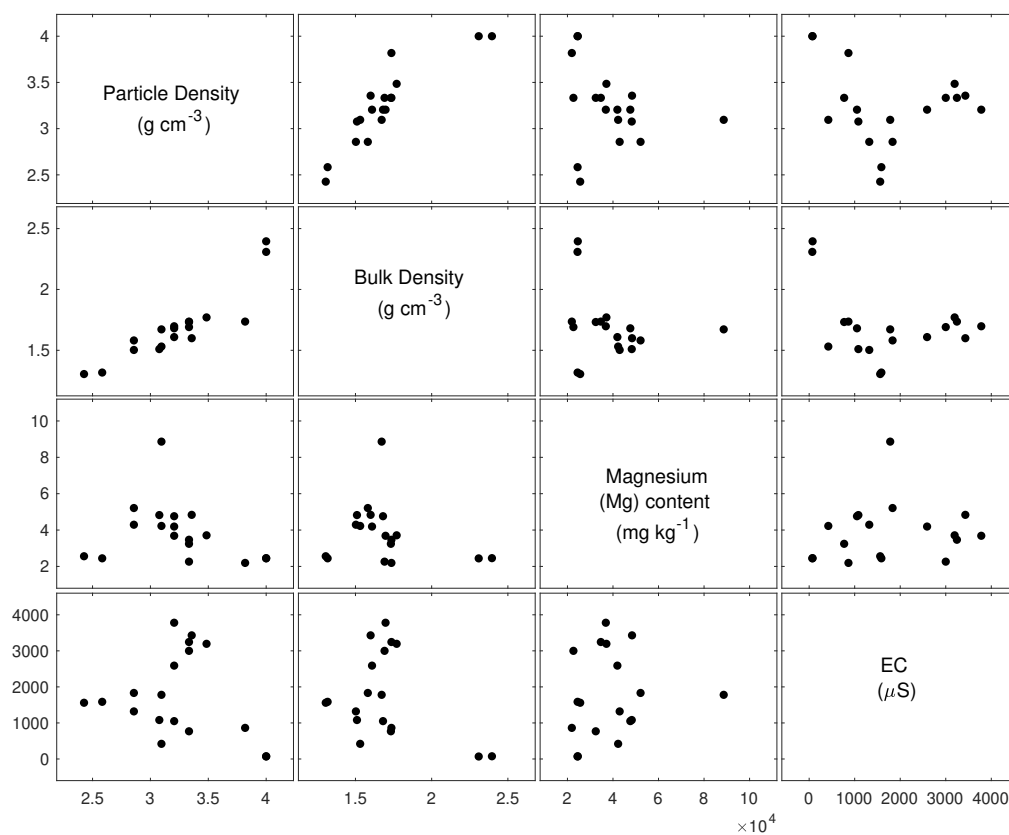


Figure B.6. Evaluating multicollinearity of explanatory variables of cumulative P removal by uncoated steel slags: particle density and bulk density showed a significant correlation.

C. ADDITIONAL CHARACTERIZATION RESULTS OF STEEL SLAG AND FLOW-THROUGH SAMPLES

Table C.1. pH of randomly selected flow-through samples.

<i>Uncoated slags</i>			<i>70% Coated slags</i>			<i>100% Coated slags</i>		
Sample	pH ₀ ⁽¹⁾	Samples pH ²	Sample	pH ₀ ⁽¹⁾	Samples pH ²	Sample	pH ₀ ⁽¹⁾	Samples pH ²
Slag 4	7.36	6.88, 6.77, 6.62	Slag 10	5.82	6.06, 6.20, 6.12	Slag 1	5.73	4.99, 5.34, 5.52
Slag 4	6.54	6.33, 6.41, 6.48	Slag 10	5.69	6.10, 6.46, 6.30	Slag 1	5.46	5.71, 5.97, 5.96
Slag 4	7.27	6.89, 6.73, 6.6	Slag 11	6.30	8.56, 8.32, 8.17	Slag 2	5.54	5.39, 5.73, 5.77
Slag 5	6.27	6.05, 6.19, 6.26	Slag 11	5.76	8.38, 8.03, 7.80	Slag 2	5.55	5.02, 5.53, 5.67
Slag 5	6.25	5.97, 6.16, 6.16	Slag 12	5.59	8.43, 7.83, 7.46	Slag 3	5.56	5.41, 5.84, 5.92
Slag 5	6.55	6.17, 6.42, 6.38	Slag 12	5.68	8.04, 7.72, 7.51	Slag 3	5.56	4.74, 5.32, 5.55
Slag 6	6.14	5.9, 6.05, 6.06				Slag 4	5.49	5.07, 5.74, 5.90
Slag 6	6.06	5.89, 6.07, 6.11				Slag 4	5.59	5.44, 5.68, 5.82
Slag 7	7.89	6.61, 7.61, 7.8, 7.94				Slag 5	6.85	5.08, 5.52, 5.58
Slag 7	7.32	8.08, 8.02, 8.15, 8.12				Slag 5	5.83	4.80, 5.34, 5.5
Slag 8	8.68	7.66, 7.67, 7.88, 7.9				Slag 6	5.70	4.85, 5.39, 5.5
Slag 8	8.36	7, 7.18, 7.02, 7.6, 7.65				Slag 6	5.92	5.1, 5.54, 5.66
Slag 9	6.56	6.05, 6.74, 7.01, 7.09				Slag 7	5.79	5.91, 5.54, 6.45
Slag 9	7.46	6.46, 7.24, 7.36, 7.32				Slag 7	6.11	6.03, 6.39, 6.45
Slag 12	7.72	10.21, 8.98, 8.71, 8.53				Slag 8	8.74	6.35, 6.75, 6.82
Slag 12	8.67	9.38, 8.57, 8.09, 8.1				Slag 8	6.74	6.20, 6.53, 6.54
Slag 15	7.74	7.04, 7.05, 6.7				Slag 9	6.39	6.08, 6.68, 6.68
Slag 15	6.63	6.45, 6.55, 6.34				Slag 9	6.24	6.06, 6.64, 6.61
Slag 17	7.92	6.37, 7.02, 7.14, 7.23						
Slag 17	7.68	6.98, 7.04, 7.15, 7.24						
Slag 17	6.47	6.33, 6.14, 6.33						
Slag 17	6.27	7.99, 8, 7.73						
Slag 18	7.51	7.01, 6.98, 7.15, 7.21						
Slag 18	7.31	5.94, 5.94, 6.07, 6.11						
Slag 18	7.38	8.62, 7.98, 7.76						
Slag 18	7.45	7.96, 7.69, 7.51						

¹ pH of first collected sample;

² pH of randomly selected effluent samples (in order of collection).

Table C.2. Micro-constituents of steel slag samples: concentrations of Boron (B), Chromium (Cr), Cobalt (Co), Manganese (Mn), Sodium (Na), Nickel (Ni), Lead (Pb), Sulfur (S), Silica (Si) and Zinc (Zn) as measured in the digestions.

Sample	mg kg ⁻¹										
	B	Cr	Co	Mn	Na	Ni	Pb	S	Si	Zn	
Slag 1	X	0.00	325.05	4.38	4824.67	1004.45	393.69	205.74	10267.00	485.84	50.71
	S	0.00	563.00	1.08	416.31	92.94	528.38	288.10	467.82	420.79	23.84
Slag 2	X	0.00	270.23	4.28	4368.83	1048.22	67.26	163.72	10615.00	491.94	54.22
	S	0.00	468.06	0.60	752.10	130.12	21.86	212.98	397.88	430.77	47.50
Slag 3	X	0.00	613.59	4.45	13091.17	414.90	272.73	191.06	2220.00	526.34	417.67
	S	0.00	735.49	1.43	3859.82	84.36	118.39	244.67	2182.38	458.21	124.15
Slag 4	X	0.00	525.49	5.71	12062.50	359.56	186.73	183.89	1535.08	553.22	465.55
	S	0.00	700.29	2.23	3471.30	68.68	77.33	213.55	973.39	485.54	130.33
Slag 5	X	0.00	237.10	5.48	5448.50	714.55	109.81	191.51	8511.50	592.25	80.02
	S	0.00	410.67	1.03	2013.04	295.37	20.52	246.62	1704.88	577.51	32.40
Slag 6	X	0.00	314.07	6.41	5814.83	639.81	124.07	182.58	7512.67	620.51	102.68
	S	0.00	543.98	1.14	532.00	79.04	74.70	216.59	523.94	539.38	71.36
Slag 7	X	0.00	364.46	1.92	7499.33	681.34	58.16	210.99	16506.67	615.62	66.45
	S	0.00	626.17	0.83	1190.50	55.29	8.04	288.97	1447.42	531.11	9.05
Slag 8	X	0.00	291.97	2.06	6040.00	665.14	45.59	304.10	15781.67	586.15	60.04
	S	0.00	505.70	1.01	660.35	34.97	17.20	438.21	2747.35	547.14	7.34
Slag 9	X	0.00	1024.01	1.26	14578.33	449.98	215.67	187.14	1685.77	561.08	139.28
	S	0.00	538.80	0.53	1006.06	23.06	179.94	275.94	1232.61	485.53	65.02
Slag 10	X	0.00	1029.07	0.92	15481.25	497.57	123.69	87.33	1668.05	728.15	162.76
	S	0.00	454.43	0.40	851.42	9.64	32.28	107.16	1217.92	629.55	28.89
Slag 11	X	25.12	1362.07	1.92	16600.00	454.51	317.66	139.76	1815.52	423.26	295.60
	S	43.50	744.98	2.58	1443.03	33.99	292.17	221.04	1233.38	366.07	360.82
Slag 12	X	25.35	1125.18	0.21	15263.33	592.59	236.75	97.92	1608.75	661.72	60.42
	S	43.91	150.26	0.43	2738.87	354.65	64.63	146.26	1239.73	574.63	43.21
Slag 13	X	6.18	1323.39	0.08	16231.11	450.13	219.22	147.16	1785.30	531.52	75.69
	S	10.71	466.01	0.14	2152.02	109.73	30.98	220.29	1327.06	460.76	99.58
Slag 14	X	0.00	835.77	0.00	16872.50	372.68	166.87	91.81	2247.18	381.54	30.56
	S	0.00	827.71	1.48	673.89	131.39	71.03	151.03	1759.20	336.31	24.52
Slag 15	X	1.83	1303.55	0.17	16670.00	522.10	136.27	143.01	1752.32	667.31	98.56
	S	3.18	599.00	0.49	1511.22	156.28	9.29	227.46	1229.53	581.30	86.91
Slag 16	X	0.00	1836.91	1.59	23143.33	485.88	208.75	72.36	1980.67	547.85	58.34
	S	0.00	1233.00	1.03	11774.44	28.77	34.73	94.95	1331.35	499.44	49.42
Slag 17	X	0.00	1288.11	1.80	16437.50	443.51	128.75	208.84	2002.35	513.97	71.89
	S	0.00	533.21	2.13	2330.42	43.97	29.12	263.64	1348.21	445.82	64.88
Slag 18	X	0.00	1627.87	1.56	18458.33	487.73	220.05	169.28	2205.62	520.50	125.99
	S	0.00	728.39	1.27	881.23	2.58	161.73	263.94	1712.67	449.78	76.93

[†]Average and standard deviation calculated across 6 replicates: 2 uncoated, 2 70% coated and 2 100% coated.

D. EFFECT OF RESIDENCE TIME ON PHOSREDEEM

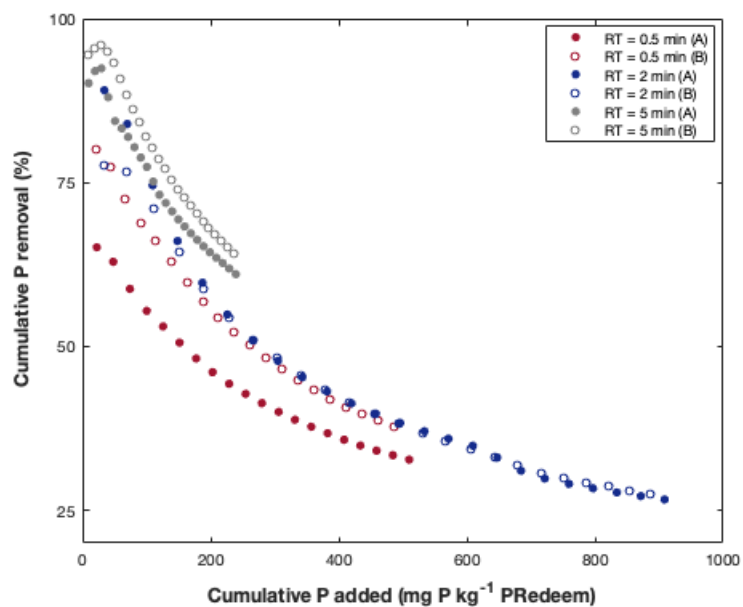


Figure D.1. Phosphorus (P) removal by PhosRedeem in flow-through experiments using different residence times (RT). Experiments were performed with input solution of 0.5 mg P L⁻¹.

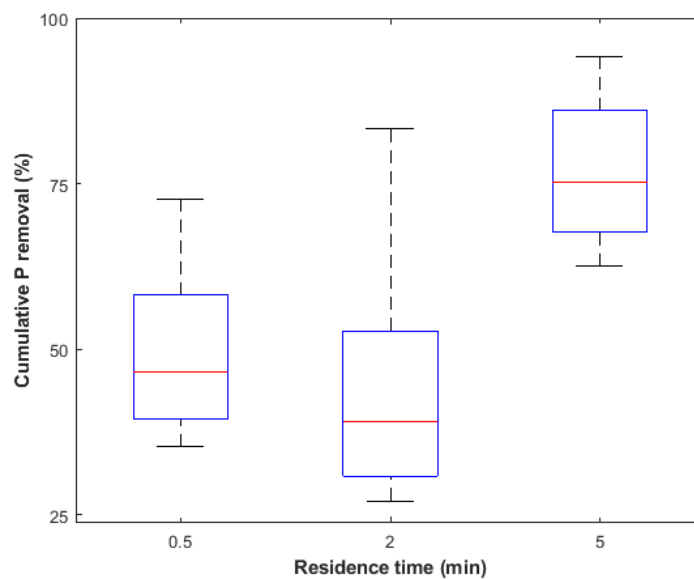


Figure D.2. Box plot: effect of residence time (RT) on P removal performance of PhosRedeem.

E. SUMMARY OF SORPTION-DESORPTION CYCLES

Table E.1. Alcan phosphorus (P) sorption and desorption results. Each row represents one regeneration treatment. The first ten rows refer to 0.5 mg L⁻¹ P, the second ten are 50 mg L⁻¹ P experiments.

Replicate ⁽¹⁾	S0 P Sorbed ⁽²⁾	D0 P Desorbed ⁽²⁾	Net P Cycle 0	S1 P Added P Sorbed	D1 P Desorbed	Net P Cycle 1	S2 P Added P Sorbed	Net P ⁽³⁾
mg P kg ⁻¹ PSM								
A.20.0.10.1	11,463	10,704	759	2453	1343	834	3362	4124
A.20.0.10.2	11,463	10,884	579	2533	2377	-221	2984	4290
A.20.0.05.1	11,463	9752	1711	2821	1123	-429	2986	1976
A.20.0.05.2	11,463	8860	2604	2848	1055	-932	2936	2582
A.5.0.05.1	11,463	4385	7079	2634	51	-607	2610	5049
A.5.0.05.2	11,463	6956	4508	2701	1188	-1287	2773	4354
A.5.6.05.1	11,463	6809	4654	2688	744	-1478	2951	3515
A.5.6.05.2	11,463	7617	3846	2821	1618	-1692	2999	4159
A.5.24.05.1	11,463	5293	6170	2596	1011	-2155	2609	4858
A.5.24.05.2	11,463	5210	6254	2559	1496	-2655	2582	5530
A.20.0.10.1	14,493	12,916	1577	19,496	4767	9749	19,635	5643
A.20.0.10.2	14,493	13,246	1246	21,034	4313	10,878	20,479	4300
A.20.0.05.1	14,493	12,641	1852	18,872	3513	10,400	19,142	3415
A.20.0.05.2	14,493	10,877	3616	19,844	3123	12,037	20,366	5077
A.5.0.05.1	14,493	5130	9363	17,579	7206	-477	21,049	14,183
A.5.0.05.2	14,493	5232	9261	18,066	8473	-955	18,195	13,242
A.5.6.05.1	14,493	8132	6361	18,196	2313	10,197	18,592	8791
A.5.6.05.2	14,493	8406	6087	17,455	5909	6452	17,463	12,292
A.5.24.05.1	14,493	7729	6764	18,781	6921	2515	17,921	10,088
A.5.24.05.2	14,493	7933	6560	23,141	5767	8635	17,795	11,015

- ⁽¹⁾ Each two replicates refer to a regeneration treatment, defined by (a) volume of KOH (measured in pore volumes, or PV), (b) recirculation and (c) residence time. The identification of the replicates follows the notation: X.PV.RC.RT.Replicate, with X being the initial of the PSM (A for Alcan, B for Biomax or P for PhosRedeem). ⁽²⁾ Total sorbed and desorbed P include rinse P concentrations. ⁽³⁾ $(P_{S0} + P_{S1} + P_{S2}) - (P_{S0R} - P_{S1R}) + (P_{D0} - P_{D1}) - (P_{D0R1} + P_{D0R2} + P_{D1R1} + P_{D1R2})$, where P_{Sx} and P_{Dx} are the P concentrations adsorbed in the sorption phases and desorbed in desorption phases, respectively. P_{SxR} and P_{DxRy} are the P concentrations observed in the rinse solution after each sorption or desorption phase.

Table E.2. Biomax phosphorus (P) sorption and desorption results. Each row represents one regeneration treatment. The first ten rows refer to 0.5 mg L⁻¹ P, the second ten are 50 mg L⁻¹ P experiments.

Replicate ⁽¹⁾	S0 P Sorbed ⁽²⁾	D0 P Desorbed ⁽²⁾	Net P Cycle 0	S1 P Added	S1 P Sorbed	D1 P Desorbed	Net P Cycle 1	S2 P Added	S2 P Sorbed	Net P ⁽³⁾
mg P kg ⁻¹ PSM										
B.20.0.10.1	7744	6871	941	947	548	1401	-1002	1156	881	900
B.20.0.10.2	7744	7294	518	1030	881	1329	-1180	1064	847	849
B.20.0.05.1	7812	7920	-108	1040	357	1537	-854	1203	722	-635
B.20.0.05.2	7812	5689	2123	1063	722	1386	-1045	1170	538	1928
B.5.0.05.1	7812	1721	6091	1059	-274	779	555	1075	365	5335
B.5.0.05.2	7812	1903	5909	1050	365	630	55	1134	467	6042
B.5.6.05.1	7812	4812	3000	1231	270	3647	-2687	1249	760	316
B.5.6.05.2	7812	5041	2771	1322	760	2533	-1971	1393	549	1480
B.5.24.05.1	7812	4784	3028	1107	447	2141	-1481	1221	744	2010
B.5.24.05.2	7812	4558	3254	458	744	2578	-2864	1203	813	2164
B.20.0.10.1	18,675	16,110	2565	22,872	4995	5753	12,124	22,332	5350	1105
B.20.0.10.2	18,675	16,210	2465	17,296	5344	5394	6558	18,124	3845	-142
B.20.0.05.1	18,675	11,547	7128	22,254	2929	6293	13,032	19,547	2232	2009
B.20.0.05.2	18,675	12,110	6565	17,923	2203	6017	9703	23,586	5578	5068
B.5.0.05.1	18,675	7800	10,875	20,310	8509	9417	2385	21,775	7169	7569
B.5.0.05.2	18,675	8245	10,430	19,032	6982	10,116	1934	21,711	8297	7553
B.5.6.05.1	18,675	9097	9578	23,939	3427	6147	14,365	24,318	9822	12,196
B.5.6.05.2	18,675	9931	8744	20,803	9765	5680	5358	21,197	5606	7612
B.5.24.05.1	18,675	10,237	8438	21,140	7182	10,131	3827	21,162	10,014	7263
B.5.24.05.2	18,675	10,096	8579	20,053	9836	9436	781	23,148	10,903	8988

⁽¹⁾ Each two replicates refer to a regeneration treatment, defined by (a) volume of KOH (measured in pore volumes, or PV), (b) recirculation and (c) residence time. The identification of the replicates follow the notation: X.PV.RC.RT.Replicate, with X being the initial of the PSM (A for Alcan, B for Biomax or P for PhosRedeem. ⁽²⁾ Total sorbed and desorbed P include rinse P concentrations. ⁽³⁾ ($P_{S0} + P_{S1} + P_{S2}$) - ($P_{S0R} - P_{S1R}$) + ($P_{D0} - P_{D1}$) - ($P_{D0R1} + P_{D0R2} + P_{D1R1} + P_{D1R2}$), where P_{Sx} and P_{Dx} are the P concentrations adsorbed in the sorption phases and desorbed in desorption phases, respectively. P_{SxR} and P_{DxRy} are the P concentrations observed in the rinse solution after each sorption or desorption phase.

Table E.3. PhosRedeem phosphorus (P) sorption and desorption results. Each row represents one regeneration treatment. The first four rows refer to 0.5 mg L⁻¹ P, the following six are 50 mg L⁻¹ P experiments.

Replicate ⁽¹⁾	S0 P Sorbed (2)	D0 P Desorbed (2)	Net P Cycle 0	S1 P Added	S1 P Sorbed	D1 P Desorbed	Net P Cycle 1	P Added	S2 P Sorbed	Net P ⁽³⁾
mg P kg ⁻¹ PSM										
P.20.0.10.1	1376	0	1376	1190	1036	0	1035	1277	129	2540
P.20.0.10.2	1376	3	1373	1150	1021	0	1021	1154	102	2496
P.20.0.05.1	1376	0	1376	1125	862	21	842	1261	212	2429
P.20.0.05.2	1376	0	1376	1098	887	0	887	1242	201	2463
P.20.0.10.1	15,292	2198	13,095	19,671	18,048	145	17,903	19,781	1333	30,746
P.20.0.10.2	15,292	2402	12,891	19,627	18,294	164	18,129	18,885	1251	30,686
P.20.0.05.1	15,292	1555	13,737	19,306	20,967	197	20,816	19,096	776	33,698
P.20.0.05.2	15,292	1355	13,937	19,783	19,008	34	19,027	15,899	1370	32,697
P.5.6.05.1	15,292	1522	13,770	18,489	18,791	195	18,679	17,473	294	31,075
P.5.6.05.2	15,292	1463	13,829	18,753	18,459	181	18,380	18,187	349	30,871

⁽¹⁾ Each two replicates refer to a regeneration treatment, defined by (a) volume of KOH (measured in pore volumes, or PV), (b) recirculation and (c) residence time. The identification of the replicates follow the notation: X.PV.RC.RT.Replicate, with X being the initial of the PSM (A for Alcan, B for Biomax or P for PhosRedeem. ⁽²⁾ Total sorbed and desorbed P include rinse P concentrations. ⁽³⁾ ($P_{S0} + P_{S1} + P_{S2}$) - ($P_{S0R} - P_{S1R}$) + ($P_{D0} - P_{D1}$) - ($P_{D0R1} + P_{D0R2} + P_{D1R1} + P_{D1R2}$), where P_{Sx} and P_{Dx} are the P concentrations adsorbed in the sorption phases and desorbed in desorption phases, respectively. P_{SxR} and P_{DxRy} are the P concentrations observed in the rinse solution after each sorption or desorption phase.

VITA

Isis Stacanelli Pires Chagas Scott was born and raised in Divinópolis, Minas Gerais, Brazil. After moving to the capital of the state, Belo Horizonte, to complete her high school studies, she joined the Department of Agronomic Engineering at the Federal University of Lavras (UFLA), one of the top three universities in the field nationally. During her undergraduate studies, Isis received a scholarship from the Brazilian government and completed a 6-month internship at the National Soil Erosion Research Laboratory (NSERL), following her interests on soil and water conservation. She returned to West Lafayette after graduating to pursue her Master's degree. Isis joined the Department of Agronomy at Purdue University in 2014, and under the supervision of Dr. Chi-hua Huang and Dr. Laura Bowling, she studied transport of phosphorus and phosphorus sorption media. After graduation in 2016, Isis started her PhD studies, continuing working on phosphorus transport and excess dissolved phosphorus mitigation with Dr. Chad Penn and Dr. Huang.